

# Coupled Flow in Groundwater Systems: The Study of Bulkflow Parameters

**Teboho Shakhane**

A dissertation submitted in accordance with the requirements  
for the degree

***Magister Scientiae***

in the

**Faculty of Natural and Agricultural Sciences**

**Institute for Groundwater Studies (IGS)**

**University of the Free State**

**Bloemfontein**

Supervisor: Prof. G. Steyl

August 2011



## DEDICATION

This thesis comes as a dedication to my late father, Mokhethi Nathnael Shakhane, who passed away in 2007: Thank you dad for instilling the love for education in me and ensuring that the route to greater heights has always been paved; you removed the roof and the ceiling above my head so that now the sky is only the limit!

“PARENTS WHO ARE AFRAID TO PUT THEIR FOOT DOWN USUALLY HAVE  
CHILDREN WHO STEP ON THEIR TOES.”

“THE WISE TURN THE DARK COLOURS OF SADNESS AND PAIN  
INTO THE MOST BEAUTIFUL RAINBOW”

Chinese quotes

## DECLARATION

I, Shakhane Teboho, declare that this thesis hereby submitted by me for the Master of Science degree at the University of the Free State is my own independent work and has not previously been submitted by me at another university/faculty. I further more cede copyright of the thesis in favour of the University of the Free State.

# X

Shakhane Teboho  
2008034429



## ACKNOWLEDGMENTS

The research in this thesis emanated from a *bulk flow parameter* project pioneered by Water Research Commission (WRC). The financing of the project by WRC is deservedly hereby gratefully acknowledged thereupon.

Also this piece of work would have not been of any success had it not been of the integral parts plaid by:

- My mentors, Professor Gerrit Van Tonder and Professor Gideon Steyl, for all their technical guidance and advice with this piece of work: MANY THANKS!!
- My hero and spring of knowledge, Prof. J.F. Botha. I pass my humble and sincere gratitude to you for being there for me whenever the situation did warrant. Your input has been vital in ensuring that this work was ultimately successful. THANK YOU PROF!!
- Johan van der Merwe for your assistance in the soil analysis. Despite the hectic schedule of the lab at the time, you persisted and went out of your way to work overtimes in order to have me helped. Thank you for all that,
- Mr Eelco Lukas for all your parental guidance and openness for help at any time,
- Mrs Lorinda Rust for your parental support, your love that gave us courage to keep coming to IGS every morning has surely not gone unnoticed,
- Dora du Plessis for your willingness to edit my thesis,
- My colleagues (better put, my brothers) Modreck Gomo and Khahliso Clifford Leketa: Through difficult situations and hardships we stood firm by each other, soldiered on and eventually prospered,
- Fannie de Lange whose technical expertise was of utmost vitality in ensuring that suggested practical methodologies were properly executed,
- My friend Nico van Zyl for always creating a conducive environment for at IGS; I always enjoyed being around you my brother

- My mom ('Mateboho), late father (Mokhethi), brothers (Mpolelo, Tlali and Shakhane), the one and only sister (Mapaseka), my aunt ('Malibuseng Mokete) my cousins (Mojabeng, Moliehi and Peter Phofu), my grannies (Mokhethi and 'Mapeter Phofu) for their prolonged moral support and encouragement and the entire Mokheseng family.
- Institute for Groundwater studies at large, my kind regards for awarding me an opportunity and financing my studies to advance this far in my academics. I am really indebted and humbled by many wonderful experiences you exposed me to during my spell at IGS- MY HEARTY THANKS!!!
- God for giving me strength and life to reach this point in life.

□

“BEHIND EVERY ABLE MAN, THERE ARE ALWAYS OTHER ABLE MEN.”

Chinese quote

## Summary

This study was aimed at studying bulkflow parameters in groundwater systems at littoral zone of the Modder River. In this thesis, all the aspects were synthesised and exemplified by incorporating a multidisciplinary perspective to develop a sound conceptual framework of the alluvial stream aquifer system.

Hydraulic characterisation of the near aquifer system was achieved by acquiring data from a 6-spot pattern well network from which lithological, aquifer hydrogeology, and groundwater hydrogeochemistry characterisations were comprehensively undertaken.

The aquifer overburden was estimated to have the permeability of 2.42m/d when its textural classification was found on average to consist of 22% clay+silt and 77% very fine sand. The geology of the study area is typical of the Karoo geology. This was affirmed by massive mudstone bedrock of the Eccca group underlying the study domain. The unconsolidated sediments of gravel, sand and silt, overlie this Karoo mudstone. Therefore, the aquifer is a three units and unconfined alluvial stream aquifer situated in the alluvial deposits along the course of the Modder River. The main units of the system are the upper unit, middle unit and lower aquitard made up of the overbank-fine sand deposits, gravel and mudstone respectively.

Groundwater is a bicarbonate type water and falls along a mixing line from sulfate-chloride type water to calcium-magnesium type water. This water was found to be both unpolluted sodium enriched and chloride enriched strongly be attributed to forestation of the site where evapotranspiration rates are widespread. Groundwater plots close and parallel to GMWL indicating that recharge is primarily derived from the direct infiltration of precipitation.

The  $\delta^{18}\text{O}$  and  $\delta\text{D}$  composition of water from the sampled wells indicates that water from all wells drilled in the Riparian or Bank storage aquifer is isotopically lighter than water from wells located on the Terrestrial aquifer. Tritium ranges are indicative of modern water suggesting that the possible influx source might have been precipitation or precipitation derived water. In other words, the groundwater gets recharged with modern rainfalls and has short circulation time in the ground indicative of short travel time. The plot of pH-Tritium indicates that the majority of the

samples fall within the range 6 to 8.5 attributed to recharges with modern and highly neutralised rainfalls. This also suggests short groundwater circulation time in the ground. The groundwater samples with the lowest nitrate concentration were the ones with the lowest tritium level indicating that, although the groundwater source lies on agricultural land, it has not been contaminated by nitrate fertilizers.

Groundwater head differences yield the hydraulic gradients from terrestrial aquifer towards riparian aquifer. On average the hydraulic gradient is 0.0083. Flow direction over the entire study domain generally trend SE, sub-perpendicular to the regional surface water flow direction. The EC-profiles show the gravel unit as a major groundwater conduit as shown by a jump in EC values at this unit and this unit is the same water source for all the wells that intercepted the gravel.

The transmissivity of the site's aquifer ranges between  $0.3\text{m}^2/\text{d}$  and  $164\text{m}^2/\text{d}$ . Highest transmissivity estimated at a maximum level are observed in wells located in the riparian aquifer. The unconfined aquifer specific yield is in the order of 0.005-0.023. Darcy velocity was estimated at  $4.16\text{m}/\text{d}$  for CYS1BH4 and natural flow velocity for this well was ultimately estimated at  $1.81\text{ m}/\text{d}$ . On the other hand, Darcy velocity for CYS1BH3 was estimated at  $9.01\text{ m}/\text{d}$  with natural flow velocity ultimately estimated at  $3.92\text{ m}/\text{d}$ . Last in the list is CYS1BH5 whose Darcy velocity was estimated at  $11.24\text{ m}/\text{d}$  and natural flow velocity ultimately estimated at  $22.4\text{ m}/\text{d}$ . The estimated velocities are relatively high and this observation holds true for transmissivities so high.

Baseflow calculations gave a negative value signifying no base flow contribution of groundwater in to the river. This suggests that most groundwater is used up by the riparian vegetation.

## CONTENTS

DEDICATION .....	II
DECLARATION.....	III
ACKNOWLEDGMENTS.....	IV
Summary.....	VI
List of Figures.....	XIII
List of Tables.....	XVII
List of equations .....	XVIII
1 PREAMBLE AND SITE BACKGROUND INFORMATION .....	1-1
1.1 Presentation and justification .....	1-1
1.2 Site inventory and overview: Physiographic setting .....	1-2
1.2.1 Location.....	1-2
1.2.2 Topography .....	1-3
1.2.3 Climatology (rainfall climate and evaporation) .....	1-3
1.2.4 Hydrography and drainage .....	1-4
1.2.5 Hydrogeological Setting.....	1-8
1.3 Scope: Aims and objectives .....	1-10
1.3.1 Aims/general objectives.....	1-10
1.3.2 Specific Objectives .....	1-10
1.4 General study approach to meeting the objectives .....	1-10
2 DEFINITIONS AND OVERVIEW OF ASPECTS, CONCEPTS AND TECHNICAL BACKGROUND .....	2-12
2.1 Introduction and remarks .....	2-12



2.2	Bulk flow parameters.....	2-12
2.2.1	Darcian or bulk velocity.....	2-12
2.2.2	Seepage velocity .....	2-14
2.2.3	Hydraulic conductivity .....	2-15
2.2.4	Transmissivity.....	2-17
2.2.5	Storativity.....	2-19
2.2.6	Groundwater level, gradient and direction of flow.....	2-22
2.2.7	Soil .....	2-23
2.3	Geotechnical Criteria.....	2-23
2.4	Conclusion .....	2-25
3	WELLFIELD OR NETWORK DESIGN .....	3-26
3.1	Introduction .....	3-26
3.2	Borehole configurations .....	3-26
3.3	Well construction and completion.....	3-28
3.3.1	CYS1BH1 .....	3-28
3.3.2	CYS1BH2 .....	3-29
3.3.3	CYS1BH3, CYS1BH4, CYS1BH5 and CYS1BH6 .....	3-29
3.4	Borehole development .....	3-31
3.5	Conclusion .....	3-32
4	PHYSICAL AND GEOMETRICAL CONFIGURATION OF THE AQUIFER SYSTEM .....	4-33
4.1	Introduction .....	4-33
4.2	Soil analysis .....	4-33
4.2.1	Hydrogeological properties of the soil.....	4-34
4.2.2	Soil index properties .....	4-34
4.2.2.1	Soil Type .....	4-34

4.2.3	Hydraulic conductivity .....	4-36
4.2.3.1	In-situ methodology .....	4-37
4.3	Geology.....	4-42
4.3.1	Regional Lithostratigraphy .....	4-42
4.3.2	Site geology.....	4-44
4.3.2.1	Drilling efforts .....	4-44
4.3.3	Geologic modelling.....	4-49
4.4	Conclusions.....	4-52
5	ISOTOPIC AND HYDROCHEMICAL CHARACTERISTICS.....	5-53
5.1	Introduction .....	5-53
5.2	Fieldwork.....	5-54
5.3	Hydrogeochemical characterisation .....	5-55
5.3.1	Chemical differences for different waters.....	5-55
5.3.2	Results and discussion.....	5-56
5.4	Isotopic characteristics.....	5-61
5.4.1	$\delta^{18}\text{O}$ and $\delta\text{D}$ .....	5-61
5.4.2	Tritium.....	5-62
5.4.3	Results and discussion.....	5-64
5.4.3.1	$\delta^{18}\text{O}$ and $\delta\text{D}$ .....	5-64
5.4.4	Tritium.....	5-69
5.5	Conclusions.....	5-73
5.5.1	Hydrogeochemical characteristics .....	5-73
5.5.2	Isotopic characteristics .....	5-74
6	GENERAL GROUNDWATER FLOW AND GRADIENTS.....	6-77
6.1	Introduction .....	6-77
6.2	Magnitude and direction of gradient.....	6-77

6.2.1	Groundwater levels.....	6-78
6.2.2	<i>Groundwater direction and slope</i> .....	6-81
6.2.2.1	Small-scale gradients and mathematical preliminary .....	6-82
6.2.2.2	Single large-scale gradient.....	6-84
6.2.2.3	Results and discussions.....	6-87
6.3	Deducing flow section .....	6-89
6.3.1	Borehole Electrical Conductivity (EC) Profiling .....	6-89
6.3.2	Pumping test.....	6-91
6.4	Conclusions.....	6-92
7	AQUIFER HYDRAULIC AND PHYSICAL PARAMETISATION .....	7-94
7.1	Introduction .....	7-94
7.2	Hydraulic parameters .....	7-94
7.2.1	Fieldwork, results and discussion .....	7-95
7.3	Baseflow component.....	7-97
7.4	Transport parameters.....	7-99
7.4.1	Groundwater tracer testing .....	7-100
7.4.1.1	Background to Single well point dilution test .....	7-100
7.4.1.2	Fieldwork, results and discussion.....	7-101
7.4.1.3	Methodology.....	7-102
7.5	Conclusions.....	7-108
8	CONCLUSIONS, PERSPECTIVES AND FLOW SYSTEM CONCEPTION..	8-109
8.1	Introduction .....	8-109
8.2	Characterisation Methodology.....	8-109
8.2.1	Borehole selection.....	8-110
8.2.2	Physical configuration of the aquifer system.....	8-110
8.2.3	Isotopic and hydrochemical characteristics .....	8-110

8.2.4	General groundwater flow.....	8-111
8.2.5	Physical hydraulic characterisation.....	8-112
8.3	Proposed Conceptual model (Schematisation) .....	8-112
9	REFERENCES .....	9-115
10	ANNEXE A: SOIL ANALYSIS.....	10-125
10.1	Infiltration Test.....	10-125
10.2	Soil Index Properties .....	10-127
10.2.1	Bouyoucos procedure for soil classification .....	10-127
11	ANNEXE B: LITHOLOGIC DESCRIPTIONS.....	11-129
12	ANNEXE C: ENVIRONMENTAL ISOTOPIC AND HYDROCHEMICAL CHARACTERISTICS .....	12-133
13	ANNEXE C: GROUNDWATER FLOW AND HYDRAULIC PARAMETER CHARCTERISATION.....	13-134

## List of Figures

Figure 1-1: Geographic location of study area (circled) and the insert map of South-Africa-provinces on which the study area is located.....	1-2
Figure 1-2: Long-term average Monthly daily rainfall for the study area.....	1-4
Figure 1-3: The major dams along the Modder River (DEAT, 2001). ....	1-5
Figure 1-4: The Modder river drainage (DEAT, 2001) .....	1-6
Figure 1-5: Baseflow from the Modder river banks at the study area. ....	1-7
Figure 1-6: The Modder river images during dry and wet periods at the weir in the vicinity of the study site. ....	1-7
Figure 1-7: Modder River downstream of the weir during dry periods .....	1-8
Figure 1-8: The location of the Modder River catchment.....	1-9
Figure 2-1: Schematic illustration of parameters in Darcy's law (Freeze and Cherry 1979).....	2-13
Figure 2-2: Macroscopic and Microscopic concepts of groundwater flow (Freeze and Cherry, 1979). ....	2-14
Figure 2-3: Overview of methods used to determine the hydraulic conductivity....	2-16
Figure 2-4: Graphical estimation of hydraulic conductivity (McKinney, 2009) .....	2-17
Figure 2-5: Diagrammatic aquifer model for illustrating Transmissivity concept in a confined aquifer (Heath, 1987).....	2-19
Figure 2-6: Diagrammatic aquifer model for illustrating Darcy's law and Transmissivity concept in an unconfined aquifer (Heath, 1987). ....	2-19
Figure 2-7: Specific yield concept for use in computing Storativity of an unconfined aquifer (Hermance, 2003). ....	2-20
Figure 2-8: Storativity concept and illustration in a confined aquifer (Hermance, 2003).....	2-21
Figure 2-9: Sketch showing the relation between hydraulic heads and water levels in two observation wells—Well1.and well2 (modified from Taylor and Alley, 2001)..	2-22
Figure 2-10: Groundwater exploration chart (technical framework) for characterisation programme (Roscoe Moss Company, 1990). ....	2-25
Figure 3-1: The pilot network for groundwater characterisation in the project site and the insert map for the wells in the study site.....	3-27
Figure 3-2: Elevation contour map at the study area.....	3-27
Figure 3-3: Inside casing wrapped with a fine mesh (bedim). ....	3-29

Figure 3-4: CYS1BH1 construction counterfeiting gravel envelope well and the borehole cap. ....	3-30
Figure 3-5: Borehole backwashing development with the aid of the rotafoam and the settleable solids test using Imhoff cone.....	3-31
Figure 4-1: Figure showing the position and configuration of soil sampling (ABH: Augured Borehole). ....	4-34
Figure 4-2: Soil grain composition.....	4-36
Figure 4-3: Auguring of the holes on which infiltration test was executed. ....	4-38
Figure 4-4: Conceptual diagram of an inversed auger-hole method illustrating the infiltration from a water-filled auger-hole into the soil and relevant measurements (modified from: Oosterbaan and Nijland, 1994).....	4-38
Figure 4-5: Fall of the water level plotted against time .....	4-40
Figure 4-6: Lithostratigraphy of the Modder River Catchment (DEAT, 2001).....	4-43
Figure 4-7: Calcrete deposits (left) as recognised from the surface and dolerite rocks (right) of the dyke located near the study site.....	4-44
Figure 4-8: Cable tool method and cable tool rig (insert) used for drilling at the study site.....	4-45
Figure 4-9: Gravel pebbles and boulders sampled during drilling of CYS1BH3 at a depth of 11-18 metres. ....	4-47
Figure 4-10: Lenses of sand, gravel and mudstone floor within Modder river channel .....	4-47
Figure 4-11: Continuous samples of sediment/geology for respective boreholes (A and C=fine sand, B=mudstone, D=gravel). ....	4-48
Figure 4-12: The 3D Multilog showing borehole distribution at the study area for more detailed an descriptive well logs, the reader is referred to ANNEXE B. ....	4-48
Figure 4-13: 3D Lithology model for the site.....	4-50
Figure 4-14: East–West lithological cross section. ....	4-51
Figure 4-15: Lithology fence diagram.....	4-51
Figure 5-1: A Google image showing location of the sampled sites. ....	5-54
Figure 5-2: Trilinear diagram (Piper) used in the hydrogeochemical interpretations. 5-56	
Figure 5-3: Characterisation of the water chemistry both from boreholes and river water. ....	5-58
Figure 5-4: Graphical comparison of water chemistry from different wells. ....	5-58

Figure 5-5: Stiff plots of water samples from the study area. ....	5-59
Figure 5-6: Box –and-Whisker differentiation of waters based on EC values.....	5-59
Figure 5-7: A vegetated CYS1BH3 location zone. ....	5-60
Figure 5-8: Evolution of Environmental Isotopes (Craig, 1961). ....	5-62
Figure 5-9: $\delta D - \delta^{18}O$ plot of groundwater and the river water.....	5-64
Figure 5-10: Bank storage at the study area. ....	5-66
Figure 5-11: Figure illustrating the riparian and terrestrial aquifer concept (van Tonder, 2011).....	5-66
Figure 5-12: Comparison between Tritium values from four wellfields in the study site.....	5-71
Figure 5-13: Plot of Tritium concentrations based on pH. ....	5-72
Figure 5-14: Plot of Tritium concentrations based on nitrate. ....	5-73
Figure 5-15: A Google image showing wells drilled in the bank storage aquifer (enclose). ....	5-75
Figure 6-1: A hydrograph of monthly groundwater levels and bar graph of monthly precipitation.....	6-79
Figure 6-2: Water level as a function of elevation. ....	6-81
Figure 6-3: Cross product output depicting estimated groundwater flow direction inferred from CYS1BH3, CYS1BH1 and CYS1BH2. ....	6-83
Figure 6-4: Cross product output depicting estimated groundwater flow direction inferred from CYS1BH5, CYS1BH1 and CYS1BH2. ....	6-84
Figure 6-5: Schematic illustration of a right handed Cartesian co-ordinate system (Botha, 1994). ....	6-85
Figure 6-6: Schematic of Cartesian graph plane illustration on which the groundwater direction is read on the plane. ....	6-86
Figure 6-7: The contour map showing horizontal groundwater flow direction in three dimensions. ....	6-88
Figure 6-8: A map illustrating and depicting groundwater flow direction.....	6-89
Figure 6-9: Borehole conductivity log for CYS1BH3.....	6-90
Figure 6-10: Borehole conductivity log for CYS1BH4.....	6-90
Figure 6-11: Borehole conductivity log for CYS1BH5.....	6-91
Figure 6-12: Pumping test showing the drawdown behaviour in boreholes CYS1BH3 and CYS1BH5.....	6-92
Figure 7-1: A Cooper Jacob fit for CYS1BH3. ....	7-96

Figure 7-2: A Cooper Jacob fit for CYS1BH1. ....	7-96
Figure 7-3: Neuman fit for CYS1BH3 pumping test data.....	7-97
Figure 7-4: Reference evapotranspiration (mm/d) map of South Africa for the month of January (Savva and Frenken, 2002). ....	7-99
Figure 7-5: Barker model applied to CYS1BH4 used for as abstraction borehole during pumping test.....	7-102
Figure 7-6: Set-up schematisation for point dilution test used during tracer testing (modified from GHR 611, 2010). ....	7-104
Figure 7-7: Field setup for executed point dilution test.....	7-104
Figure 7-8: Point-dilution curve obtained during the CYS1BH4 tracer test.....	7-105
Figure 7-9: Point-dilution curve obtained during the CYS1BH3 tracer test.....	7-106
Figure 7-10: Point-dilution curve obtained during the CYS1BH5 tracer test.....	7-107
Figure 8-1: A Proposed methodology to constructing the conceptual model.....	8-109
Figure 8-2: Map showing the estimated hydraulic properties of the site water bearing material. ....	8-114
Figure 8-3: Schematic section for the hydrogeologic conceptual model.....	8-114
Figure 11-1: 2D lithological logs. ....	11-131
Figure 11-2: 2D lithological logs. ....	11-132
Figure 13-1: GRADIENT XLS Microsoft excel used to estimate the groundwater gradient and direction of flow (Devlin, 2002). ....	13-135
Figure 13-2: A cooper Jacob fit for CYS1BH2 (a drying well).....	13-136
Figure 13-3: A Cooper Jacob fit for CYS1BH4. ....	13-136
Figure 13-4: A Cooper Jacob fit for CYS1BH6 (a drying well).....	13-137
Figure 13-5: Neuman fit for CYS1BH3 pumping test data.....	13-137
Figure 13-6: Neuman fit for CYS1BH5 data. ....	13-138



## List of Tables

TABLE 4-1: SOIL TEXTURAL ANALYSIS FROM IGS LAB.....	4-35
TABLE 4-2: RANGE OF K-VALUES BY SOIL TEXTURE (Smedema and Rycroft, 1983).....	4-37
TABLE 4-3: INFILTRATION TEST RESULTS FROM CYS1_ABH1 (r=0.105m, D'=0.7m).....	4-41
TABLE 4-4: COMPUTED K VALUES FOR EACH OF THE TESTED HOLES.....	4-42
TABLE 5-1: TRITIUM BASED CATEGORISATION OF GROUNDWATER AGE (Clark and Fritz, 1997; Zouari <i>et al.</i> 2003).....	5-63
TABLE 5-2: STABLE ISOTOPIC COMPOSITIONS.....	5-68
TABLE 5-3: TRITIUM (T.U) RESULTS.....	5-70
TABLE 6-1: SUMMARY OF MEASURED WATER LEVELS 2011/02/09.....	6-78
TABLE 6-2: GROUNDWATER GRADIENT AND DIRECTION OF FLOW.....	6-88
TABLE 7-1: AQUIFER PARAMETERS ESTIMATED FROM PUMPING TEST ....	7-97
TABLE 7-2: FLOW DIMENSION (n) AND FLOW THICKNESS (b) FOR RESPECTIVE WELLS OBTAINED FROM BARKER MODEL.....	7-102
TABLE 7-3: PARAMETER VALUES OBTAINED FROM THE TRACER TEST...	7-107
TABLE 10-1: INFILTRATION TEST RESULTS CYS1_ABH2.....	10-125
TABLE 10-2: INFILTRATION TEST RESULTS CYS1_ABH3.....	10-125
TABLE 10-3: INFILTRATION TEST RESULTS FOR CYS1_ABH4.....	10-126
TABLE 10-4: INFILTRATION TEST RESULTS FOR CYS1_ABH5.....	10-126
TABLE 12-1: SUMMARISED WATER QUALITY DATA FROM DIFFERENT WELLS.....	12-133
TABLE 13-1: TIMELY GROUNDWATER LEVEL DATA (MEASUREMENTS ARE GIVEN IN MAMSL).....	13-134

## List of equations

Equation 2-1 .....	2-13
Equation 2-2 .....	2-14
Equation 2-3 .....	2-16
Equation 2-4 .....	2-18
Equation 2-5 .....	2-18
Equation 2-6 .....	2-20
Equation 2-7 .....	2-21
Equation 4-1 (Oosterbaan and Nijland, 1994) .....	4-39
Equation 5-1 (Craig, 1961) .....	5-61
Equation 5-2 (Gat and Gonfiantini, 1981) .....	5-62
Equation 6-1 .....	6-82
Equation 6-2 (Botha, 1994) .....	6-82
Equation 6-3 .....	6-82
Equation 6-4 .....	6-84
Equation 6-5 .....	6-86
Equation 6-6 .....	6-87
Equation 7-1 .....	7-100
Equation 10-1 .....	10-127
Equation 10-2 .....	10-128

# 1 PREAMBLE AND SITE BACKGROUND INFORMATION

## 1.1 Presentation and justification

Over 95% of the world's total fresh water supply is stored beneath the earth's ground subsurface (Schwartz, 2003). It is stored in the rock pores and fractures having sufficient spaces and connectivity for both storage and flow. The geological formation having pores and fractures that hold water or permit its economically viable movement under ordinary field conditions is called an aquifer (Botha, 1994). Aquifers may be located nearby and hence abutting surface water bodies thereby, one way or the other, influencing the surface water body in question, i.e., acting as influent (losing to groundwater), effluent (gaining from groundwater) or both. Hypothetically therefore, withdrawal of water from streams can deplete ground water; conversely, pumpage of ground water can deplete water in surface bodies. The afore mentioned process can only occur if and only if groundwater and surface water systems in question are proved to be connected. Understanding and quantifying the implications of both the physical and chemical groundwater processes to surface water bodies or vice versa has become a fast growing subject in hydrogeological studies (Winter *et al.*, 1998). These require thorough near-surface water body or interface characterisation of the groundwater systems. The characterization may entail measurements of bulk flow concepts and spatial patterns of flow at the groundwater-surface water interface affecting the interaction (Sophocleous, 2002). This characterisation is important in determining whether or not there is an interaction between groundwater and surface water bodies; subsequently, enabling an effective management of both surface and groundwater resources without compromising the other.

This thesis subsequently seeks to characterise groundwater/aquifer systems at the groundwater-surface water interface. The results are aimed at contributing to building of a comprehensive dataset for testing of groundwater surface water interaction methodologies. All aspects are synthesised and exemplified at a local scale to build a sound conceptual model at Krugersdrift (WRC).

## 1.2 Site inventory and overview: Physiographic setting

### 1.2.1 Location

The study area is located within the Free State province in South Africa, north-west of the city of Bloemfontein. It is located within the Upper Orange Water Management Area which is divided into three reaches or catchments; namely the Upper, the Middle and the Lower Modder catchments with the study area being predominantly within the upper Riet/Modder River catchment. The exact location is in the riparian region of the Modder River [Afrikaans name *Modder* is *mud* which affiliates the river with high sediment loads, (Tsokeli, 2005)] approximately 800m's downstream of the Kruggersdrift dam (Figure 1-1).

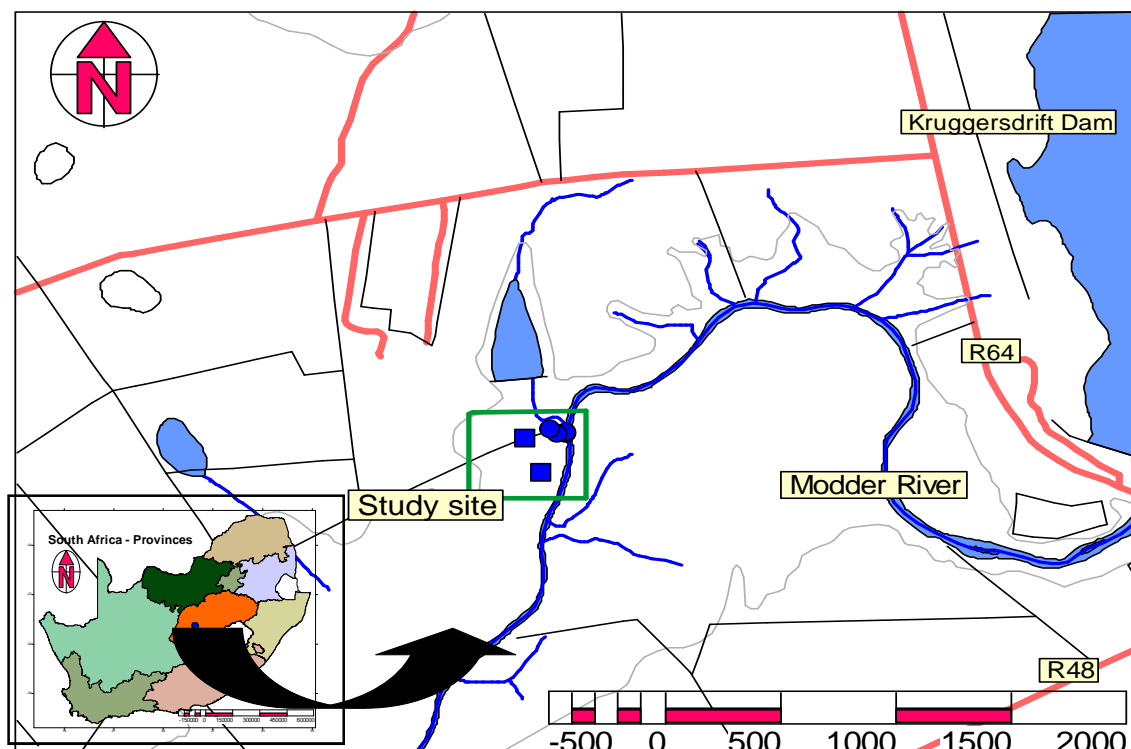


Figure 1-1: Geographic location of study area (circled) and the insert map of South-Africa-provinces on which the study area is located.

### 1.2.2 Topography

The landscape of the Modder River basin is generally flat, lying between 1000 and 1500m in elevation. The study area itself lies between 1237 and 1255mamsl elevation in the shallow open valley; almost on the knitpoint of the Modder River banks where the land unit is gentle, undulating to flat in nature. Part of the study area extends on the upland where the unit presents more accentuated, moderately steep to almost flat sloping. Surrounding the study area is the undulating, flattening topography that opens up into wide plains making most of the area surrounding the study area relatively flat. The relief of the study area is generally very low (>2%).

### 1.2.3 Climatology (rainfall climate and evaporation)

Rainfall in Modder River catchment varies temporally in summer and winter. Summer is regarded as the time-period between December and February. This period, most of the days, is generally hot with clear skies normally with considerable widespread showers. Also very common in summer are short and intermitted thundershowers and hailstorms. On the other hand, winter is regarded as the time period between May and August, the period that is very cold (Gugulethu *et al.* 2009).

Mean annual precipitation (MAP) for the area is in the range of 400-500mm (Midgley *et al.*, 1994). Rainfall in this area shows a significant temporal variation where most of the precipitation is experienced in the wet season (November stretching until March April) with the maximum rainfall period being from December to February (Figure 1-2) (Gugulethu *et al.*, 2009). Weather stations in the Modder River catchment have shown that none of the stations receive more than 100mm in any rainy month (Gugulethu *et al.*, 2009). Conversely, extremely low precipitation amounts ( $\leq 10$ mm) are recorded in winter. The study area therefore has a fairly arid climate with low and erratic rainfall because there is never a time when more than 100mm was recorded. These climatic conditions have groundwater implications in that even small summer rainfall events can result in a considerable water table rise (Gasca and Ross, 2009) in areas of high recharge.

Evaporation in the Modder River C50k quaternary catchment is estimated to be in the range of 1800-2000mm (Symons Sunken-pan) (Midgley *et al.*, 1994). Symons

Sunken-pan (S-pan) is a pan that is used to hold water during observations for the determination of the quantity of evaporation at a given location. It combines or integrates the effects of several climate elements: temperature, humidity, rain fall, solar radiation, and wind. It is a square in geometry with side length of 1.83m and 0.61m in depth. This pan is installed in the ground with a 76mm rim above ground level (Shahin, 2002).

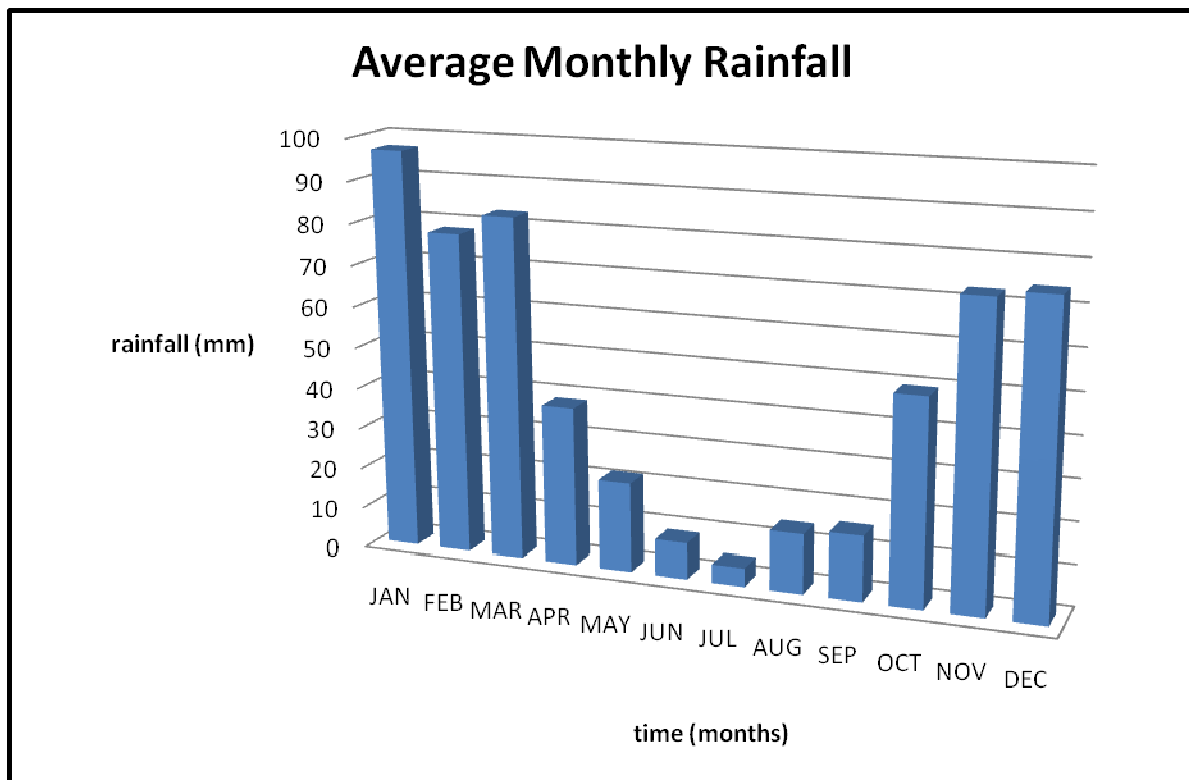


Figure 1-2: Long-term average Monthly daily rainfall for the study area.

#### 1.2.4 Hydrography and drainage

The following dams drain into the Modder River: Rustfontein, Mockes and Krugersdrift Dams (DEAT, 2001) (Figure 1-3). From upstream of the Krugersdrift Dam, Modder River drainage displays more of dentritic nature in which a couple of tributaries feed into the stem river (Modder). Non-perennial and sizeable tributaries or headstreams of the Modder River are located eastward and comprise Klein Modder, Sepane, Koranna, Doring, Renoster and Krom tributaries (Figure 1-4).

Below the Krugersdrift Dam, numerous pans exist. The pans are filled up following torrents of summer rainfall (BKS, 2002) although they seldom overflow thereby contributing very little (2,5mm) into the stem river (Midgley *et al.* 1994a).

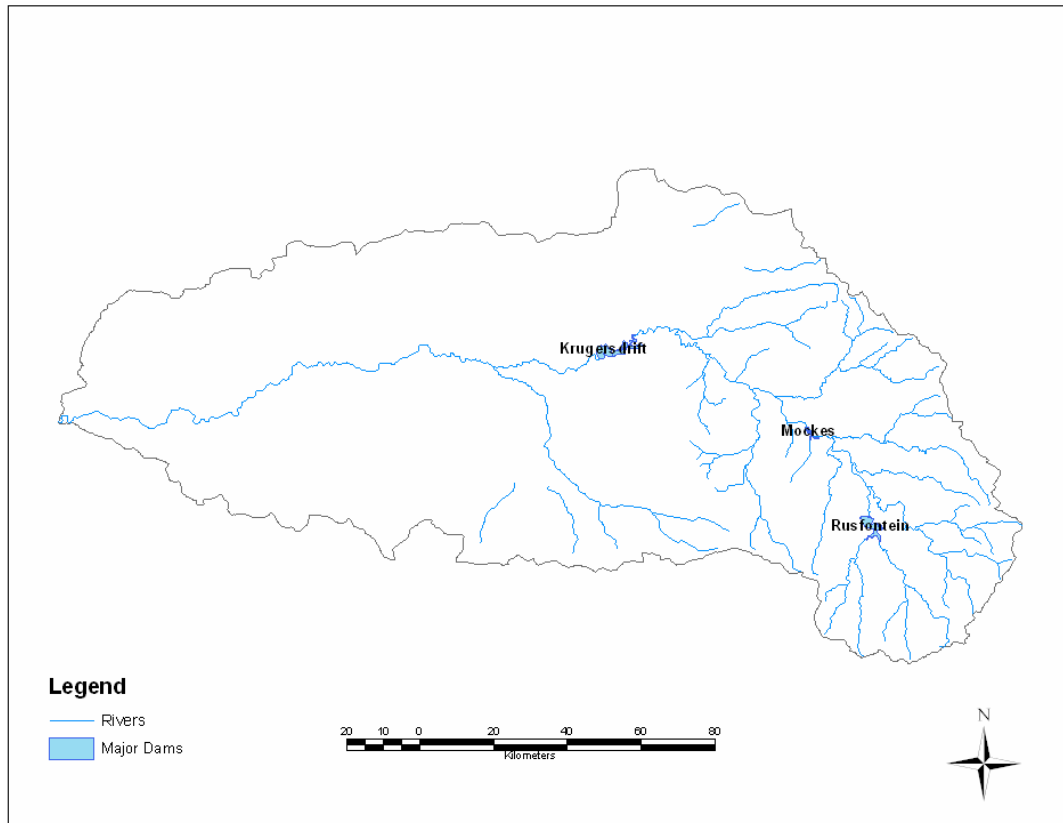


Figure 1-3: The major dams along the Modder River (DEAT, 2001).

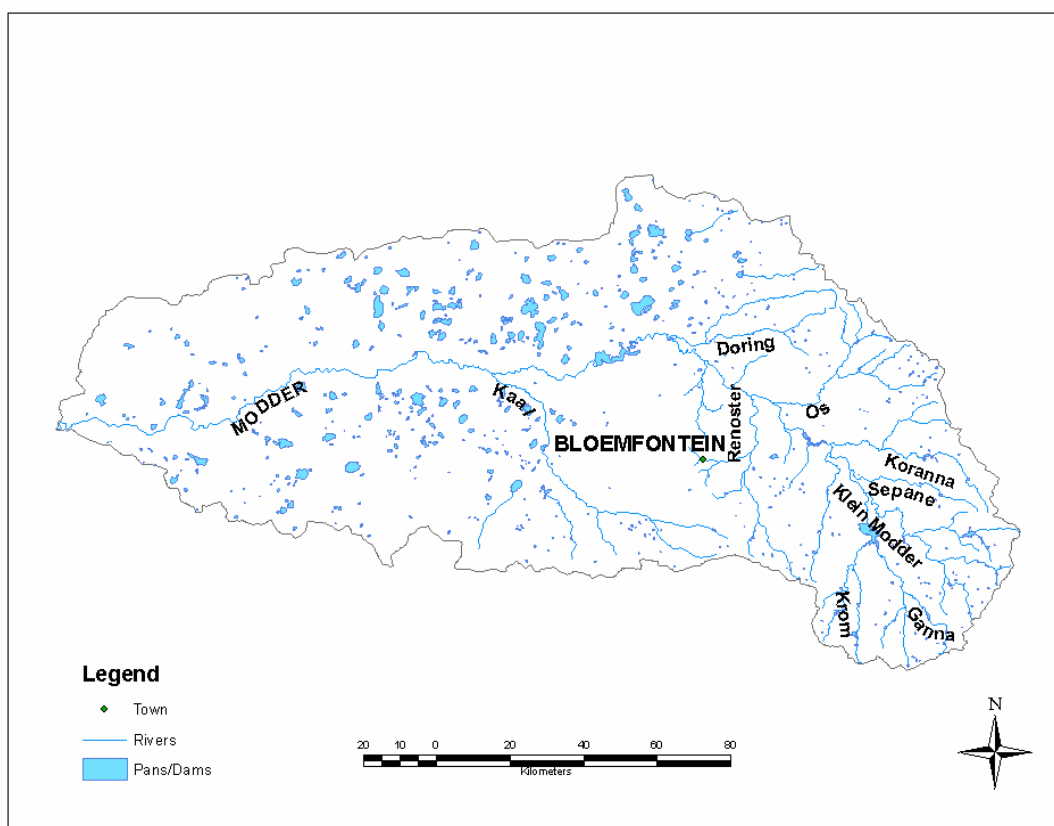


Figure 1-4: The Modder river drainage (DEAT, 2001)

Runoff in the Modder River catchment is moderate with the mean annual runoff estimated to range between 2.5mm-5mm; this is the result of the relatively flat topography (BKS, 2002). Modder River flows along the base of the upland riparian region where additional water is contributed by baseflow emerging directly from the river banks (Figure 1-5). Baseflow is defined as the water contribution into the surface water bodies from the combination of both interflow and groundwater discharges (Parsons, 2004). This seepage, only identifiable on the eastern side of the river, is located about 10m below the ground; otherwise, the river feeds its waters from the Krugersdrift Dam.

Flow of the river waters downstream of the Krugersdrift Dam is relatively minimal to almost stagnant because the river flows through an area of very low gradient. It is dammed with a broad weir some  $\pm 500\text{m}$  downstream the dam making the river stage relatively higher compared to other regions of the river (Figure 1-6). Subsequently,



the river displays more marshy and eutrophic characteristics with dead snags and fallen trees downstream of the weir (Figure 1-7).



Figure 1-5: Baseflow from the Modder river banks at the study area.



Figure 1-6: The Modder river images during dry and wet periods at the weir in the vicinity of the study site.



Figure 1-7: Modder River downstream of the weir during dry periods

### 1.2.5 Hydrogeological Setting

Groundwater plays a major role in the sustainability of the economy and represents a large potential resource for the Modder River catchment. Studies undertaken by DWAF in the Upper Orange catchment revealed that the groundwater abstraction in C52K (Figure 1-8) is estimated at 14.6 million m<sup>3</sup>/a (Darcy, 2004).

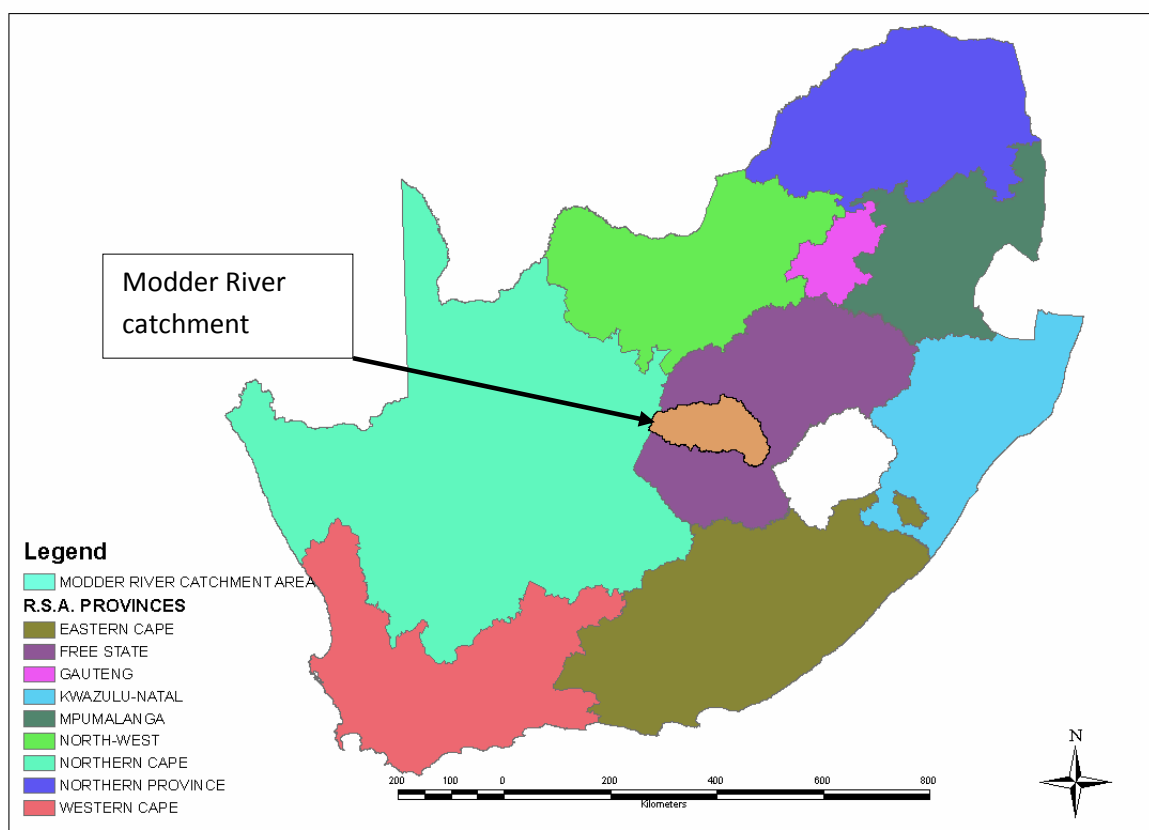


Figure 1-8: The location of the Modder River catchment.

The geological characterisation reveals that the geological stratification in the area comprises Ecca and Beaufort Group (Chapter 3) differing in groundwater occurrences. Groundwater occurrence in the Ecca Group is principally associated with dolerite contact zones, joints and bedding planes. The characterisation also reveals the availability of calcrete in the area whose high porosity can enhance recharge to the aquifer (DWA, 2004). Borehole yields in the catchment are thought to be in the range of 0.5-2.0 l/s on average although over 10% of the recorded boreholes exhibit yields exceeding 5.0 l/s (DWA, 2004). The Adelaide Subgroup of the Beaufort Group on the other hand has been extensively intruded by dolerite sills and by dolerite dykes. Groundwater in these instances occurs in joints and fractures on the contact zones, weathered dolerite zones, weathered and jointed sedimentary rocks and on bedding planes (Botha, 1998).

Groundwater is generally of acceptable quality owing to the rural nature and lack of heavy industry and mining in the area. Elevated nitrate levels have been recorded in

some boreholes, the situation mainly attributed to agricultural practices (Meyer, 2003). The groundwater in the area can be classified as Ca/Mg(HCO<sub>3</sub>)<sub>2</sub> type water (DWA, 2004).

## **1.3 Scope: Aims and objectives**

### **1.3.1 Aims/general objectives**

This dissertation aims at studying geohydrological processes with coupled flow in groundwater systems at littoral zone of the Modder River. In this thesis, all the aspects are synthesised and exemplified by incorporating a multidisciplinary perspective to develop a sound conceptual framework of the site hydrogeology.

### **1.3.2 Specific Objectives**

The set of specific objectives of the dissertation are to:

- Characterise site geology and present a comprehensive lithological conceptual model,
- Describe the chemical conditions of the water within the aquifer system in order to delineate groundwater flow systems and determine the origins and mixing relationships between different waters; and,
- Describe the physical conditions of the water within the aquifer system by applying suitable techniques in order to measure and estimate both baseflow contribution into the river system, aquifer hydraulic and transport properties for the aquifer system. This is used to develop an understanding of groundwater flow and transport capabilities

## **1.4 General study approach to meeting the objectives**

The dissertation is structured in a way that will address and answer the general objective of the study by taking into account different aspects as follows:

- Chapter one aims at establishing the aim and hence the objectives of the study by briefly looking at the background of the study.
- Chapter two sought to present the literature pertaining to aspects, concepts and techniques based on this study only.
- Chapter three is chiefly aimed at development and design of a groundwater monitoring network so as to ensure that aims and objectives of the project will be met.
- Chapter four follows with a comprehensive characterisation of site geology and soil in order to identify and model gross lithological variations. This chapter is included in the dissertation because the movement of groundwater is controlled to a large extent by both the geological and soil framework of a given area.
- Chapter five sought to characterise groundwater systems based on the analysis of the hydrogeochemical and isotopic facies,
- Chapter six then follows to calculate magnitude, direction of groundwater flow gradient as well as identifying flow section.
- Chapter seven sought to quantify physical hydraulic characteristics and transport properties for the site.
- Chapter eight integrates all the chapters and develops the refined and revised site conceptual model. After the assimilation and interpretation of the site characterisation data, a revised conceptual model that best suits the observed data or conclusions from each of the afore-mentioned chapters, a hydrogeological conceptual model for the aquifer in question is developed.

## **2 DEFINITIONS AND OVERVIEW OF ASPECTS, CONCEPTS AND TECHNICAL BACKGROUND**

### **2.1 Introduction and remarks**

Understanding of groundwater systems requires a fully fleshed description of all the properties that govern the systems. This is known as a groundwater characterisation programme. Selection of tools or methodologies together with parameters to be studied wholly depends on the goals, objectives or the scope of the study. As a result therefore, this chapter sought to present the literature pertaining to the core and basic concepts and gives an overview of the geotechnical criteria habitually used during geohydrological characterisation.

### **2.2 Bulk flow parameters**

Flow concepts frequently used in groundwater studies are referred to as hydraulic bulkflow parameters. Hydraulic bulkflow parameters are constitutive parameters used in hydrogeological studies to describe and quantify the influence of the matrix geometry to groundwater flow and storage properties of aquifers (Botha, 1998). They must be known in order to describe the hydraulic aspects of a saturated groundwater system under study. Amongst other bulkflow parameters, the following are looked at in this thesis: Darcy's velocity, seepage velocity, hydraulic conductivity, transmissivity, storativity, water level, groundwater gradient and direction of flow.

#### **2.2.1 Darcian or bulk velocity**

Laminar flow of groundwater through a granular and porous media is described by Darcy's law, stating that the volumetric rate ( $\mathbf{q}$ ) of groundwater is proportional to the hydraulic loss and inversely proportional to the length of the flow path (Walton, 1970). This relationship forms the basis from which most of the groundwater flow equations are derived and serves as the foundation of quantitative groundwater resource evaluation studies (Walton, 1970).

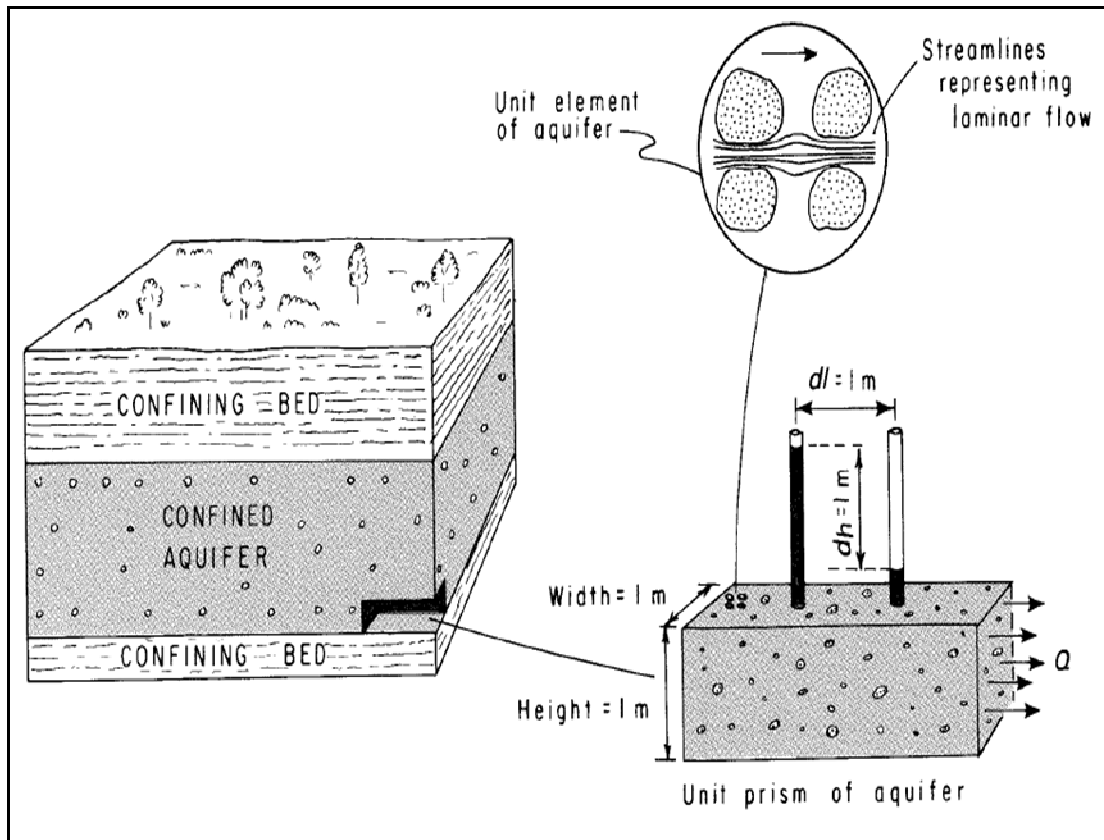


Figure 2-1: Schematic illustration of parameters in Darcy's law (Freeze and Cherry 1979).

Darcy's law is expressed mathematically as:

$$q = K \frac{dh}{dl}$$

Equation 2-1

Where:  $q$  = specific discharge, also known as the Darcy velocity or Darcy flux,

$K$  = hydraulic Conductivity hydraulic conductivity (L/T),

$D_h = h_1 - h_2$  = hydraulic head loss where  $h_1$  and  $h_2$  are the hydraulic heads measured at Points 1 and 2 respectfully; and,

$dl = L_1 - L_2$  is Length difference between points  $L_1$  and  $L_2$  (L).

The velocity, expressed in Equation 2-1, assumes macroscopic scale and that flow occurs over the entire cross section of the aquifer without regard to pore spaces. As a result therefore, the velocity is thought to be hypothetical, representing average

bulk flow velocity in the direction of the decreasing uniform head (Roscoe Moss Company, 1990).

### 2.2.2 Seepage velocity

Seepage velocity (pore or true velocity) is defined as the volumetric flow rate per unit interconnected pore space (Schwartz, 2003). Unlike bulk velocity/specific discharge, seepage velocity is a microscopic velocity associated with actual paths of individual water particles moving through the pores of the medium. In addition, specific discharge can be measured while the seepage velocity cannot be practically measured; therefore, average values are usually presented (Figure 2-2).

Pore velocities are vital in the cases of groundwater pollution and solute transport in which case the actual paths of individual water particles moving through the pores of the medium need to clearly be defined. Real velocity values are computed taking into account the effective surface, and hence effective porosity, allowing the flow.

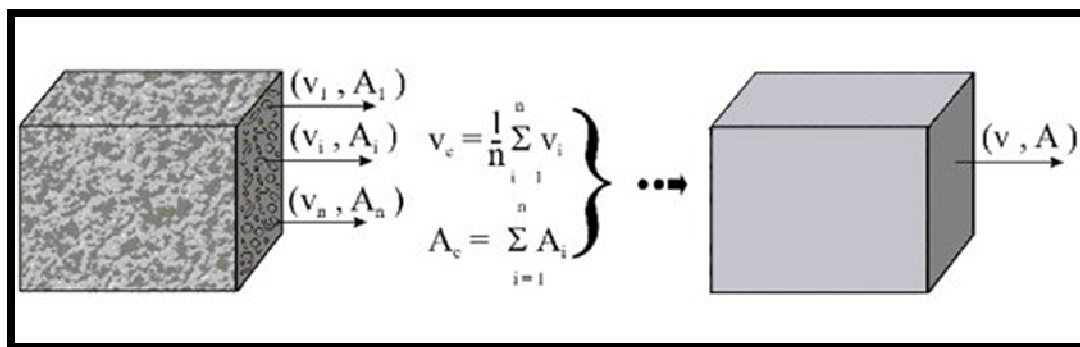


Figure 2-2: Macroscopic and Microscopic concepts of groundwater flow (Freeze and Cherry, 1979).

$$v = \frac{q}{\eta_e} = \frac{Q}{\eta_e A}$$

Equation 2-2



Where;  $v_e$  = pore or linear velocity of the flow,

$n_e$  = effective/kinematic porosity of the water-transmitting medium or porosity available for fluid flow

### 2.2.3 Hydraulic conductivity

The ease with which water flows through the saturated geological formation (aquifer) is influenced by hydraulic conductivity of the formation through which flow occurs. Hydraulic conductivity is therefore the measure of the ease with which water moves through the porous material defined herein as the rate of flow through the medium's cross-section under a unit hydraulic gradient (Institute for Groundwater Studies, 2007). It is used in Darcy's law as a constant of proportionality where it relates specific discharge to hydraulic gradient (Hem, 1970). Hydraulic conductivity differs from formation to formation where it is generally higher by several magnitudes in the fractured aquifers systems (Kruseman and de Ridder, 1994) following which are aquifer systems with high effective porosity (sands and gravels) and last are silts and clayey aquifers. Several methodologies are available for determining hydraulic conductivity both in situ and in laboratory (Figure 2-3).

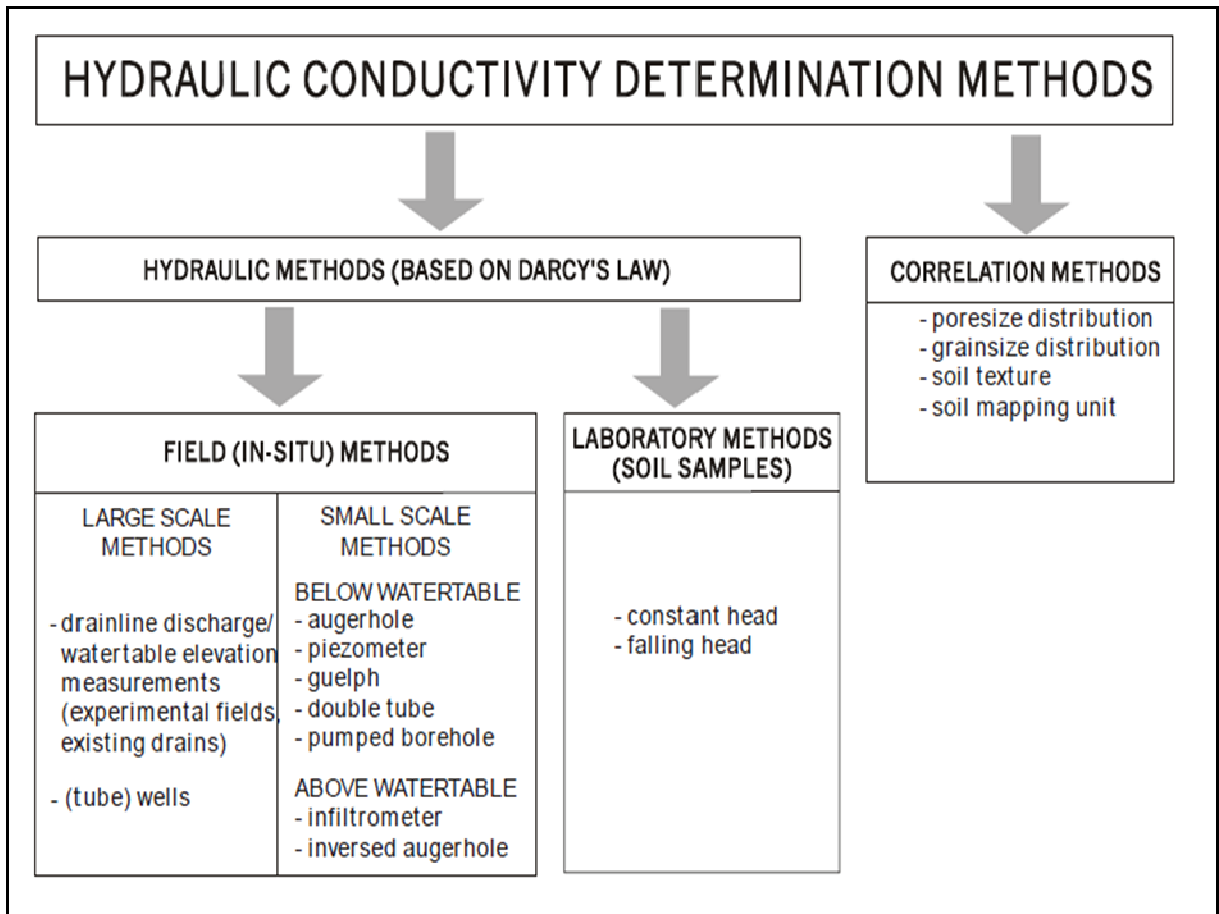


Figure 2-3: Overview of methods used to determine the hydraulic conductivity.

Hydraulic conductivity can be obtained from a plot of real groundwater velocity,  $q$ , and head gradient (Figure 2-4). Otherwise Equation 2-3 can be rearranged to estimate intrinsic conductivity. However, hydraulic conductivity depends not only on the formation type but also on the fluid properties such as viscosity and density, the incorporation of which yields the following form of Darcy's equation that can be rearranged to estimate for hydraulic conductivity.

$$q = k_i \left( \frac{\rho g}{\mu} \right)$$

Equation 2-3

Where;  $k_i$  = intrinsic or specific permeability depending on the rock properties,

$\mu$  = the fluid viscosity,

$\rho$  = fluid density; and,

$g$  = acceleration due to gravity.

Intrinsic permeability  $K_i$  is essentially a function of the diameter of the pore throats that provide interconnected flow pathways and networks through the rock; the larger the square of the mean pore diameter, the higher the intrinsic permeability. It must be noted however that intrinsic permeability is important in cases of contaminations.

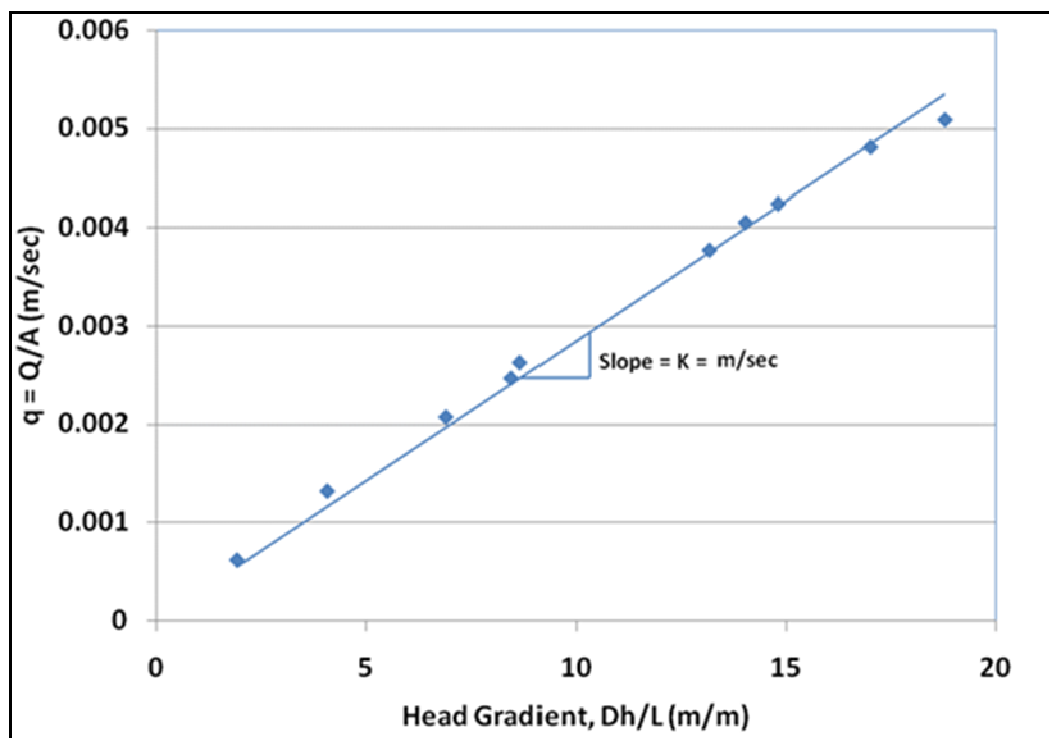


Figure 2-4: Graphical estimation of hydraulic conductivity (McKinney, 2009)

#### 2.2.4 Transmissivity

The term transmissivity defines the aquifer characteristic as the rate at which water of average kinematic viscosity is transmitted per unit width through the entire vertical strip of aquifer thickness per unit hydraulic gradient (Bear, 1979). In short, it defines

how transmissive an aquifer is in moving water through pore spaces (Roscoe Moss Company, 1990). For every aquifer type of a known thickness (b) upon which flow occurs through the entire thickness, transmissivity can be estimated from the product of the average hydraulic conductivity and the saturated thickness of the aquifer (b) (Spitz and Moreno, 1996). This is expressed mathematically as:

$$T = Kb \text{ (Confined aquifer)}$$

$$T = K\bar{D} \text{ (Unconfined aquifer)}$$

Equation 2-4

Where; T = transmissivity (L<sup>2</sup>/T)

K = Hydraulic conductivity

b = aquifer thickness in the confined aquifer (L)

$\bar{D}$  = average saturated thickness in the unconfined aquifer (L).

Darcy's equation can also be used to develop a relationship pertaining to its transmissivity (Schwartz, 2003). The relationship is expressed as thus:

$$Q = -WT \frac{dh}{dl}$$

Equation 2-5

Where; W= width of the aquifer in question

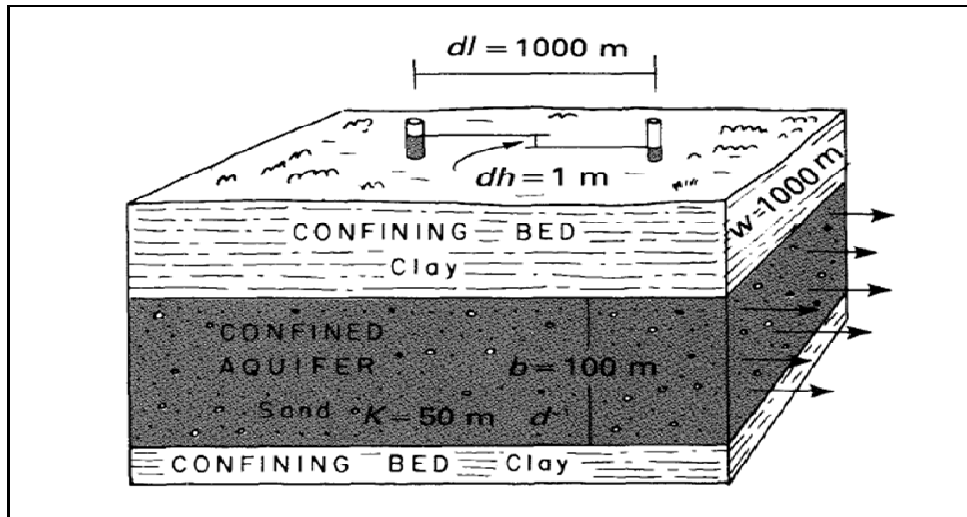


Figure 2-5: Diagrammatic aquifer model for illustrating Transmissivity concept in a confined aquifer (Heath, 1987).

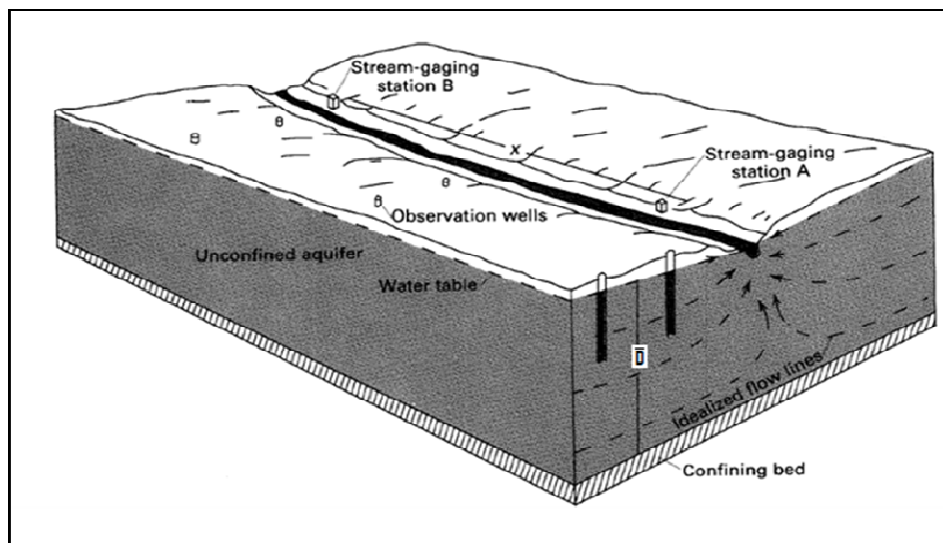


Figure 2-6: Diagrammatic aquifer model for illustrating Darcy's law and Transmissivity concept in an unconfined aquifer (Heath, 1987).

### 2.2.5 Storativity

Storativity is defined as a volume of water that a permeable unit will absorb or expel from storage per unit surface area due to the decline or increase in average hydraulic head. For a phreatic/unconfined aquifer, it is expressed mathematically as:

$$S = S_y(\eta_e) + \bar{D}S_s = S_y$$

Equation 2-6

Where;  $S_y$  = Specific yield [defined as the ratio of the volume of water that drains from a saturated aquifer owing to the attraction of gravity to the total volume of the aquifer] =  $\eta_e$  (effective porosity)

$\bar{D}$  = Average thickness (L)

$S_s$  = specific [ amount of water per unit volume of a saturated formation that is stored or expelled from storage owing to compressibility of the mineral skeleton and the pore water unit change in head].

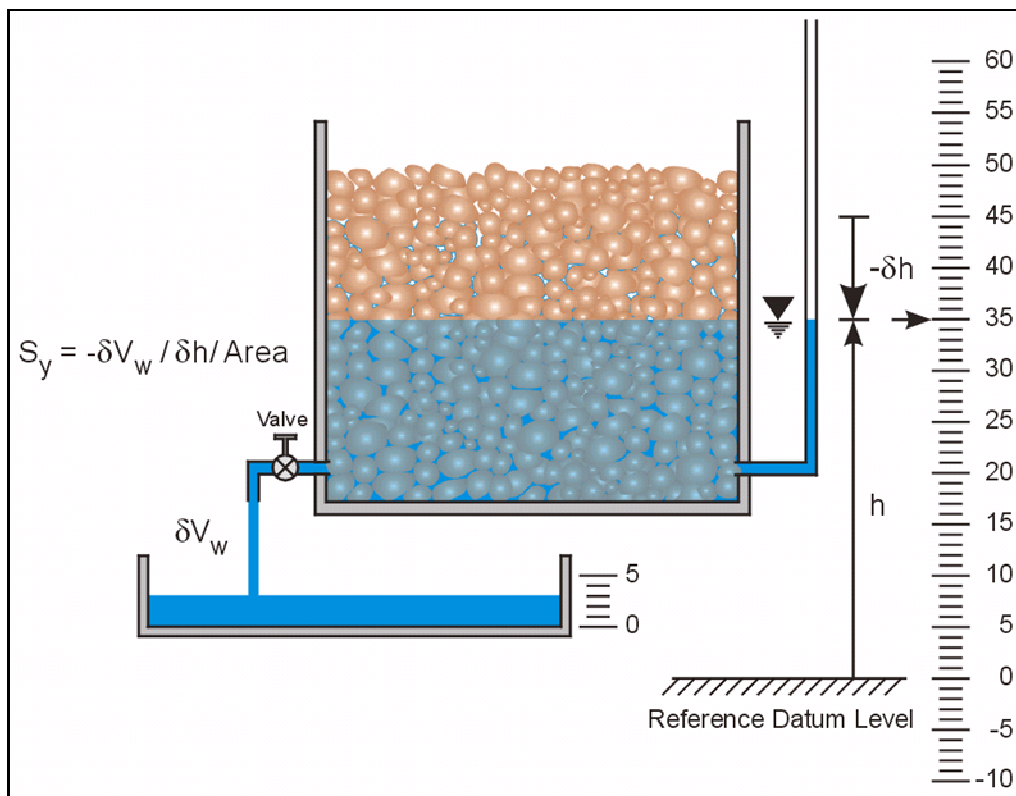


Figure 2-7: Specific yield concept for use in computing Storativity of an unconfined aquifer (Hermance, 2003).

For practical purposes, unconfined aquifer storativity equals the effective porosity (specific yield) and hence represents the drainable pore volume (Roscoe Moss Company, 1990).

For a confined aquifer, due to compressibility and elasticity of both water and the aquifer, storativity is defined as the product of saturated thickness and specific storativity expressed mathematically as:

$$S = bS_s$$

Equation 2-7

Where;  $b$  is an average thickness of the aquifer ( $L$ ).

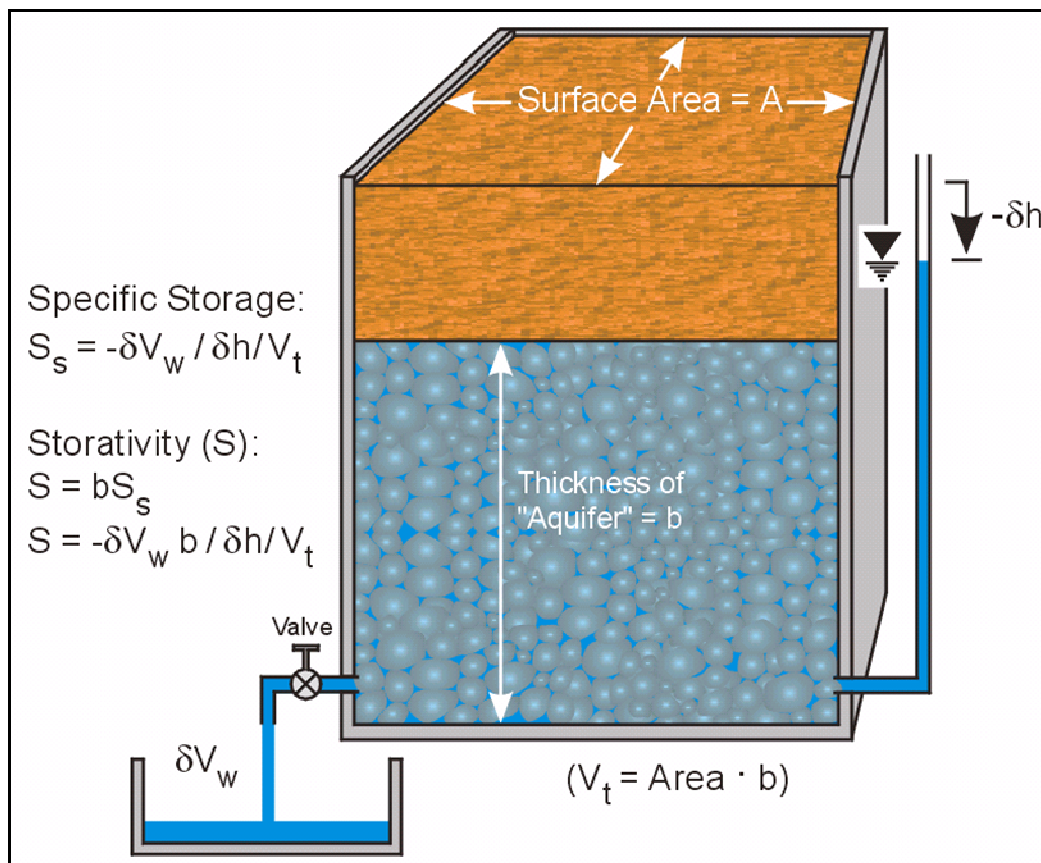


Figure 2-8: Storativity concept and illustration in a confined aquifer (Hermance, 2003).

### 2.2.6 Groundwater level, gradient and direction of flow

Water level, otherwise commonly known in the groundwater discipline as rest water level or static water level, is defined by groundwater dictionary as the natural groundwater level measured in a given well and not influenced by both artificial discharge or recharge. Hydraulic head (often simply referred to as “head”) is an indicator of the total energy available to move ground water through an aquifer. Hydraulic head is measured by the height to which a column of water will stand above a reference elevation (or “datum”), such as mean sea level (Figure 2-9) (Taylor and Alley, 2001). A water-level measurement made under static conditions, such as non-pumping, is a measurement of the hydraulic head in the aquifer at the depth of the screened or open interval of a well. In a nutshell, hydraulic heads in the aquifers are determined by the elevation of the water level in the well relative to the sea level.

Because hydraulic head represents the energy of water, ground water flows from locations of higher hydraulic head to locations of lower hydraulic head. The change in hydraulic head over a specified distance in a given direction is called the hydraulic gradient (Groundwater dictionary, IGS).

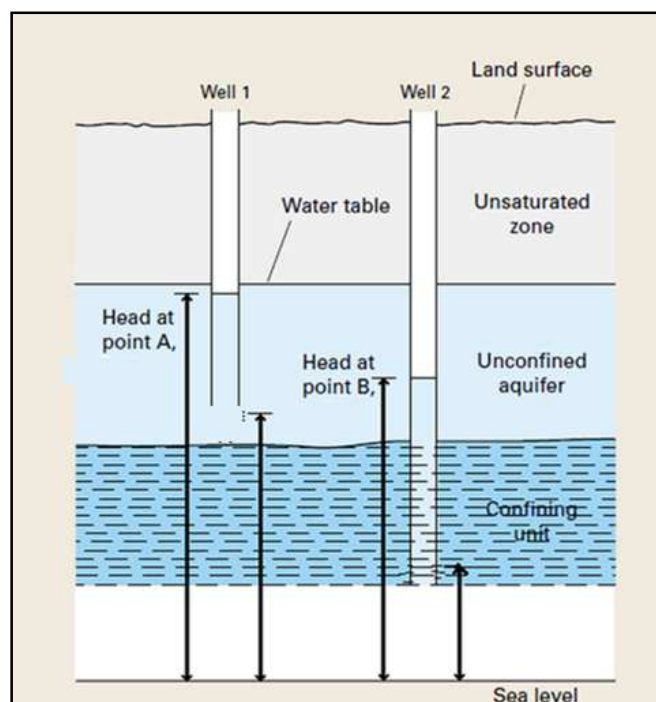


Figure 2-9: Sketch showing the relation between hydraulic heads and water levels in two observation wells—Well1.and well2 (modified from Taylor and Alley, 2001).



### 2.2.7 Soil

Soil is a loose mass of chemically and physically weathered rock fragments, sometimes mixed with organic matter and constituted by pore space (Engle *et al.*, 1991). The soil is a controlling factor in the groundwater recharge processes because it may hold the water in soil pores, release it to plant roots or the atmosphere, or allow it to pass through to the underlying groundwater body. The following physical properties of soil are observed in this dissertation:

- Texture and particle size - Texture describes coarseness of the soil; therefore, the relative proportion of sand, silt, and clay in a soil determines its texture. The coarsest soil particles are sand while clay particles are the finest with silt being the intermediate. The significance of texture in groundwater is that it influences the porosity, hydraulic conductivity as well as the chemical activity of a given soil (Troeh and Thompson, 1993). Sandy soils contain mostly large pores with little water holding capacity, and excess water through them drains easily. The combination of low chemical activity and rapid water movement through sandy soils makes them more vulnerable to leaching of contaminants than finer-textured soils. Soils which consist mostly silt or clay have more of small pores, that do not drain water readily and their small particles provide a vast surface area on which sorption can take place thereby limiting leaching of contaminants to groundwater bodies. Subsequently, the risk of groundwater contamination is much less in environments characterised by fine textured soils. (Engle *et al.*, 1991)

## 2.3 Geotechnical Criteria

The geotechnical criteria habitually used in groundwater characterisation programme are outlined in Figure 2-10. Based on the scope and/or objectives and the answers sought, some of the steps may be rendered unnecessary thereby not being used; other methods can also be borrowed. However much that might be the case, the ultimate steps engaged must answer the following basic questions of characterisation:

- Where does groundwater come from?
- Where does it go, its rate of movement and storage?
- What is the nature of the aquifer system? (Roscoe Moss Company, 1990).

The basic steps, in their chronologic order, are as follows:

- Project definitions
- Preliminary groundwater studies
- Hydrologic aspect
- Identification of uncertainties
- Adoption of geophysical methods of investigation
- Synthesis of acquired data (Roscoe Moss Company, 1990).

For a detailed explanations and descriptions of the exploration chart, step-by-step, the reader is referred to Roscoe Moss Company (1990).

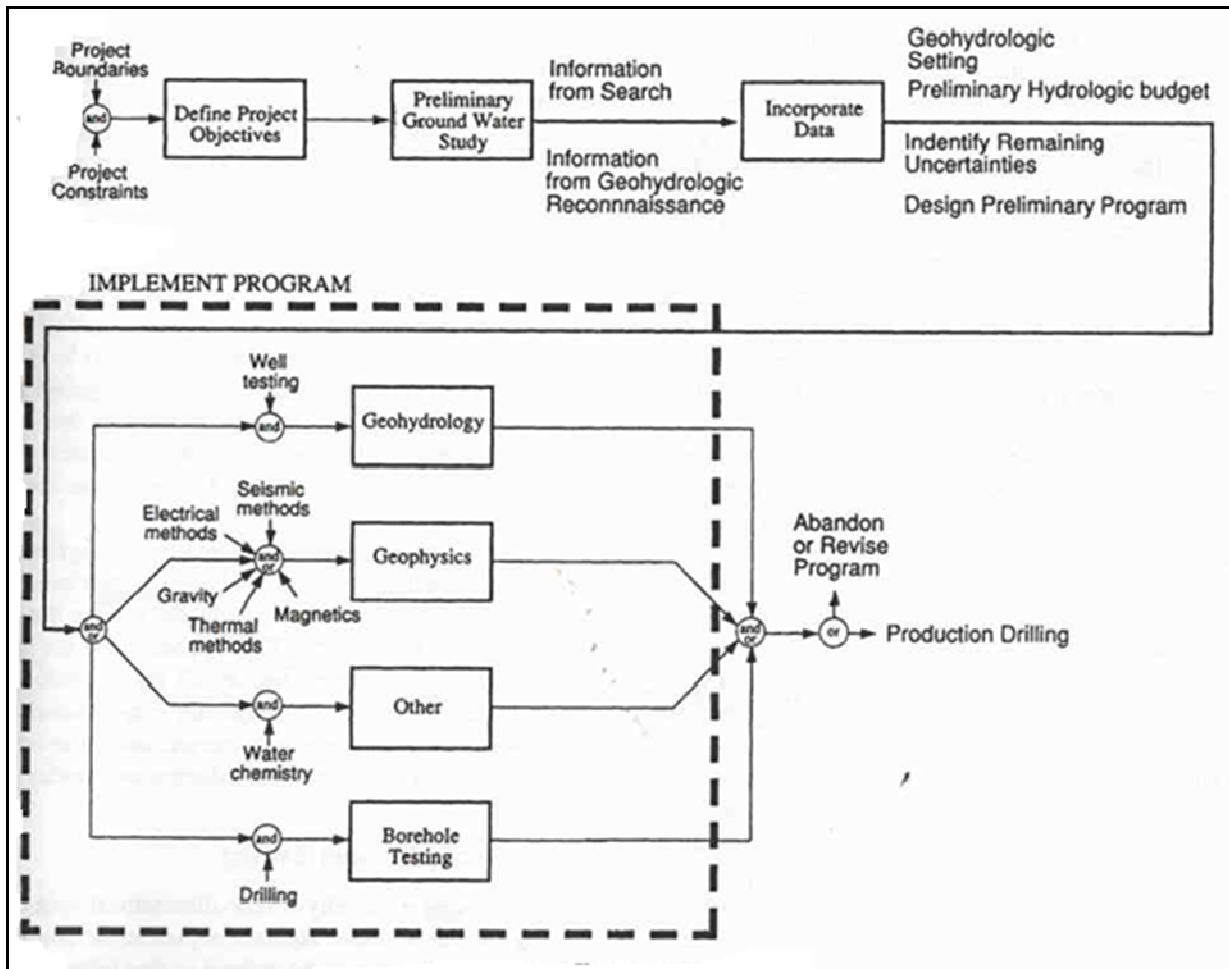


Figure 2-10: Groundwater exploration chart (technical framework) for characterisation programme (Roscoe Moss Company, 1990).

## 2.4 Conclusion

It is important to note that the material presented here is only intended to introduce and define the concepts in order to provide an indication of their significance in groundwater characterisation and is not intended to present detailed descriptions. The following chapters will execute some of the geotechnical criterions in order to characterise the defined concepts.

## **3 WELLFIELD OR NETWORK DESIGN**

### **3.1 Introduction**

The development and design of a groundwater monitoring network was based on the technical level objective: to estimate state variables with acceptable accuracy levels. Based on this objective, a dense local and pilot network was developed. Dense local and pilot networks are usually developed to serve specific purposes and their configuration depends largely on the subject studied, and the answers sought (Jousma and Roelofsen, 2004). The final product of a design is a plan showing the arrangement, spacing of wells and specifications containing details on well construction and completion, including information on well diameter, depth, and position of screens or open hole, the type of casing and screens.

### **3.2 Borehole configurations**

The study was conducted on the farm owned by Mr Charl Yssel [CYS1 (BH1, BH2, BH3, BH4, BH5 and BH 6)] cluster of CYS wellfield at the Modder river project site. Thirty five boreholes were drilled over the entire project site from which a 6-spot pattern well array or pilot network was selected to answering the aim of this particular study (The other boreholes were used by two PhD students and another MSc student for the same study). The study site, comprising two triangulated arrays, approximately measures ~237m × 200m over which the six boreholes of varying depths below ground surface were selected. Two triangulated array was chosen by the author to aid in establishment of the groundwater flow fields/directions also to ensure that all the lithological units would be intercepted. Figure 3-1 shows the location of the boreholes at the entire project site with the zoomed insert map of those in the study site. Boreholes CYS1BH4, CYS1BH5 and CYS1BH6 are widely spaced from each others and therefore make their own bigger triangle whilst CYS1BH1, CYS1BH2 and CYS1BH3 too make their own small triangle. The elevation contour map shows CYS1BH6 as being located at the highest elevation followed by CYS1BH4 and CYS1BH5 which are more or less on the same elevation. The elevation dip towards CYS1BH3 and further down to CYS1BH1 and CYS1BH2 which are almost at the same elevation (Figure 3-2).

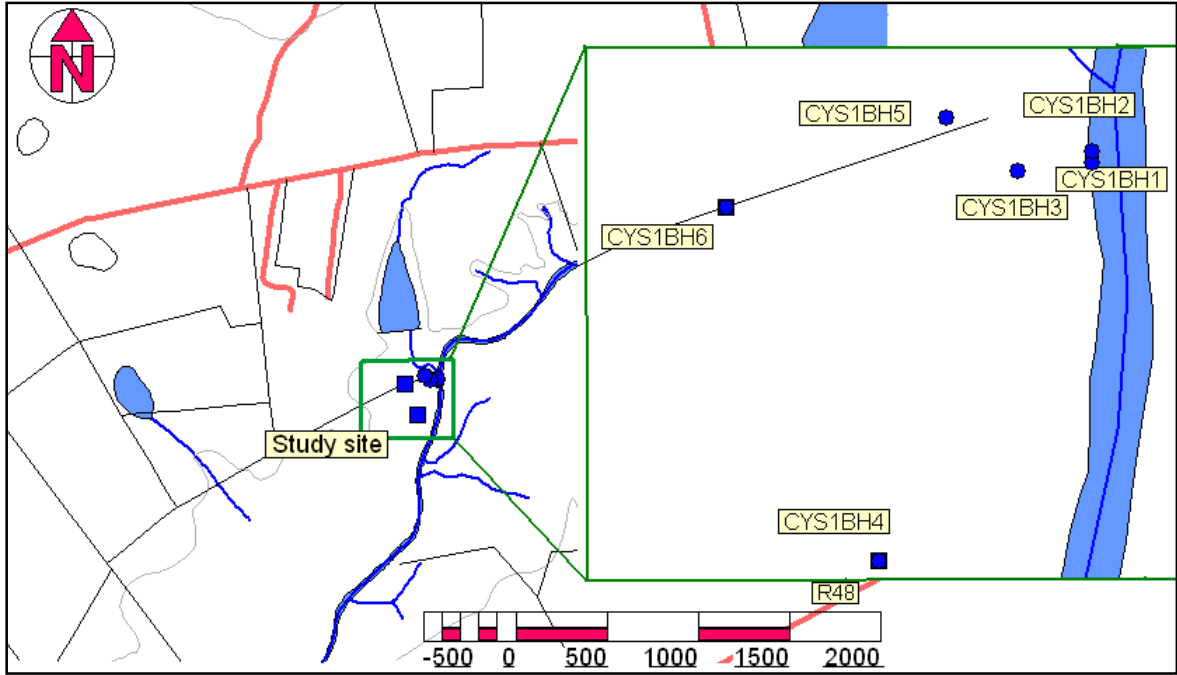


Figure 3-1: The pilot network for groundwater characterisation in the project site and the insert map for the wells in the study site.

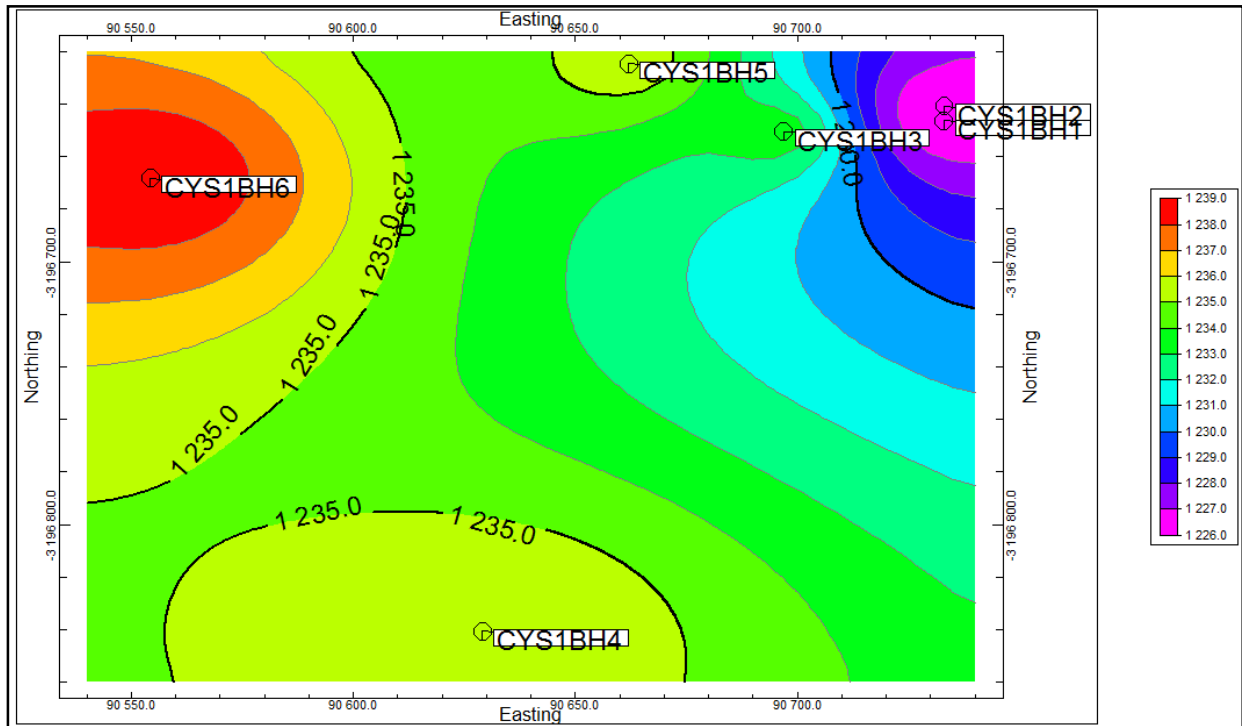


Figure 3-2: Elevation contour map at the study area.

### 3.3 Well construction and completion

Following borehole drilling completion, sediments from the drilling operation are usually not mobilised from the borehole and may alter the confidence level of obtaining both water quality and aquifer properties results accurately. As a result therefore, borehole development was a must do for all instances and purposes of this dissertation.

The general objectives of the well design and development in the project area were to:

- Enhance confidence level required to experiment for aquifer characteristics,
- Enable for aquifer representative water samples for chemical characterisation and hence,
- Ensure no surface contamination and recharge from the near-surface water recharging through the annular of the wells and the casing and so is directly through the well opening itself. This might introduce biasness and distortion of hydrogeochemical data acquired from such a borehole.
- Properly settle the gravel pack around the well screen.
- Minimize the development of drilling-induced low  $K$  zone (Skin effect) around each well.

#### 3.3.1 CYS1BH1

CYS1BH1 was constructed in a partial gravel envelope type fashion. This well was approximately 12mbgl deep and double cased with the stainless steel casing. The casing was vertically machine-slotted. The major disadvantage of this type of screening includes clogging due to parallel surfaces within the opening (Roscoe Moss Company, 1990). To account for that however, the borehole was partially gravel packed with 1.2-2.4mm dry graded silica sand to 3mbgl. A highly impermeable and powdered bentonite clay seal was added above the top filter pack to about 2.5mbgl to ensure that no water or contamination can enter the annulus from the surface. The well construction was eventually completed by setting a pump house casing in a cement grouted seal and the collar was capped with a lockable steel cap.

### 3.3.2 CYS1BH2

The 12mbgl deep CYS1BH2 was constructed in a partial gravel envelope type fashion as well. It was double cased inside by a 0.22m diameter protective casing and on the inside by a 0.12m casing. Both casings were stainless still and machine-slotted screened. The inside casing was wrapped with a fine mesh (bedim) (Figure 3-3). The borehole was partially gravel packed with 1.2-2.4mm dry graded silica sand (gravel pack) to 2.5mbgl.



Figure 3-3: Inside casing wrapped with a fine mesh (bedim).

### 3.3.3 CYS1BH3, CYS1BH4, CYS1BH5 and CYS1BH6

CYS1BH3 was drilled to an 18mbgl depth. CYS1BH4, CYS1BH5 were drilled to the depths of 30mbgl whereas CYS1BH6 was drilled to a 24mbgl depth. The construction for CYS1BH3 was all the same as in CYS1BH1 with dimensions and casing screening being the only differences. The casing for CYS1BH3 has solid sections alternating with screened sections. CYS1BH4, CYS1BH5 were gravel packed with 4-9mm dry graded silica sand to 3mbgl depth and double cased

followed by bentonite seal as in other wells. CYS1BH6 was solid cased to 8mbgl and not cased from 8mbgl to 22mbgl.

The well construction was eventually completed by setting a pump housing casings in the grouted cement seal and the collars were capped with lockable steel caps. The elevated flush mount concrete pad was developed around all the boreholes to prevent the vertical well from acting as a conduit for downward migration of surface contamination and water.

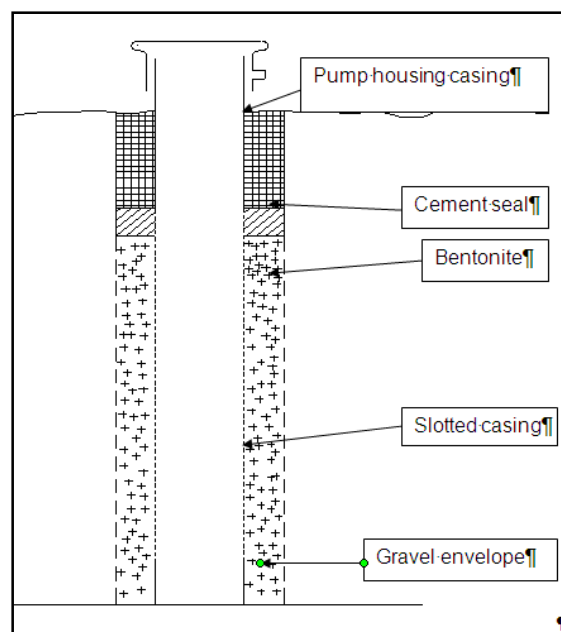


Figure 3-4: CYS1BH1 construction counterfeiting gravel envelope well and the borehole cap.

All the wells were drilled to different depths so that lithological conceptualisation, such as the geometry of different lithological units, would be approximated with minimal error. In addition, the idea was to intercept different lithological units in order to infer hydrogeology based on different units intercepted for a well refined hydrogeological conceptual model.



### 3.4 Borehole development

Shortly after the installation, all of the wells were developed until the discharge water was sediment free. The development is an integral phase of well construction and was executed using backwashing development technique that involved blowing high pressure air from the compressor to blow out the slurry up to the surface until almost clean water with little slurry was blown out of the borehole. Because of the high load of fine soil particles, rotafoam was put into the boreholes to increase the density of backwashing fluid thereby aiding in blowing as much of the sediments out. A well was determined developed by performing the settleable solids test that measures the volume of solids in one litre of sample that settles to the bottom of an Imhoff cone (Figure 3-5). If the sediments for a particular well settling in the cone reached 7ml or below, the borehole was deemed clean and the development would be ceased thereupon otherwise the blowing would be continued.



Figure 3-5: Borehole backwashing development with the aid of the rotafoam and the settleable solids test using Imhoff cone.

### 3.5 Conclusion

Hydraulic characterisation of the near aquifer system was achieved by acquiring data from a 6-spot pattern well network.

Boreholes were constructed in a partial gravel envelope type fashion to meet stipulated projects' objectives with each borehole constructed according to the encountered subsurface strata while maintaining uniformity in general construction methodology. All the wells were developed until the discharge water was essentially sediment free. With the adopted network, construction and development of the boreholes, the author strongly believes that the hydrogeological results obtained from these wells will be something to rely on in understanding the aquifer system under study and so is for future references.

## **4 PHYSICAL AND GEOMETRICAL CONFIGURATION OF THE AQUIFER SYSTEM**

### **4.1 Introduction**

Flowing groundwater is both a geologic and soil agent because geological and soil frameworks are important as they dictate and serve as a preferential groundwater flow path in the groundwater flow fields/systems. Subsequently, geological and soil frameworks for the groundwater flow system are considered the first step towards further chapters in this thesis. The primary objective of the geological and soil characterisation in this thesis is therefore to present a comprehensive lithological and soil framework for the site.

The data from previous works and that collected during drilling and soil sampling is reviewed, analysed, interpreted and correlated to obtain an understanding of the physical configuration of the aquifer system in the study site.

This chapter is therefore divided into two parts: part one focuses on the hydrogeological characteristics of the soil while part two focuses on the geologic features, both stratigraphic and structural elements, to define geometry and type of lithological units.

### **4.2 Soil analysis**

An integral part in groundwater resource management entails the assessment of groundwater recharge aspects which is unfortunately yet to be thoroughly understood mainly because recharge processes happen in the vadose zone. The vadose zone is unfortunately largely neglected by hydrogeologists (Vermaak and van Schalkwyk, 2000). Vermaak and van Schalkwyk (2000) conclude that the lack of knowledge and information about the vadose zone makes the accuracy of recharge assessments difficult to deal with. Subsequently, this section sought to describe two principal hydrogeological properties of the soil in the study area which may impact on groundwater recharge and contamination hereupon.

#### 4.2.1 Hydrogeological properties of the soil

The soil samples were collected from the test site in a way that all the samples would be homogenised composite samples (Figure 4-1). The sampled spots or test holes were randomly selected. The one metre holes were drilled with a hand rotary auger (Figure 4-3) to ensure minimal disturbance of the surrounding soil. Five soil samples were collected in the process, packed in plastic bags and submitted to the Institute for Groundwater studies laboratory to be analysed for soil type (texture).

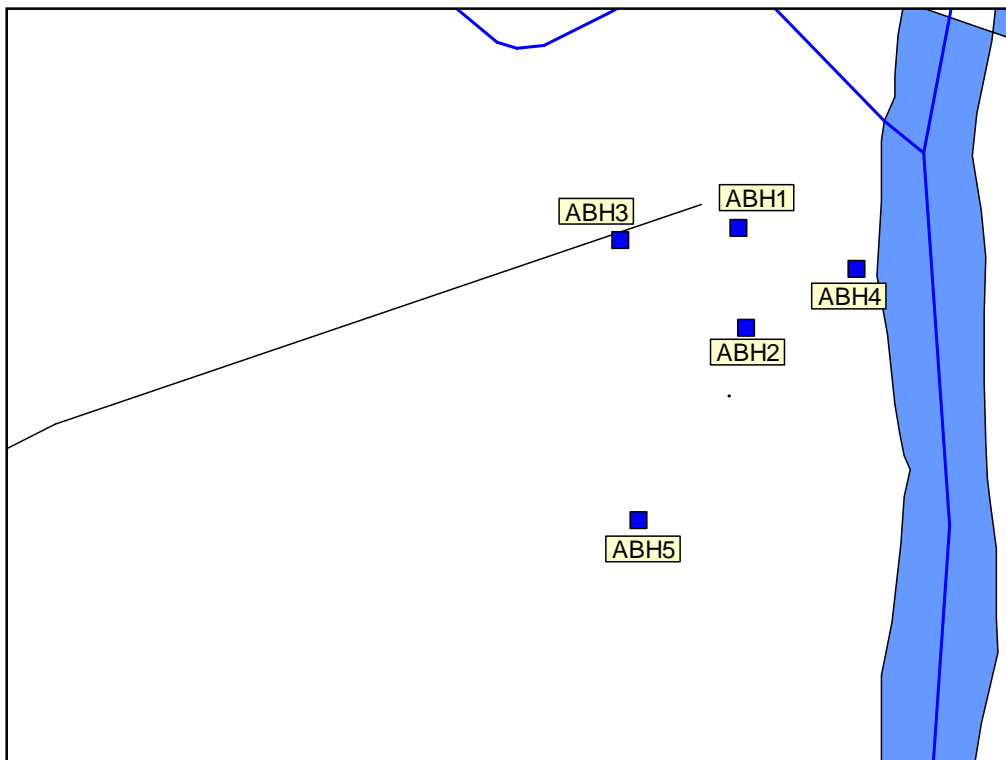


Figure 4-1: Figure showing the position and configuration of soil sampling (ABH: Augured Borehole).

#### 4.2.2 Soil index properties

##### 4.2.2.1 Soil Type

Soil type (texture) refers to the percentage of sand, silt and clay particles in the soil. Texture or textural class is often used for the correlation of K-values with other hydraulic properties of the soil such as water-holding capacity, drainable pore space and many more (Hillel, 1980). Grain size analysis of the samples was conducted

using the Bouyoucos hydrometer method otherwise known as the Rapid method. This method determines the particle size distribution of a non-destructed soil sample suspension which undergoes settling. The steps, whose procedural details can be found in the ANNEXE A, followed when undertaking this test are stipulated below:

1. Dispersion of the soil sample:
2. Separation of sand fraction:
3. Determination of clay:
4. Determination of silt.

The results of this test are summarised in Table 4-1. The soil at the study area comprises mainly fine sands constituting 75%< X>80% of the total mass of the collected soil sample. Clay constitutes 10%< X>20% while silt takes 5%< X>10% of the total soil samples collected. Both silt and clay make up 20%< X>25% (Figure 4-2). From these results, it can be seen that the overburden alluvial deposit for the study area consists largely of fine sand.

TABLE 4-1: SOIL TEXTURAL ANALYSIS FROM IGS LAB.

Client: Teboho Shakhane				Date: 14-Dec-10			
Sample nr.	Lab. nr.	4 min.	6 hour	Clay (%)	Silt (%)	Clay+Silt (%)	Fine Sand (%)
Cys1	ABH1	18	9.5	19	17	36	64
Cys1	ABH2	10	7.0	14	6	20	80
Cys1	ABH3	9	6.5	13	5	18	82
Cys1	ABH4	10	6.0	12	8	20	80
Cys2	ABH5	10	6.0	12	8	20	80

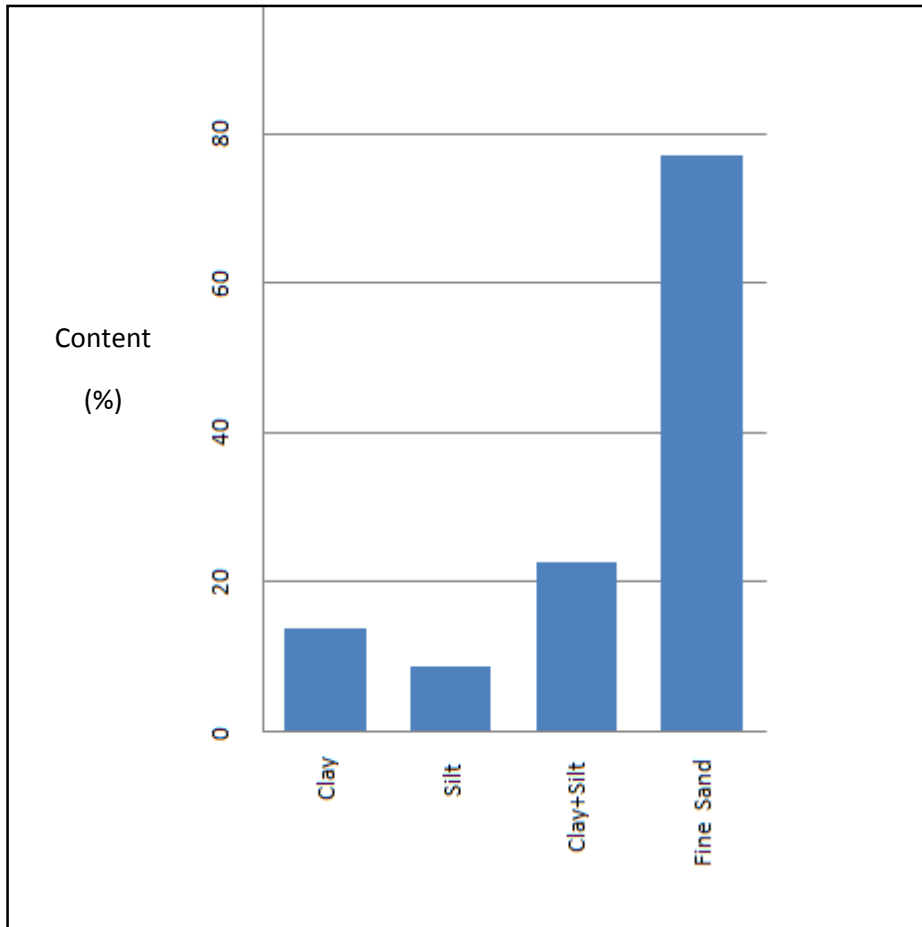


Figure 4-2: Soil grain composition.

#### 4.2.3 Hydraulic conductivity

The hydraulic conductivity ( $K$ ) of the soil is one of the most important soil properties controlling many hydrological processes. This property depends on soil texture, particle arrangement and structure and can vary in space, time and flow direction (Bagarello and Provenzano, 1996). Different soils with particular textural classes have different  $K$ - values although it is advisable to handle and treat these values with ultimate care because soils with identical texture may have quite different  $K$ -values due to differences in structure. For example, some heavy clay soils have well-developed structures and much higher  $K$ -values than those indicated in the Table 4-2 (Smedema and Rycroft, 1983).

In groundwater surface water interaction studies,  $K$  is an important parameter to estimate in order to quantify the magnitude and spatial distribution of

groundwater/surface water interaction. Because fine sands, silts and clays are often deposited on floodplains, these floodplains can have lower K values thereby restricting groundwater/surface water influxes (Rosenshen 1998; Larkin and Sharp 1992; Conrad and Beljin, 1996).

TABLE 4-2: RANGE OF K-VALUES BY SOIL TEXTURE (Smedema and Rycroft, 1983)

Texture	K (m/day)
Gravelly coarse sand	10-50
Medium sand	1-5
Sandy loam, fine sand	1-3
Loam, well structured clay loam and clay	0.5-2
Very fine sandy loam	0.2-0.5
Poorly structured clay loam and clay	0.002-0.2
Dense clay (no cracks, no pores)	≤0.002

#### 4.2.3.1 *In-situ methodology*

The in-situ physical test to determine the hydraulic conductivity of the soils was undertaken by small-scale inverted auger-hole method. Numerous small-scale in-situ methods for the determination of K-values do exist. These methods are characterised into two groups: determine K above and below the water table. (Bouwer and Jackson, 1974).

In this project however, the former method was used. Since the soil is not saturated above the water table in this technique, one must therefore apply sufficient water to obtain near-saturated conditions in order to measure the saturated hydraulic conductivity. Each hole was therefore pre-soaked several times, until the soil below

and around the hole was practically saturated. The saturation was performed by pumping water from the nearby boreholes at a very low rate in to the test holes.



Figure 4-3: Auguring of the holes on which infiltration test was executed.

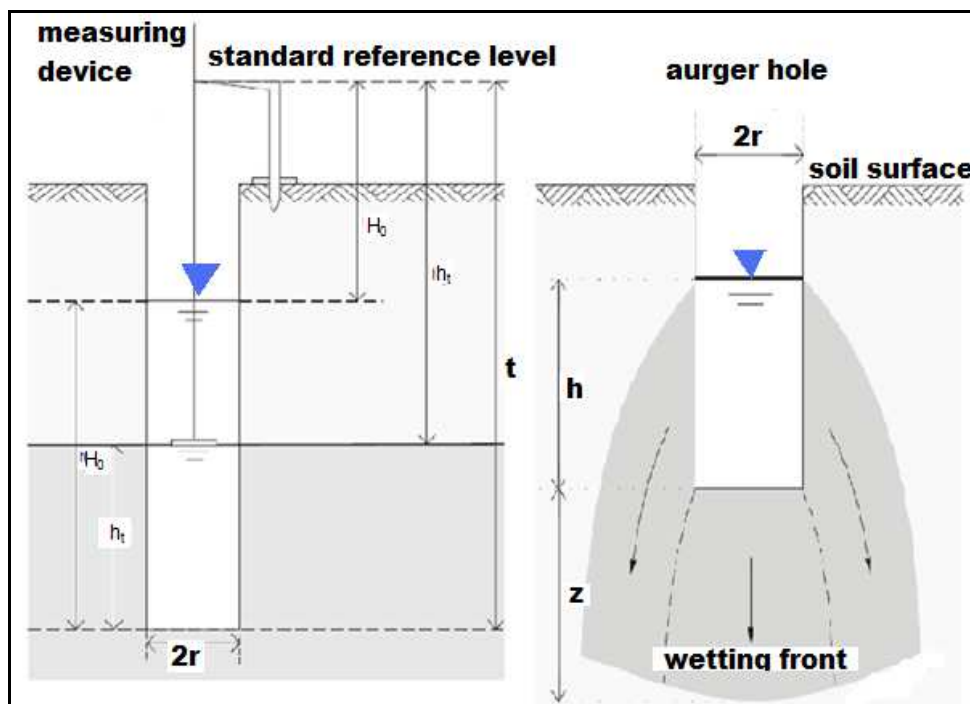


Figure 4-4: Conceptual diagram of an inversed auger-hole method illustrating the infiltration from a water-filled auger-hole into the soil and relevant measurements (modified from: Oosterbaan and Nijland, 1994).



Infiltration methods can further be divided into steady-state and transient methods and the latter were employed because it avoids the difficulty of ensuring steady-state conditions. The transient methods are based on adding the slug of water and observing the rate of head change with respect to time.

Following the saturation processes, the water was re-filled into each hole until the head reached the targeted displacement,  $H_0$  (30cm) to ensure that top soil was not going to be incorporated as it could distort the true K-values. The head loss was induced while the displacement,  $h_t$ , were recorded. The data ( $h + \frac{1}{2}r$  and  $t$ ) were then plotted on a log plot and the graph was ideally supposed to yield a straight line. When the line curved, the soil would continue to be wetted until the graph showed almost a linear trend (Figure 4-5). The straight line would imply that almost full saturation conditions have been reached (Oosterbaan and Nijland, 1994). The hydraulic conductivity of the soil was then calculated from the following formula:

$$K = 1.15r \frac{\log\left(h_0 + \frac{1}{2}r\right) - \log\left(h_t + \frac{1}{2}r\right)}{t - t_0}$$

Equation 4-1 (Oosterbaan and Nijland, 1994)

Where;  $r$  = radius of the whole

$h_0$  = Initial head (m) at the time  $t_0$  (min)

$h_t$  = final head (m) at time  $t$  (min)

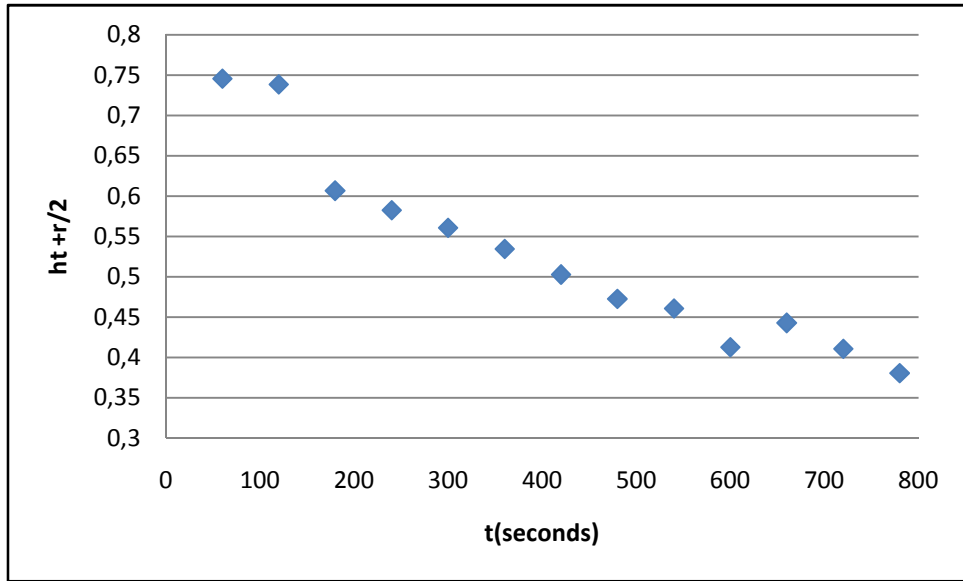


Figure 4-5: Fall of the water level plotted against time

TABLE 4-3: INFILTRATION TEST RESULTS FROM CYS1\_ABH1 (r=0.105m, D'=0.7m)

t(sec)	WL(m)	Ht=D' – WL	$H_0 + \frac{1}{2}r$
0	0.3	0.7	0.7525
60	0.307	0.693	0.7455
120	0.314	0.686	0.7385
180	0.446	0.554	0.6065
240	0.47	0.53	0.5825
300	0.492	0.508	0.5605
360	0.518	0.482	0.5345
420	0.55	0.45	0.5025
480	0.58	0.42	0.4725
540	0.592	0.408	0.4605
600	0.64	0.36	0.4125
660	0.61	0.39	0.4425
720	0.642	0.358	0.4105
780	0.672	0.328	0.3805

$$T_0=60, H_0+1/2r = 0.7455, \text{Log} (H_0+1/2r) = -0.12755$$

$$t_t= 780, H_0+1/2r = 0.3805, \text{Log} (H_t+1/2r) = -0.41965$$

$$K = 1.15 \times 0.105 \frac{-0.127552352 + 0.419655339}{(780 - 60)}$$

$$= \underline{4.90E-05\text{m/s}} = \underline{4.23\text{m/d}}$$

TABLE 4-4: COMPUTED K VALUES FOR EACH OF THE TESTED HOLES

BH	K (m/d)
CYS1ABH1	4.23
CYS1ABH2	2.27
CYS1ABH3	1.85
CYS1ABH4	3.13
CYS1ABH5	1.99
Harmonic mean K	2.42

### 4.3 Geology

Integrating geological concepts, such as relative positions and proportions of the different lithofacies is of paramount importance in order to render a realistic geological conceptual model. The geological model allows the commencement of the understanding of the conceptualisation of the groundwater flow paths in a system and the definition of the aquifer units. Without proper geological interpretation, hydrogeological interpretation is otherwise extremely questionable (Lloyd, 2006). The description of the geology for the area is primarily based on the published reports, which is augmented by geological logs of the newly drilled boreholes. Because geologic conditions govern the hydrogeologic regime, geologic conditions were investigated and recorded. The ultimate knowledge was used to establish the proper logistical configuration of the aquifer system at the site.

#### 4.3.1 Regional Lithostratigraphy

The regional geological setting of the study area consists mainly of rocks of the Karoo Sequence comprising the following lithostratigraphic units and dichotomy: Ecca and Beaufort Groups of Mesozoic-Paleozoic stratigraphic sequence (Figure

4-6). These beds are predominantly carbonaceous shale, mudstone, siltstone and fine-grained sandstone sediments from the Adelaide Subgroup (Hogan, 2008).

Beds of Beaufort group underlie the greater part of the Karoo region covering the central region. It consists principally of alteration of the intercalated arenaceous sandstones and argillaceous mudstones (grey to reddish and red to purple mudstone) strata (Tshokeli, 2005). In general, Beaufort lithofacies are related to the deposition of sediments.

The Ecca Group comprises of thick succession of carbonaceous shale (dark bluish-green to grey massive shale, olive-green micaceous shale/mudstone, and light green to greenish-grey shale), mudstone, siltstone and fine-grained sandstone. The calcrete deposits, occurring widely distributed in the study area, are also identifiable from the surface over a wide range (Figure 4-6). The area is interspersed in places with sills that intruded the Karoo Super Group during the Mesozoic Era (Midgley *et al.*, 1994) (Figure 4-6).

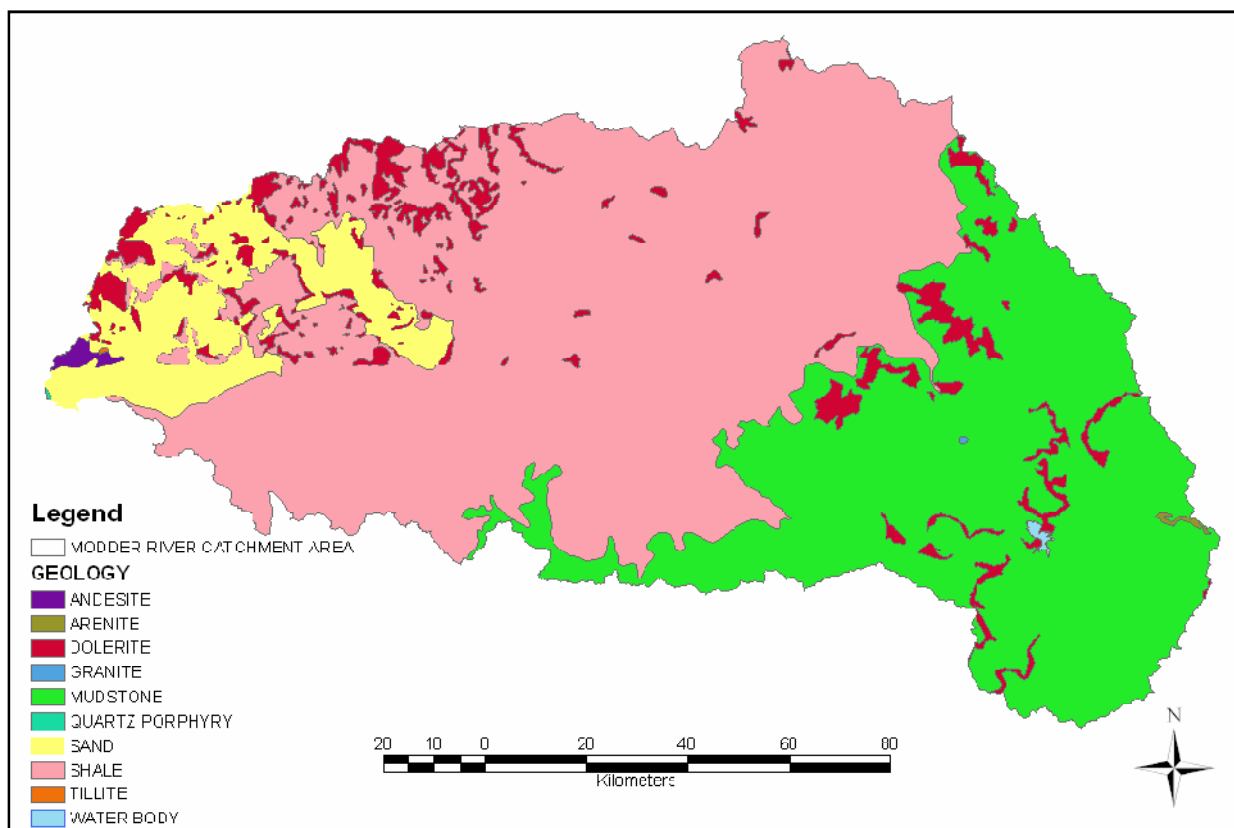


Figure 4-6: Lithostratigraphy of the Modder River Catchment (DEAT, 2001).



Figure 4-7: Calcrete deposits (left) as recognised from the surface and dolerite rocks (right) of the dyke located near the study site.

### 4.3.2 Site geology

#### 4.3.2.1 Drilling efforts

Lithostratigraphic data was acquired during drilling. The objective was to drill boreholes from which long term monitoring would be done. Subsequently, the borehole drilling programme at the site needed to fulfil a number of rigorous criteria namely:

- The recovery of depth representative rock samples to describe the aquifer lithology and nature of variation with depth,
- Minimise disturbance to the borehole wall and maintaining borehole stability in to allow in-situ tests; and,
- Hydro-geochemical and isototope sampling for subsequent hydraulic characterisation.

Previous works in most parts of the Karoo based geology indicates that drilling using cable-tool percussion techniques are suitable to satisfy the afore-mentioned criteria. This drilling method, best suited for moderate to hard rock, was used to drill all 35 boreholes on the site. The method, powered by compressed air, involves the use of percussion by repeatedly lifting and dropping a heavy string of drilling bit suspended

on a steel cable from a truck-mounted rig into a borehole to chop the lithological material. The material is pulverized at the bottom of the borehole forming slurry which is then removed up the borehole by air pressure. Steel casing is often used to keep the borehole open during drilling in unstable materials. The advantage of this drilling technique is that: 1) it is suitable for a wide variety of rocks; 2) it is possible to drill to considerable depths; 3) no water is required and relatively inexpensive. During drilling, the following main drawbacks were identified: 1) the boundaries between geological layers cannot be precisely located; 2) slow penetration rates especially in hard rocks and clays (under 250psi or 18bar air pressure, penetration rates ranged between 0.08m/s and 0.5m/s); 3) problems can occur with unstable rock formations.



Figure 4-8: Cable tool method and cable tool rig (insert) used for drilling at the study site.

#### 4.3.2.1.1 Lithologic borehole logs

The lithostratigraphic units recognised at the site, their thickness and gross lithology, were depicted and presented in columnar sections based on the six selected boreholes (Figure 4-12). The analysis of the lithological logs has allowed detailed elaboration of the lithological set-up for the study site (Figure 4-11).

From the geological logs of CYS1BH1, two units were intercepted. The upper unit, 11 metres thick, is constituted by single grained and very fine sand matrix plus minor amounts of clayey and silty levels. This lithotype is underlain by the gravely strata one metre thick (11m-12m). CYS1BH2 on the other hand penetrates only one unit. This unit comprises brown and very fine matrix of 12 metres (0-12m).

CYS1BH3 and CYS1BH4 display two units. The first unit comprises a single grained and very fine sand matrix plus minor amounts of clayey and silty levels identical with those in CYS1BH1 and CYS1BH2 respectively. Lying below is the unit represented by sand and gravel succession with very small to medium sized pebbles and cobble (Figure 4-9).

Borehole CYS1BH5 exhibits three units. The first two units of CYS1BH5 are identical to that of CYS1BH3 and CYS1BH4. Below the first unit lies a highly impermeable and massive mudstone that forms the base for the Modder River (Figure 4-10). Johanson *et al.*, (1996) ascribe the existence of mudstone floor in the river environments to the fact that the river might have been typical of rivers in the Beaufort formations where rivers were mostly of high-sinuosity type with extensive floodplain muds predominating over lenticular channel sands. This mudstone is concluded to be a confining aquiclude because mudstones of the Karoo Supergroup are in general highly impermeable (Vermaak and van Shalkwyk, 2000). The contact between the second and the third unit displays light brown gravely river sand with some mudstone pebbles.

The last is CYS1BH6 that exhibits quite a different set of geological successions. It comprises the first fine sandy 4m unit. This unit is underlain by a 5 metre calcrete layer followed again by 4 metre fine sand. The last unit is a highly impermeable and massive mudstone recognisable from 12 metres down to 24 metres.





Figure 4-9: Gravel pebbles and boulders sampled during drilling of CYS1BH3 at a depth of 11-18 metres.

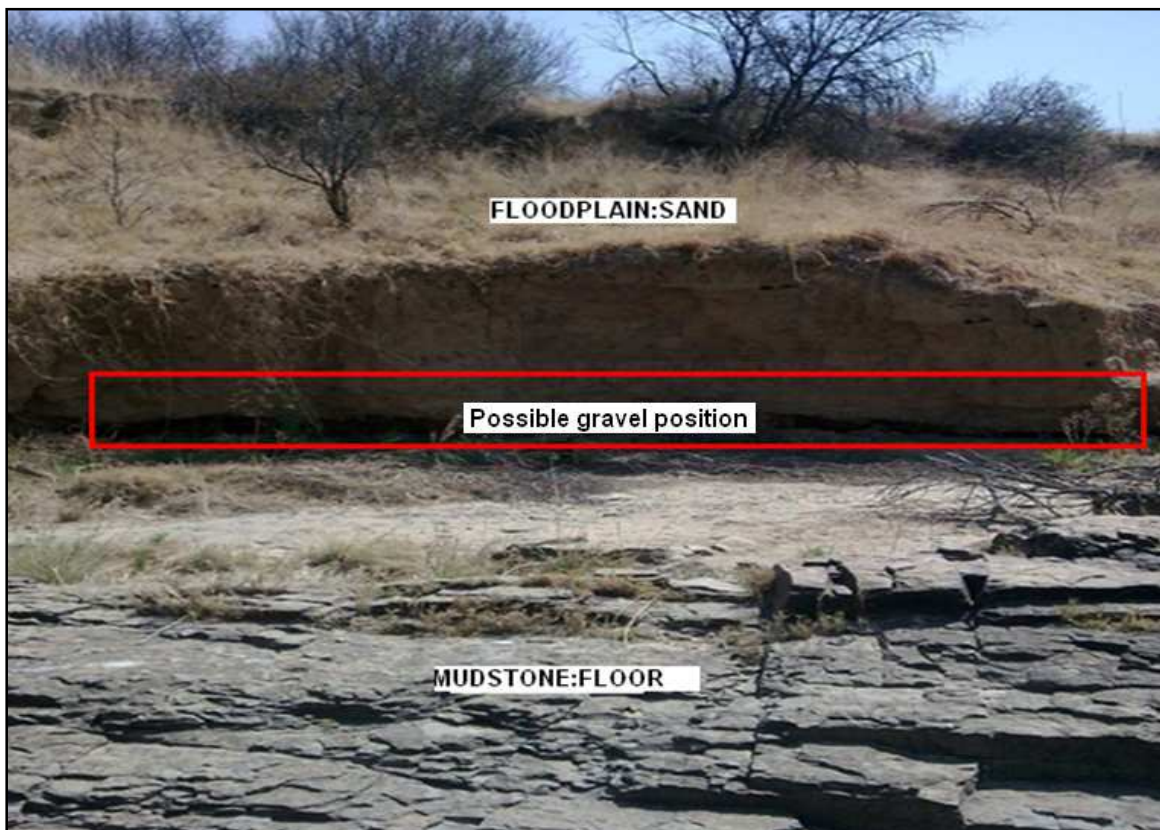


Figure 4-10: Lenses of sand, gravel and mudstone floor within Modder river channel

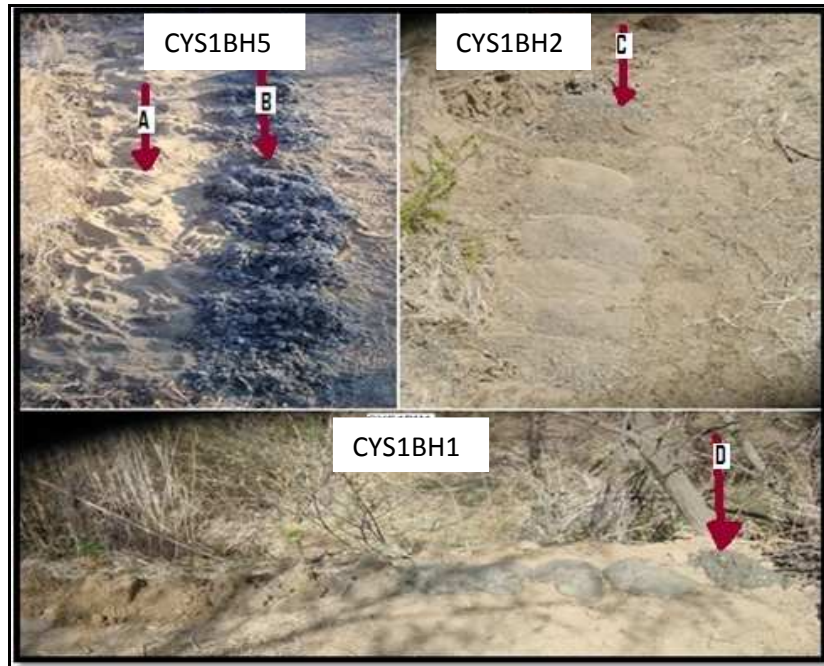


Figure 4-11: Continuous samples of sediment/geology for respective boreholes (A and C=fine sand, B=mudstone, D=gravel).

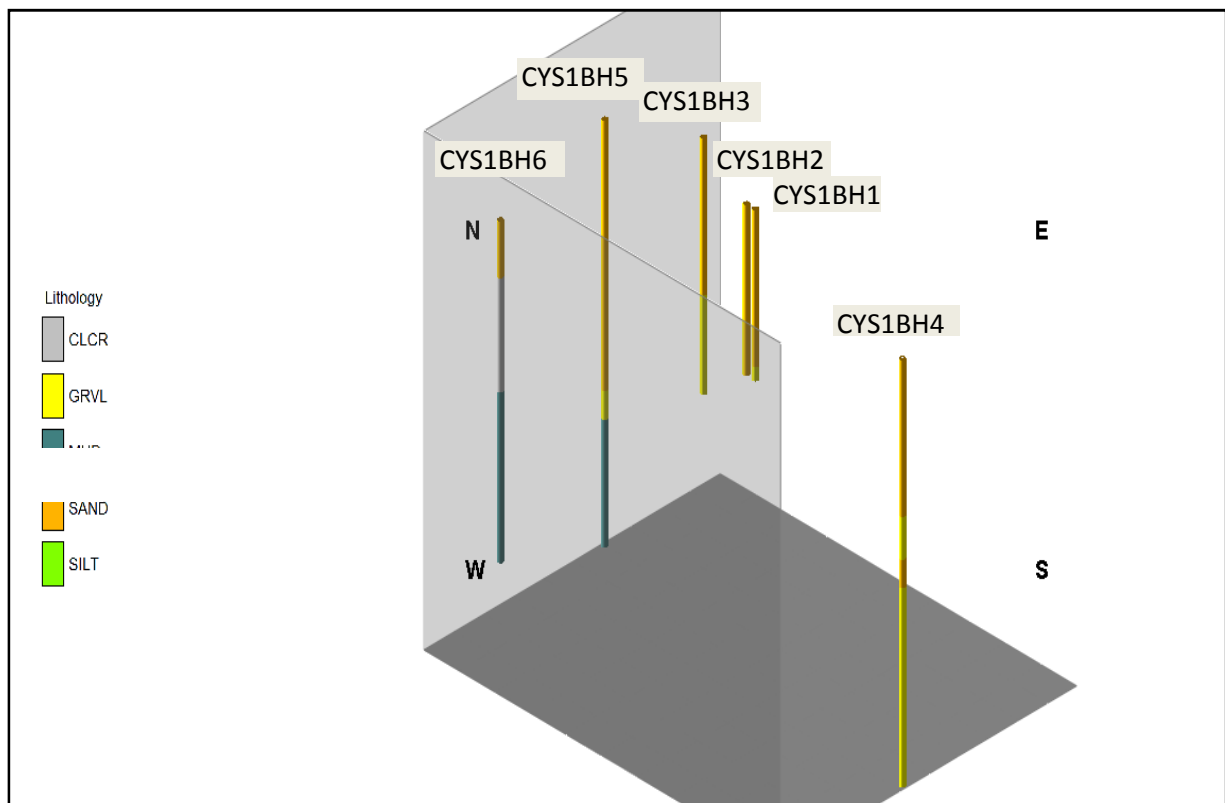


Figure 4-12: The 3D Multilog showing borehole distribution at the study area. For more detailed and descriptive well logs, the reader is referred to ANNEXE B.

### 4.3.3 Geologic modelling

A difficult reality often faced by hydrogeologists is that site geologic conditions are commonly non-ideal. However, synthesising and interpolating data from borehole logs to develop an appropriate conceptual model is a good tool that can enhance understanding of the subsurface geological condition and hence give a better understanding of the hydrogeological properties and processes of the aquifer in question.

In order to gain this additional insight into the geologic framework which includes the correlation, thickness and continuity of sand/gravel and silt/clay deposits of this specific site, it was necessary to construct a geologic model and cross sections that visually integrates the geological information obtained from well logs and soil analysis. The RockWorks software package (RockWorks-15, 2010) was used in this regard to model the geology. The software provides several methods of gridding and interpolation of well log data for building lithological models that could be used in characterisation of the subsurface (RockWorks-15, 2010). This chapter aims at applying lithological modelling techniques for characterisation of the alluvial river aquifer system using the data acquired during drilling and soil analysis. The modelling depends on using well log data and the techniques of lithologic modelling available in RockWorks.

A 3-dimensional (3D) model representing interpolated lithology types was constructed in order to provide local subsurface information to delineate aquifers and confining units (Figure 4-13). A three-dimensional geological model provides a more realistic site conceptual model for geohydrological studies especially in more complex settings. The 3D lithology model was "Sliced" across through A-A' (West-East) to create a 2D profiled cross-section diagram to reveal the subsurface geological structure (Figure 4-14). Because the lithology is interpolated across the entire project area, multiple slices were reproduced to visualise the lithologic variation in various direction (Figure 4-15).

The three lithologic categories of the Quaternary system (fine sand, sand and gravel) are represented as spatially repeated sequences that have significant spatial changes in terms of occurrence, thickness of individual categories, and elevation of top and bottom of each layer. Interfingering and presence of lenses is a main

characteristic of the sedimentary basin represented in the study area. Results of the lithologic models, two dimensional cross section and three-dimensional fence diagrams, revealed that there is no significant lithologic heterogeneity in the modelled area. However, this heterogeneity which varies spatially needs to be taken into consideration as it will have a great importance in the groundwater flow regimes because lithologic materials tend to be connected to form a certain continuation which controls flow. It is important however to note that these models depend on interpolation schemes to fill the gaps in between the boreholes and hence the lithologic representation between boreholes may not reflect the actual reality.

Based on the results, use of these lithologic models to build the groundwater flow model will be far better than assuming a homogeneous three-layer model as the model reveals directly the heterogeneity in three dimensions.

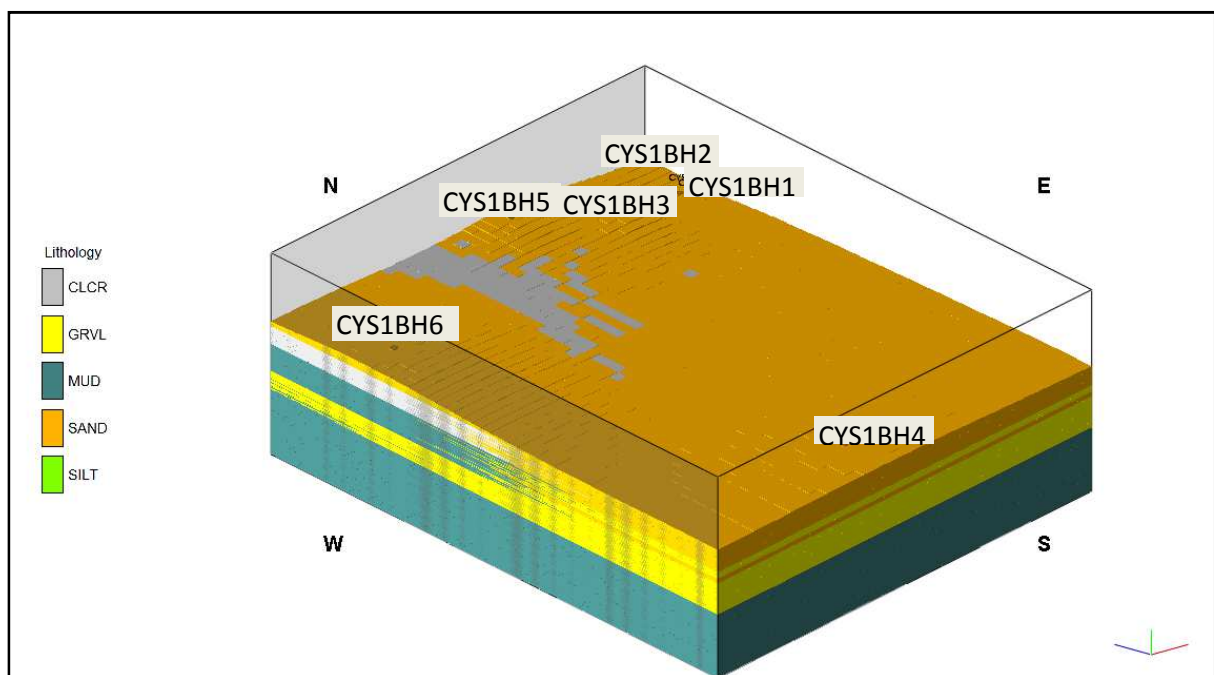


Figure 4-13: 3D Lithology model for the site.

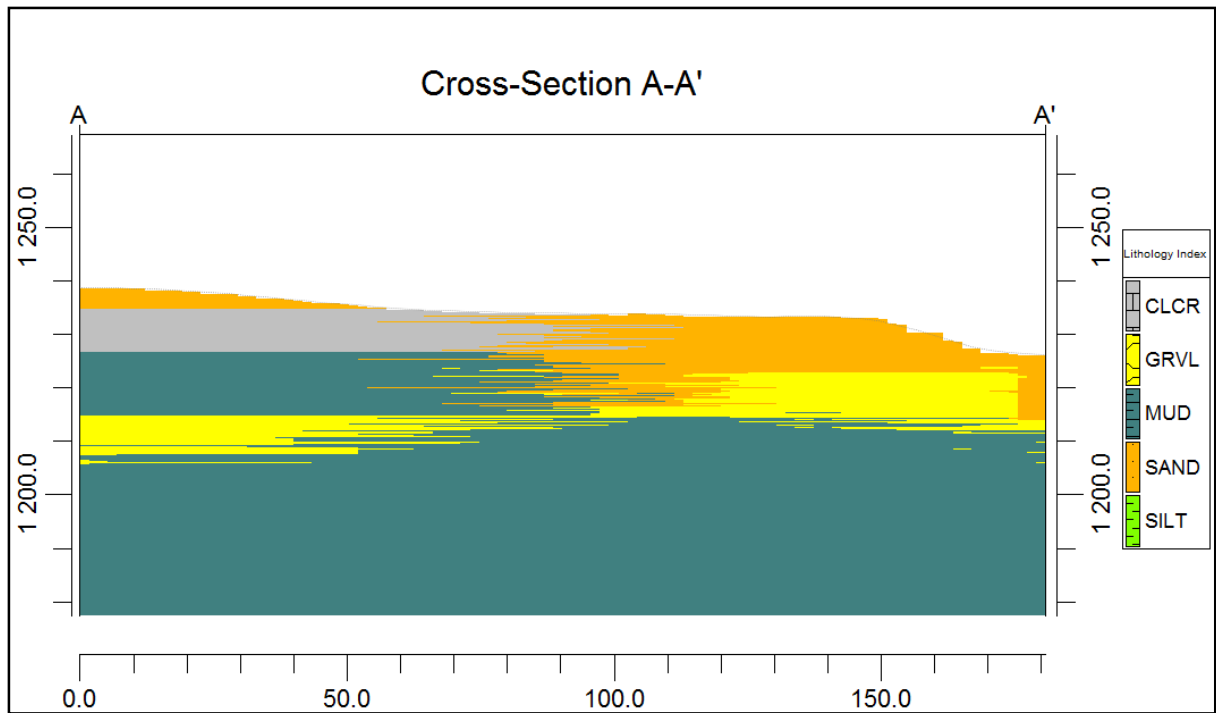


Figure 4-14: East–West lithological cross section.

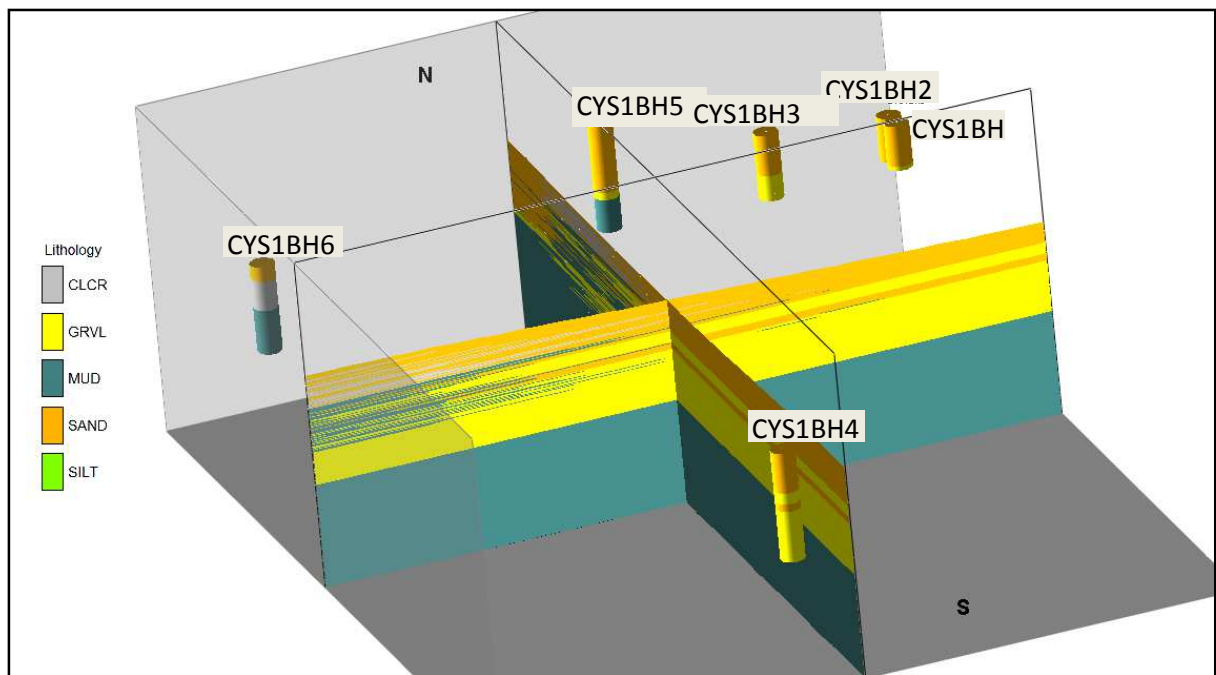


Figure 4-15: Lithology fence diagram.

## 4.4 Conclusions

Based on the aforementioned analysis and results, the following conclusions are drawn:

- Overburden was estimated from the infiltration test to be of average permeability; K is approximately equal to 2.42m/d. The *in situ* experiment was considered the most robust experiment to obtaining accurate K values for field soils (Vermaak and van Schalkwyk, 2000) because of the inherent limitations associated with empirical grain-size methods and minimal disturbances. This is because during the determination of grain size distribution, the sediment structure and stratification are destroyed. Hence, these relations yield a value of hydraulic conductivity that represents neither the vertical nor the horizontal hydraulic conductivity and is not representative of the true hydraulic properties of the subsurface. *In situ* permeameter tests have an advantage that representative sample can be tested.
- Soil textural class was found to consist an average of 22% Clay +silt and 77% very fine sand.
- The regional geological setting of the study area consists mainly of rocks of the Karoo Sequence and Super Group comprising the Ecca and Beaufort Groups.
- The aquifer is a three unit and unconfined alluvial stream aquifer situated in the alluvial deposits along the course of the Modder River. The main units of the system are the upper unit, middle unit and lower aquitard which are made up of the overbank-fine sand deposits, gravel and mudstone respectively.

The geology of the study area is typical of the Karoo Sequence. This is affirmed by massive mudstone bedrock of the Ecca group underlying the study domain. The unconsolidated sediments of gravel, sand and silt, deposited by the running water of the River (Modder River) during overflows on its banks, overlies this Karoo mudstone. The two (mudstone and alluvial deposits) are in hydraulic connection with each other. The alluvial deposits consist a range of raw materials of broken shale, mudstone and basalts typical of Karoo basin rocks (Ecca, Beaufort and Dyka respectively).

## 5 ISOTOPIC AND HYDROCHEMICAL CHARACTERISTICS

### 5.1 Introduction

The quality and isotopic composition of groundwater evolves from its primary composition (i.e. precipitation) due to constant interaction with the ambient environment, before and after recharge. Thus, the chemical and isotopic characteristics of the groundwater in question can help distinguish its origin. It is also worth noting that the movement of water between groundwater and surface water provides a major pathway for chemical and isotopic transfer between terrestrial and riparian aquifer systems.

Isotopes referred to are naturally occurring dissolved and stable isotopes of water that are used to determine source areas and hence track the movement and age of water through the aquifer systems (Winter *et al.*, 1998). Isotopes are also useful for determining the mixing of waters from different source areas. In a nutshell and driving towards the main objectives of this chapter, hydrogeochemical and isotopic information can indicate hydrological processes along groundwater flow paths and thus help delineate groundwater flow systems and determine the origins and mixing relationships between different waters (Sturchio *et al.*, 1996; Gemici and Filiz, 2001).

In this chapter, consideration is subsequently given to the combination of hydrogeochemical and isotopic indicators of both the river water and groundwater to provide means to meeting the following objectives:

- Describe and understand the chemical and isotopic characteristics of groundwater,
- Discriminate the spatial distribution of geochemical parameters at the site and hence,
- Apprehend the groundwater influx sources,
- Identify possible hydraulic interconnections between river water; and, groundwater.

## 5.2 Fieldwork

To answer the afore mentioned objectives, CYS1BH1, CYS1BH2, CYS1BH3, CYS1BH4, CYS1BH5, CYS1BH6 and some wells from CYS2 wellfield and CYS3 wellfield were sampled (Figure 5-1). The goal for ground-water sampling was as follows: to collect samples "representative" of *in-situ* ground-water conditions and the data quality objective (DQO) was to collect samples that represent the composite of the entire flow section (screen interval) of the wells. Low-flow sampling technique was used in which the water, with the intake set within the flow section, was pumped at a slow rate. Pumping was executed by pumping at a low flow rate of 0.60l/s to ensure that there was no mixing with water in the casing storage and to ensure minimal drawdown. Pumping was undertaken prior to sampling to avoid sampling of stagnant annulus water in the wellbore. Water quality indicator parameter electrical conductivity (EC) was used to determine when formation water was accessed during purging (until EC almost stabilised). The samples were then collected from the pump discharge using 1L sample bottles with airtight caps. Samples were appropriately marked and send to be analysed.

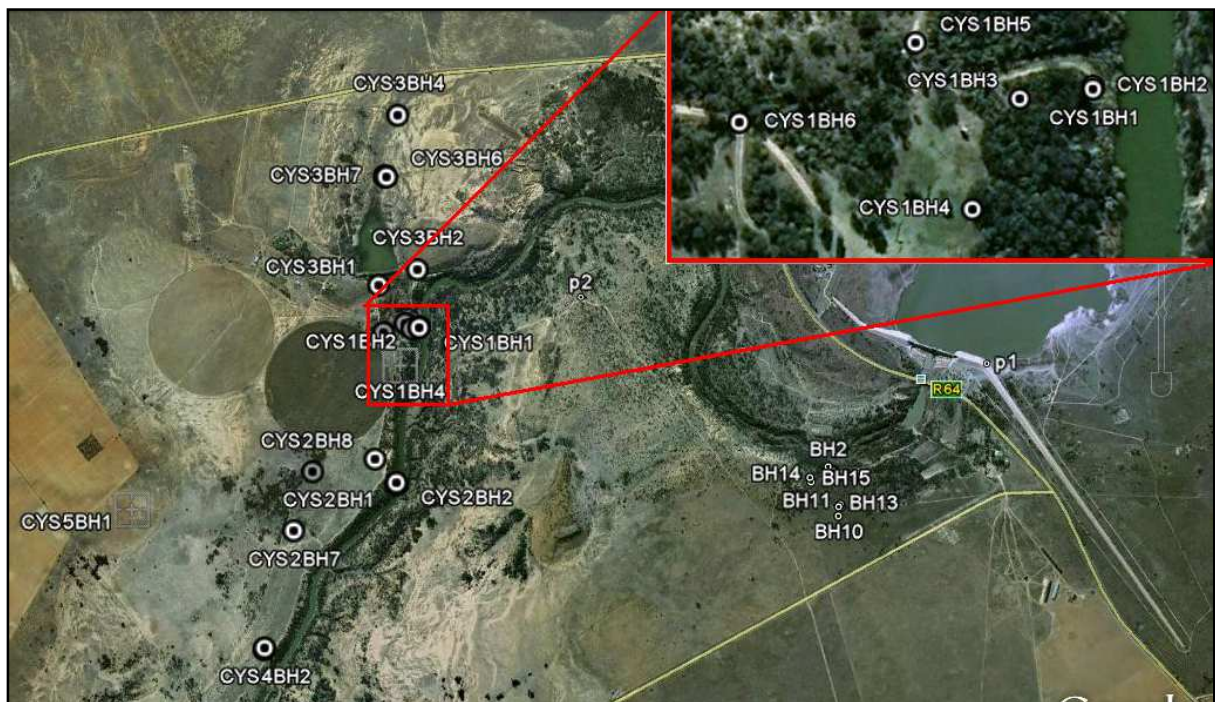


Figure 5-1: A Google image showing location of the sampled sites.



A total of 12 groundwater samples were collected over the six boreholes. Four river water samples were also collected directly from creeks at two different locations by immersing the bottle until filled. Thus, in total, 16 samples were collected from which 9 were analysed for chemistry and the other 9 for isotopes [this number excludes the samples collected from background wells (CYS2 and CYS3)]. Samples for chemistry were analysed by IGS laboratory while that for isotopes were sent to Environmental Isotope Laboratory, iThemba labs, for analysis of stable isotopes of oxygen 18 and deuterium. The samples were analysed for the following chemical parameters: EC, Na<sup>+</sup>, Ca<sup>2+</sup>, Mg<sup>2+</sup>, K<sup>+</sup>, SO<sub>4</sub><sup>2-</sup>, Cl<sup>-</sup>, MALK, Al, Fe, Mn, NO<sub>3</sub> and F<sup>-</sup>, for subsequent geochemical interpretations.

### **5.3 Hydrogeochemical characterisation**

The characterisation of ambient groundwater systems and nearby rivers can not neglect and override the groundwater chemistry and surface water chemistry and these two cannot be dealt with separately because, one way or the other, surface and subsurface flow systems interact.

#### **5.3.1 Chemical differences for different waters**

Water from different sources differs in chemical composition because of conditions in each of the sources. Since these conditions are different, they also give rise to a different chemical reaction and hence play a dominant role in controlling the chemistry of waters from different sources. A classic example is that of the water recharging groundwater from rainfall. Rainfall that ultimately recharges groundwater systems has little dissolved mineral matter. However, once this water disappears into the ground, it accumulates a large load of dissolved mineral solutes. This unique process helps distinguish groundwater from surface water.

### 5.3.2 Results and discussion

Water-chemistry data compiled was used to help characterise the spatial variations in surface and groundwater quality and to help identify the source and movement of groundwater at the site. River water and ground-water data from the CYS1 wells were used for this study. Table 12-1 summarises the chemistry data for the wells sampled as part of this study. Major-ion concentrations in surface and groundwater samples are plotted in trilinear diagrams (Figure 5-2). The trilinear diagrams show the proportions of common cations and anions for comparison and classification of water samples independent of total analyte concentrations (Hem, 1970). Trilinear diagrams can be used to identify groups of samples that have similar relative ionic concentrations (Freeze and Cherry, 1979). Other subordinate and specialised chemical plots such as stiff, Schoeller and Box-and-Whisker plots were also used.

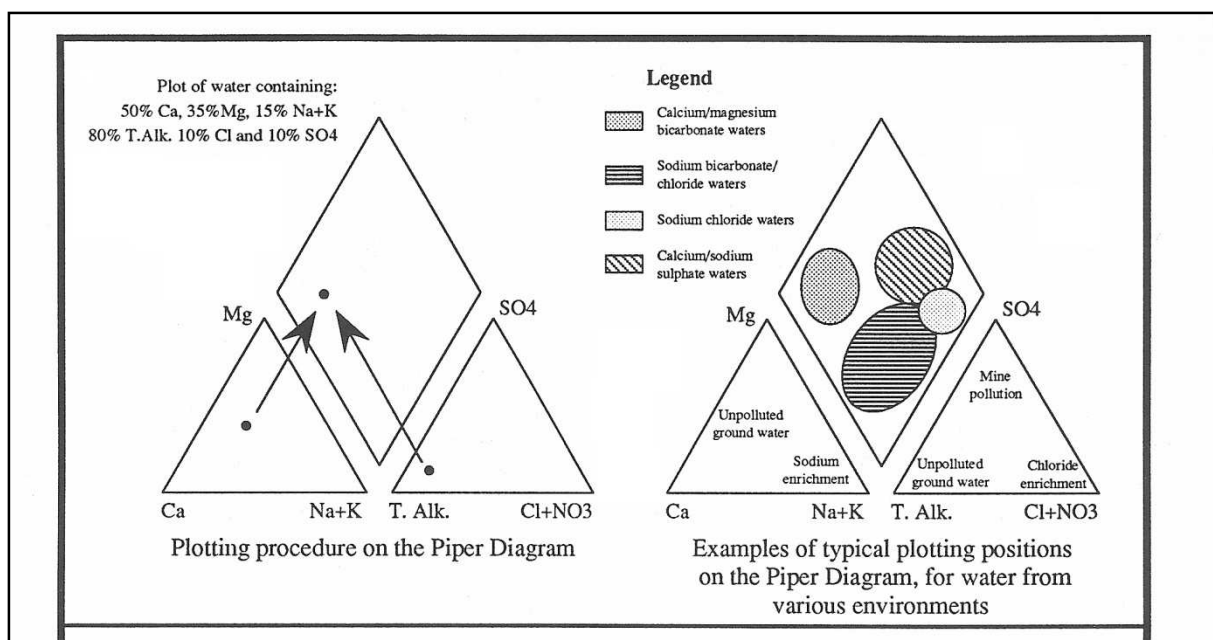


Figure 5-2: Trilinear diagram (Piper) used in the hydrogeochemical interpretations.

Hydrochemical characteristics of water samples in the study area are shown in the Piper plot in Figure 5-3. In general, this diagram shows that all the groundwater samples, together with the river water, are bicarbonate type water and fall along a mixing line from sulfate-chloride type water to calcium-magnesium type water (Figure

5-3). The Piper diagram further indicates that the analysed water is both unpolluted sodium and chloride enriched. However, the river water seems to fall between calcium/magnesium bicarbonate type water and sodium bicarbonate/chloride water. This indicates the mixing phenomena between river water and groundwater. It should be noted that water from CYS1BH2 seem to differ with the rest of the the wells because it is characterised as sodium bicarbonate/chloride water. This characteristic is similar to that of river water indicating more mixing between the two (river water and groundwater).

The values of the major parameters are presented in the Schoeller diagram (Figure 5-4). Analytical results of the river water showed that chloride and calcium were the predominant cations in solution for the six wells sampled (CYS1BH1, CYS1BH2, CYS1BH3, CYS1BH4, CYS1BH5 and CYS1BH6). The elevated concentrations of calcium and chloride in groundwater might strongly be attributed to forestation of the site where evapotranspiration rates are widespread. Natural groundwater chemistry is largely influenced by vegetation (evapotranspiration). Salts not used up by plants tend to accumulate in the soil horizon thereby being leached by infiltrating and percolating water down to the water table. This process is therefore attributed to the elevated salt species in groundwater in the area. The other possible source might be the dissolution of calcium-rich calcrete identified in the study area.

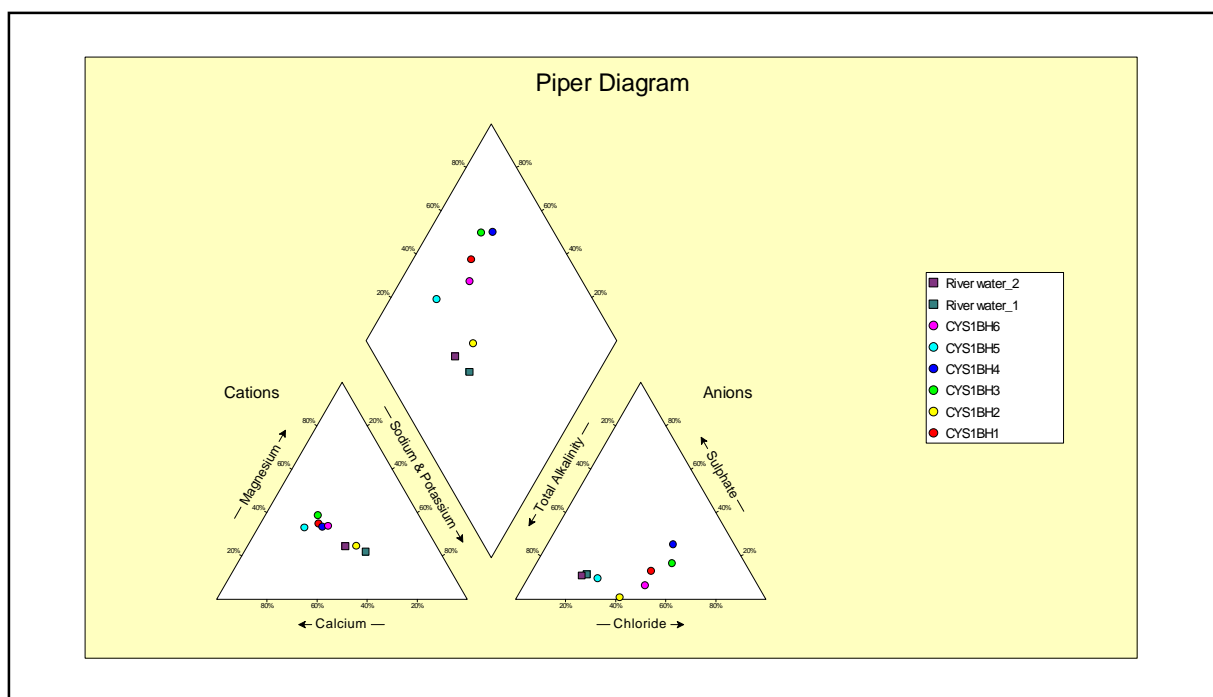


Figure 5-3: Characterisation of the water chemistry both from boreholes and river water.

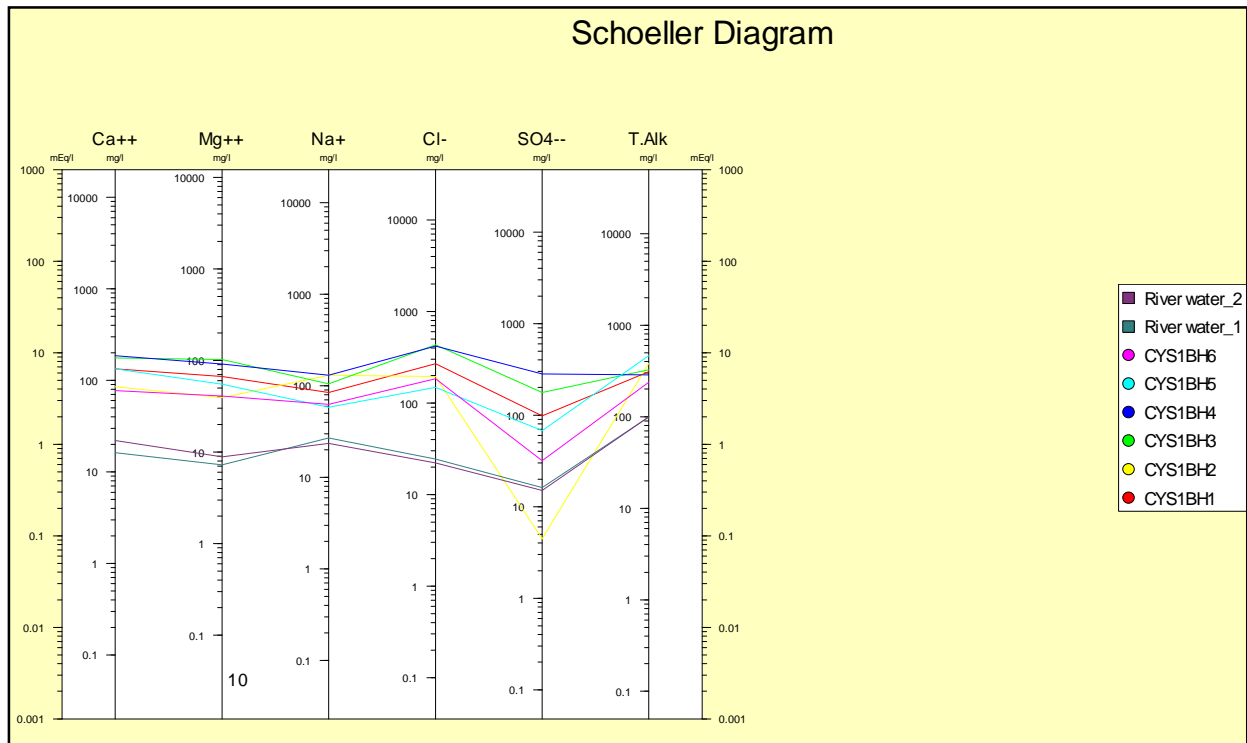


Figure 5-4: Graphical comparison of water chemistry from different wells.

The stiff diagrams for the median concentrations of the parameters under the four wellfields are presented in Figure 5-5. Wells CYS1BH1, CYS1BH3 and CYS1BH4 can be classified as Ca-Cl waters that have undergone evolution through ion exchange from recharge to discharge areas in the groundwater flow system. These results are not questionable as the three wells display similar geological makeup. These waters are differentiated slightly by their EC values in which CYS1BH3 falls towards the end of the 50% percentile with CYS1BH1 falling mid 50% percentile while CYS1BH4 falls in the 95% percentile (Figure 5-6). Well CYS1BH2 is a Na+K-HCO<sub>3</sub> water while CYS1BH6 is a Ca-Cl- HCO<sub>3</sub> water. River water on the other hand shows more of Na+K-Mg- HCO<sub>3</sub> type water characteristic.

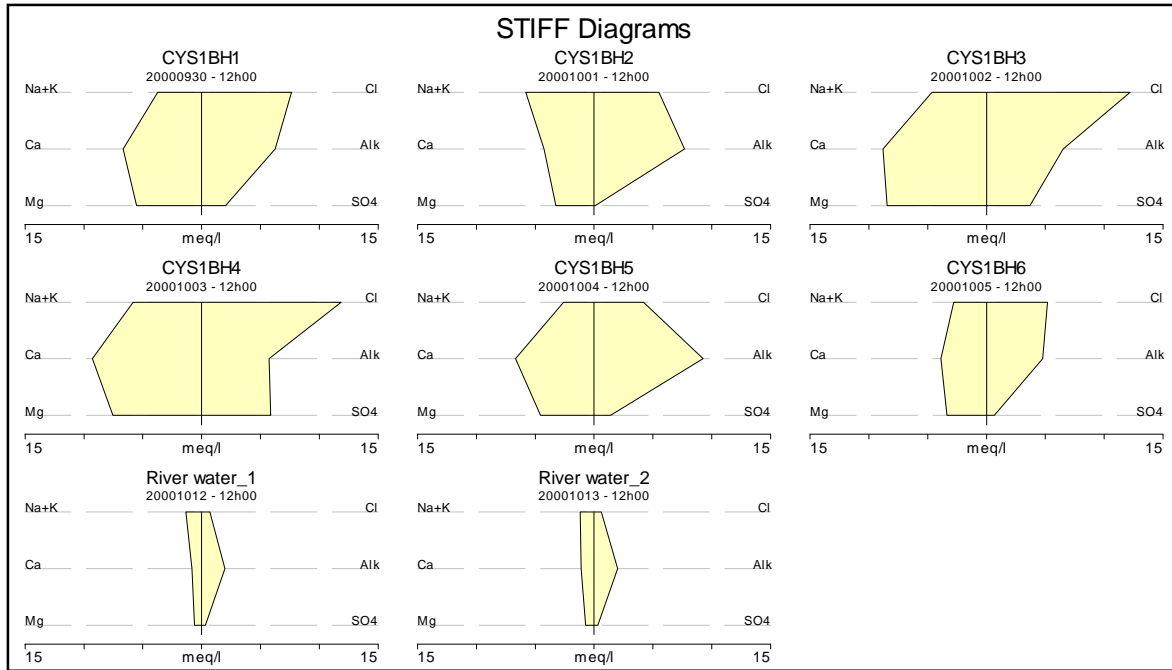


Figure 5-5: Stiff plots of water samples from the study area.

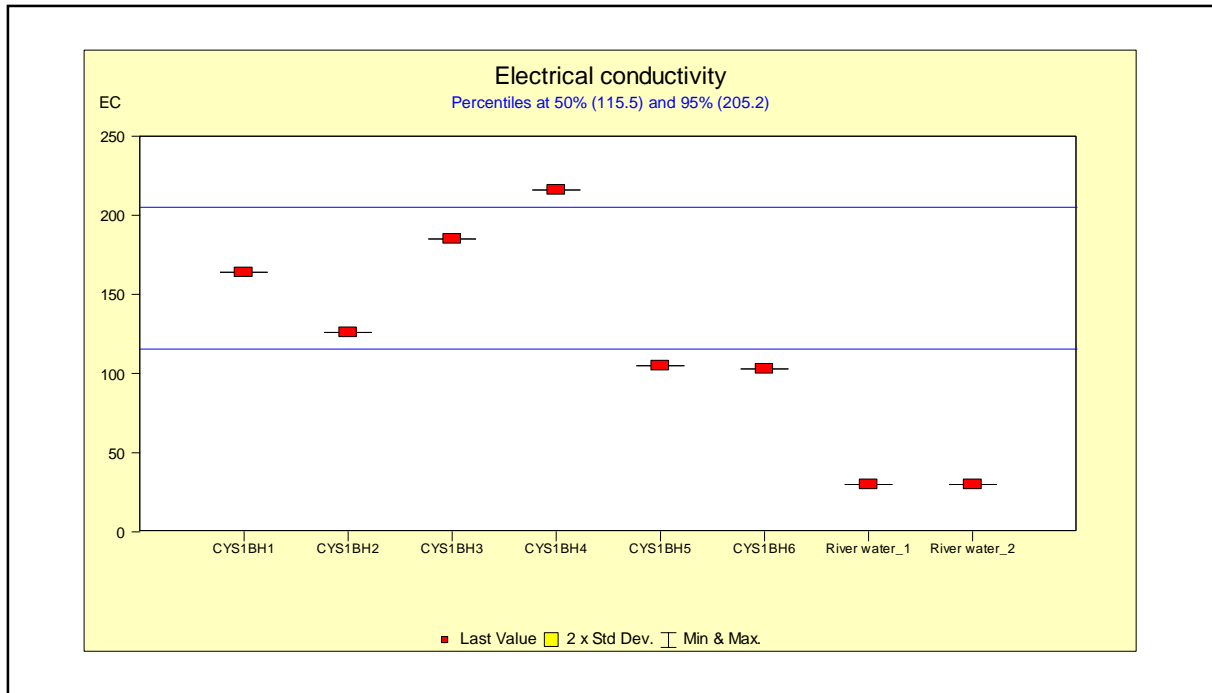


Figure 5-6: Box –and-Whisker differentiation of waters based on EC values.

Figure 5-6 further goes to illustrate that EC values are high for CYS1BH1, CYS1BH3 and CYS1BH4. The locations over which these wells are drilled is highly populated by riparian trees as well as an extensive grass masses (Figure 5-7). Evapotranspiration by these plants may cause an elevated concentration of total dissolved solids (TDSs). Since TDSs can be measured by the conventional measure of EC (EC of water is directly related to the concentration of dissolved ionised solids in the water), ions from the dissolved solids in water give water the ability to conduct electrical current hence EC. This observation can be contrasted with the low EC values observed in CYS1BH5 and CYS1BH6 which are at positions of relatively low vegetation intensities. The river water goes on to strengthen the conclusion that vegetation has a significant contribution to the elevated TDSs and hence high EC.



Figure 5-7: A vegetated CYS1BH3 location zone.

## 5.4 Isotopic characteristics

Natural water can be a combination of several stable nuclides (isotopes) such as, Tritium ( $^3\text{H}$ ) Oxygen-18 ( $^{18}\text{O}$ ) and Deuterium (D). These environmental isotopes contribute to a more productive groundwater investigation, complementing geochemistry as well as the physical hydrogeology (Usher, 2008). The relative abundance ( $\delta$ ) of oxygen-18 can be used to help infer the source and the evaporative history of water while that of Tritium can help in estimating groundwater age.

### 5.4.1 $\delta^{18}\text{O}$ and $\delta\text{D}$

With evaporation and condensation processes, both  $^{18}\text{O}$  and D are fractionated so that the water circulating from the ocean to the atmosphere and falling as rain has specific  $^{18}\text{O}$  and  $\delta\text{D}$  values that are correlated (Coplen, 1988). Fractionation causes the relative abundance of the isotopes to change because heavier isotopes ( $^{18}\text{O}$  and D) tend to be more abundant in the condensed phase (Figure 5-8).

Because the source of much of the world's precipitation is derived from the evaporation of seawater, the  $\delta^{18}\text{O}$  and  $\delta\text{D}$  composition of precipitation throughout the world clusters along and parallel to a straight line known as the global meteoric water line (GMWL) (Equation 5-1).

$$\delta\text{D} = 8\delta^{18}\text{O} + 10$$

Equation 5-1 (Craig, 1961)

Isotopic changes due to fractionation are too small to measure accurately so that the isotopic abundance is reported as positive or negative deviations of isotopes ratios away from a standard (Fritz and Fontes, 1980). In this regard, sea water being the largest uniform body of water is used as the standard (standard mean oceanic water, SMOW) with which measured concentrations are compared. The abundance ( $\delta$ ) is usually expressed as the relative difference of heavy to light isotopes with that of SMOW (Equation 5-2):

$$\delta = \frac{R - R_{SMOW}}{R_{SMOW}}$$

Equation 5-2 (Gat and Gonfiantini, 1981)

Where:  $\delta$  reported as permill

R= isotopic concentration of a sample

$R_{SMOW}$ = isotopic concentration of standard

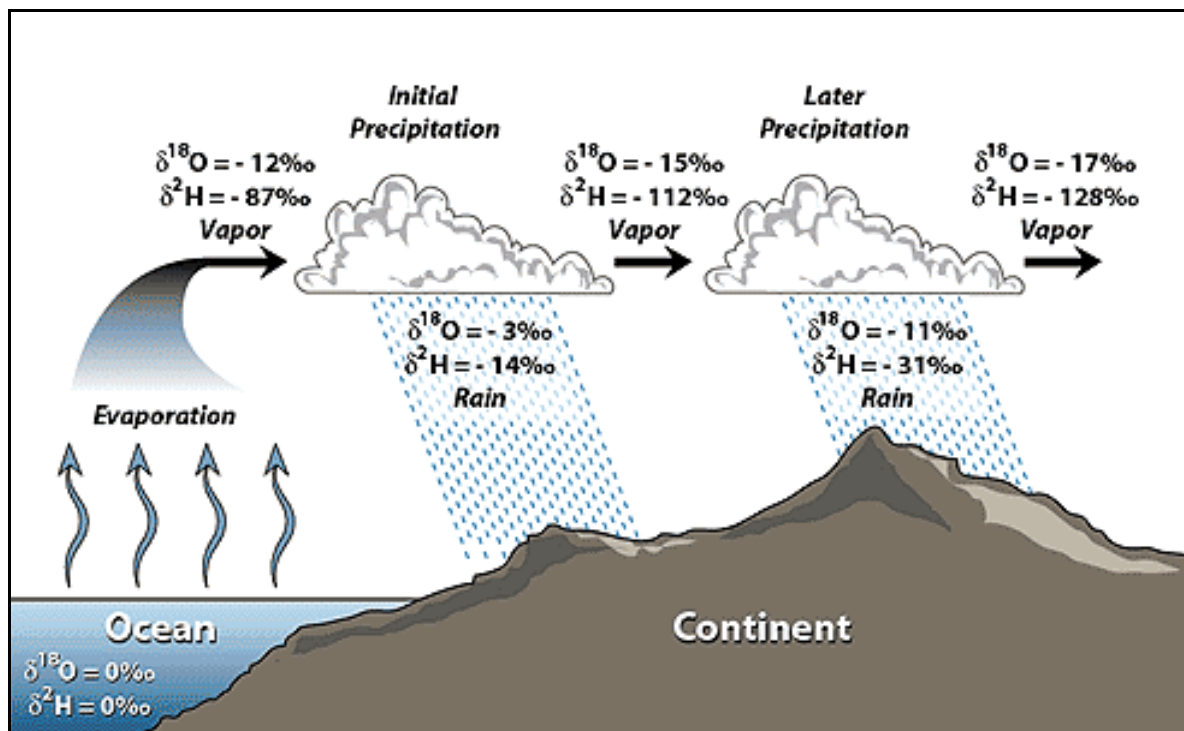


Figure 5-8: Evolution of Environmental Isotopes (Craig, 1961).

#### 5.4.2 Tritium

Tritium is a naturally occurring radionuclide that is produced during the reaction between cosmic-ray neutrons and nitrogen in the upper atmosphere (Ravikumar, and Somashekar, 2010). In the present study, an attempt was made to estimate the tritium content of the groundwater sampled from different wells in the study area in



order to distinguish influx ages. This section also discusses the relationship between the least abundant chemical species ( $\text{NO}_3$  and pH) in groundwater and tritium

Tritium concentration can be used to qualitatively determine whether or not groundwater is pre-modern (less than about 50 years in age) or modern (older than about 50 years in age) (Table 5-1) (Clark and Fritz, 1997). Tritium concentrations below 1 TU were considered to indicate that groundwater is at least 50 years old (pre-modern) and tritium values equal to or greater than 1 TU were considered as modern groundwater. Values of tritium of about 3 TU indicate a residence time of the water of about 30-40 years. Again modern age is classified depending on 3H values wherein the 3H values ranging from 1 to 8 TU could be attributed as a mixture of recent water with old groundwater and groundwater having been subjected to radioactive decay. The high tritium content value of the water can be interpreted as being due to mixing phenomena between the 'old' water of the confined aquifer and the 'recent additions' from the hydrological channel.

TABLE 5-1: TRITIUM BASED CATEGORISATION OF GROUNDWATER AGE (Clark and Fritz, 1997; Zouari *et al.* 2003)

Groundwater age (T.U)	Categorisation
<1	Old (pre-modern)
≥1	New(modern)
1-2	Mixture of old and new (radioactive decay)
9-18	Recent with activities
19->28	Thermonuclear with activities

### 5.4.3 Results and discussion

#### 5.4.3.1 $\delta^{18}\text{O}$ and $\delta\text{D}$

The isotopic composition of oxygen of samples from the study area's groundwater and river water are presented in

Figure 5-9, and plot along the GMWL as indicated on the graph. The  $\delta^{18}\text{O}$  and  $\delta\text{D}$  values for the entire suite of water samples (both groundwater and river water) ranged from  $-6.44\text{‰}$  to  $-3.85\text{‰}$  and  $-16.1\text{‰}$  to  $-44.2\text{‰}$ , respectively (Table 5-2). These values plot on the right hand side, but parallel to the GMWL. Some were overall the isotopically heaviest (least negative) water sampled while others were isotopically lightest (more negative).

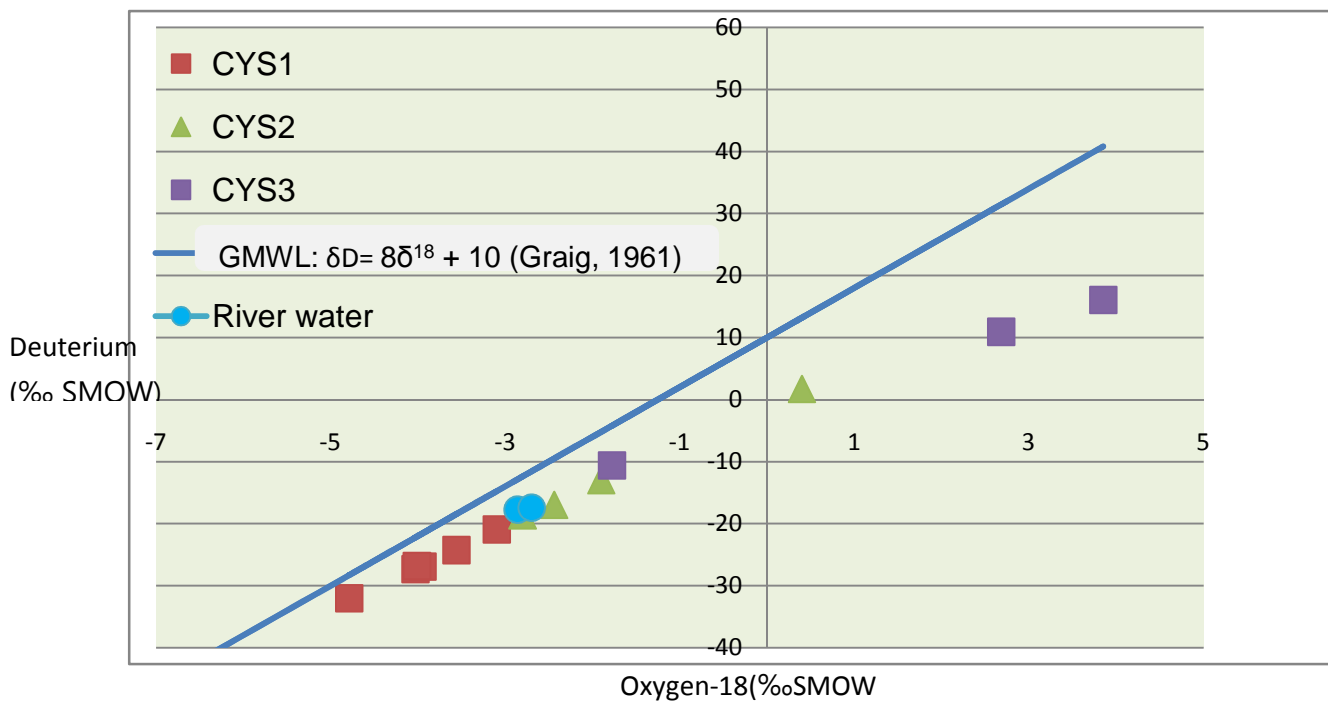


Figure 5-9:  $\delta\text{D} - \delta^{18}\text{O}$  plot of groundwater and the river water.

Water from most of the wells (CYS1BH1, CYS1BH2, CYS1BH3, CYS1BH4, CYS1BH5, CYS1BH6, CYS2BH1, CYS2BH8 and CYS3BH2) plot close and parallel to GMWL indicating that recharge is primarily derived from direct infiltration of precipitation or from the infiltration of riverbank seepage. This conclusion is accentuated by the plot of river samples along the same position and trend as the

groundwater samples. The clustering of these samples along the GMWL suggests that the samples may represent similar groundwater ages and mixing of infiltrated surface water and precipitation. Contrary to the above, some samples of CYS2BH2, CYS3BH1 and CYS3BH3) tend to scatter and the plot deviates from the GMWL indicating different mixing of infiltrated surface water and evaporated waters.

The  $\delta^{18}\text{O}$  and  $\delta\text{D}$  composition of water from the sampled wells indicates that water from all wells drilled in the “Riparian or Bank storage aquifer” is isotopically lighter than water from wells located on the “Terrestrial aquifer”. Where a river channel is in contact with an unconfined aquifer as is the case in the study area, groundwater may flow from the aquifer into the river channel, or vice versa, depending upon where the water level is lower. During a flood period, groundwater levels may be significantly raised (Figure 5-10). This process is known as bank storage (Kuchment, 2004). The aquifer system recharged directly by overbank flow is therefore referred to as a bank storage aquifer which is an interface between a river and land (Figure 5-11). The aquifer system located on the land is subsequently referred to as a terrestrial aquifer. The median  $\delta^{18}\text{O}$  and  $\delta\text{D}$  composition of samples from wells drilled in the bank storage aquifer was  $-3.56\text{‰}$  and  $-24.3\text{‰}$  while those drilled in the Terrestrial aquifer was  $-2.8$  and  $-18.7\text{‰}$  respectively.

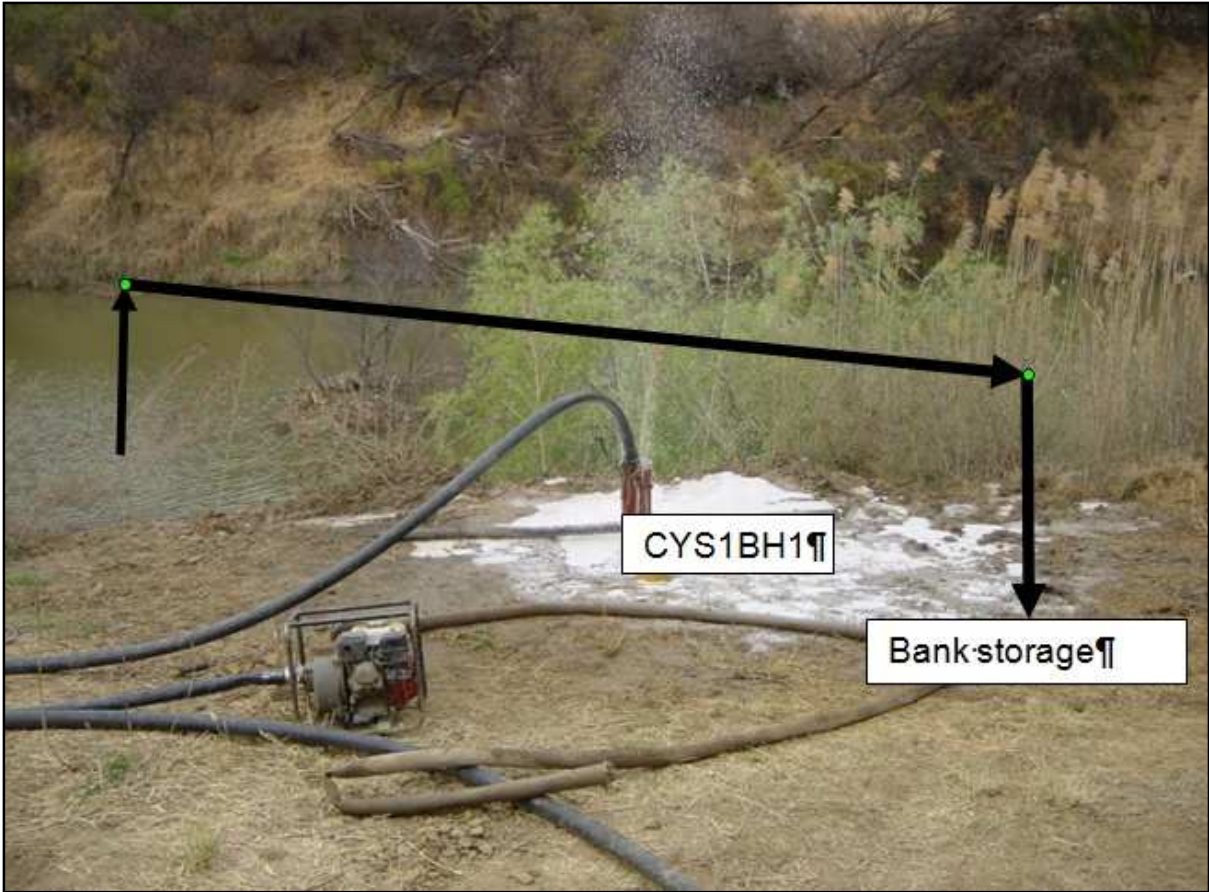


Figure 5-10: Bank storage at the study area.

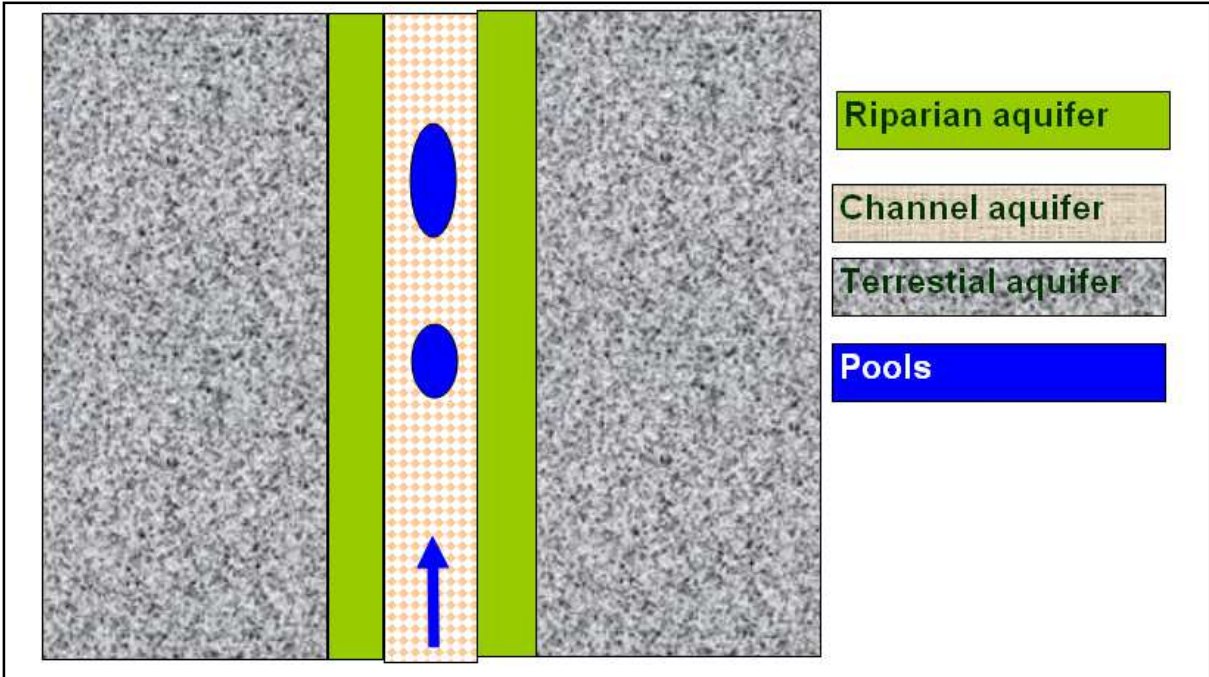


Figure 5-11: Figure illustrating the riparian and terrestrial aquifer concept (van Tonder, 2011).

Subsequently, the isotopic composition of water from riparian/bank storage aquifer well fields (CYS1, CYS2) is significantly lighter (more negative) and less evaporated, plotting only slightly off the GMWL. This implies that this water was not affected by evaporation. Recharge waters not affected by evaporation may occur in areas where precipitation and runoff infiltrate rapidly through coarse-grained alluvium and where there is negligible mixing with evaporated waters. These waters include samples from wells taken from the river, CYS1 and some wells at CYS2 wellfield (CYS2BH1, CYS2BH2, CYS2BH7, and CYS2BH8). It is important to take note that sampling was executed during the wet season. During this time, the Krugersdrift dam was overflowing thereby releasing water into the downstream channel. This process may allow for faster downstream movement, thereby minimising residence time of water and hence minimal exposure to evaporation.

Conversely, CYS3BH2 plots along and parallel to GMWL although it is drilled in the riparian aquifer. During the first three months in which the water levels were measured at the project site, this well was dry but contained water during sampling following torrents of rains. This well was drilled directly into heavily fractured dolerite. Subsequently, direct rainfall water recharged the well hence why its water tends to plot parallel and along the GMWL contrary to the rest of the terrestrial wells. The isotopic composition of water from, CYS3 well fields (CYS2BH2, CYS3BH1, and CYS3BH3) is significantly heavier (less negative), more evaporated hence plotting off the GMWL. This might be attributed to the fact that these wells are shallower so that the water might be near surface water it could be easily reached by heat and evaporated.

Waters affected by evaporation or modified by isotopic exchange after infiltration are represented by samples that plot to the far right of the GMWL. Samples from wells located on the terrestrial aquifer (CYS2BH2, CYS3BH1, and CYS3BH3) appear to have been subjected to evaporation. Recharge to these wells is meteoric, derived directly from local precipitation or storm runoff, but modified by evaporation prior to infiltration or mixed with evaporated waters from contributing sources. Contributing sources of evaporated waters in CYS3BH3 may include delayed infiltration of shallow soil water in areas with heavy soils. A stormwater retention pond (impoundment) that is open to the atmosphere provides the opportunity for

evaporation and isotopic enrichment of reclaimed water. This water might be the driving force towards the type of isotopic concentration in CYS3BH1 as this well is located directly below the impounding wall of the pond.

TABLE 5-2: STABLE ISOTOPIC COMPOSITIONS

Laboratory number	Sample Identification	$\delta D(\text{‰})$	$\delta^{18}O(\text{‰})$
IGS028	CYS1BH1	-27.30	-4.03
IGS029	CYS1BH2	-20.90	-3.10
IGS030	CYS1BH3	-26.90	-3.95
IGS031	CYS1BH4	-32.00	-4.79
IGS032	CYS1BH5	-24.30	-3.56
IGS033	CYS1BH6	-26.80	-4.01
IGS034	CYS2BH1	-13	-1.9
IGS035	CYS2BH2	1.7	-0.74
IGS036	CYS2BH7	-17	-2.44
IGS037	CYS2BH8	-18.7	-2.8
IGS038	CYS3BH1	16.1	3.85
IGS039	CYS3BH2	-10.6	-1.78
IGS040	CYS3BH3	10.9	2.68
IGS041	CYS4BH1	-44.2	-6.44
IGS042	CYS4BH2	-24.9	-3.54
IGS043	River water	-17.7	-2.86
IGS044	River water	-17.4	-2.7

#### 5.4.4 Tritium

The recorded environmental  $^3\text{H}$  content in 15 groundwater samples used for analysis at the study area varied from 0 T.U. to 4.8 T.U. with an average of 1.8 T.U. On comparing these results with standard  $^3\text{H}$  values given by Clark and Fritz (1997) and Zouari *et al.*, (2003), it is evident that almost all the samples exhibited radioactive decay (0.1 to 5 T.U.) having a mixture of pre-modern (old water) water mixed with modern (new water) recharge (Figure 5-12). Usually, natural tritium in precipitation varies approximately from 1 TU in high-precipitation regions to as high as 10 TU in arid areas (Ravikumar and Somashekar, 2010). Most samples (70%) from the study area show tritium content greater than 1T.U. (Figure 5-12) indicative of modern water in the arid region and suggesting that the possible influx source might have been precipitation or precipitation derived water. In other words, the groundwater gets recharged with modern rainfalls and has short circulation time in the ground indicative of short travel time. The aforementioned interpretation absolutely hold true because sampling was carried it out during torrents of rains. Only 30% falls below 1T.U. indicative of older water.

A closer look at each well entity shows that most wells (except CYS3 wellfield) and river water are new (modern waters). This water has average tritium concentrations of 0.9T.U. Contrarily, CYS3 wells have average tritium content of 4T.U indicative of a mixture of old and new water (radioactive decay). Water from CYS2BH1 and CYS1BH2 has an average of 3.5T.U. indicative of a mixture of old and new water.

TABLE 5-3: TRITIUM (T.U) RESULTS

Laboratory number	Sample Identification	Tritium (T.U)
IGS028	CYS1BH1	1.1
IGS029	CYS1BH2	1.20
IGS030	CYS1BH3	0.40
IGS031	CYS1BH4	1.00
IGS032	CYS1BH5	0.60
IGS033	CYS1BH6	0.60
IGS034	CYS2BH1	3.40
IGS035	CYS2BH2	3.50
IGS036	CYS2BH7	1.20
IGS037	CYS2BH8	1.10
IGS038	CYS3BH1	3.10
IGS039	CYS3BH2	4.2
IGS040	CYS3BH3	4.80
IGS041	CYS4BH1	0.00
IGS042	CYS4BH2	1.20
IGS043	River water	1.1
IGS044	River water	1.20



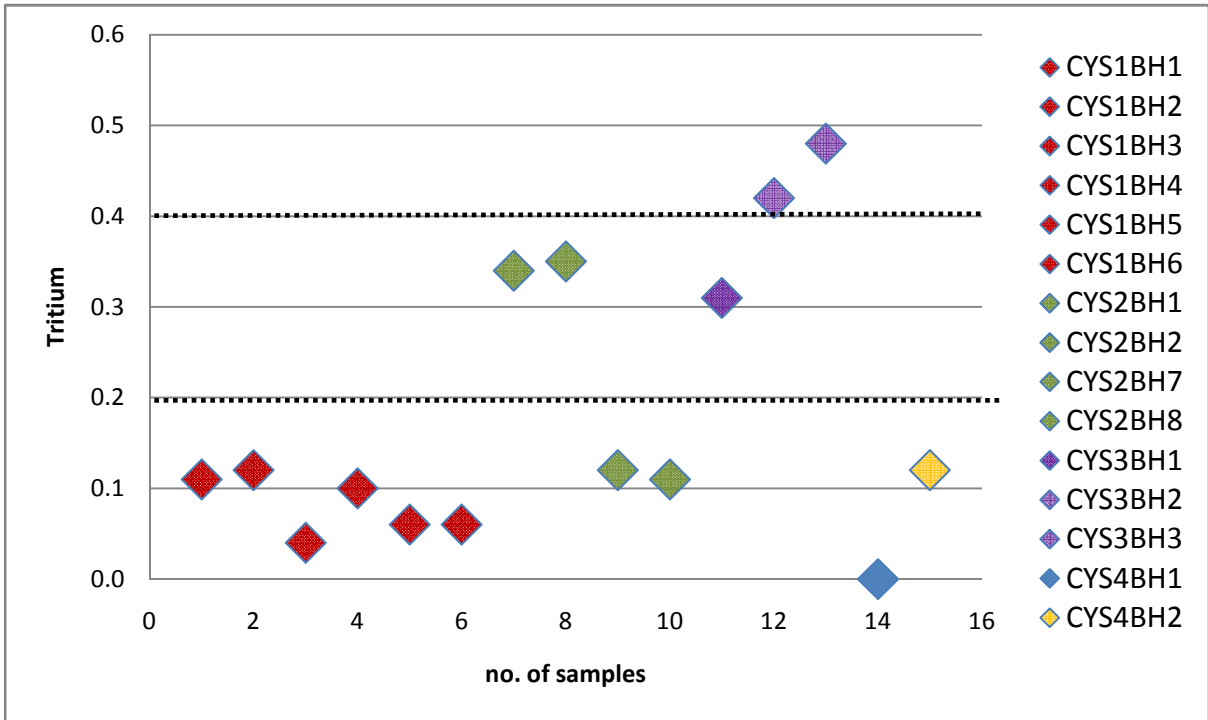


Figure 5-12: Comparison between Tritium values from four wellfields in the study site.

The plot of pH-Tritium indicated that majority of the samples fall within the pH range 6 to 8.5 attributed to recharges with modern and highly neutralised rainfalls with minerals present in the aquifer lithology (Figure 5-13) and have short circulation time in the ground. Since rain water has no minerals, when rain (modern recharge) falls down to the earth, it collects the environmental impurities along with minerals, dominated by alkaline components, particularly bicarbonates, carbonates (Ravikumar and Somashekar, 2010).

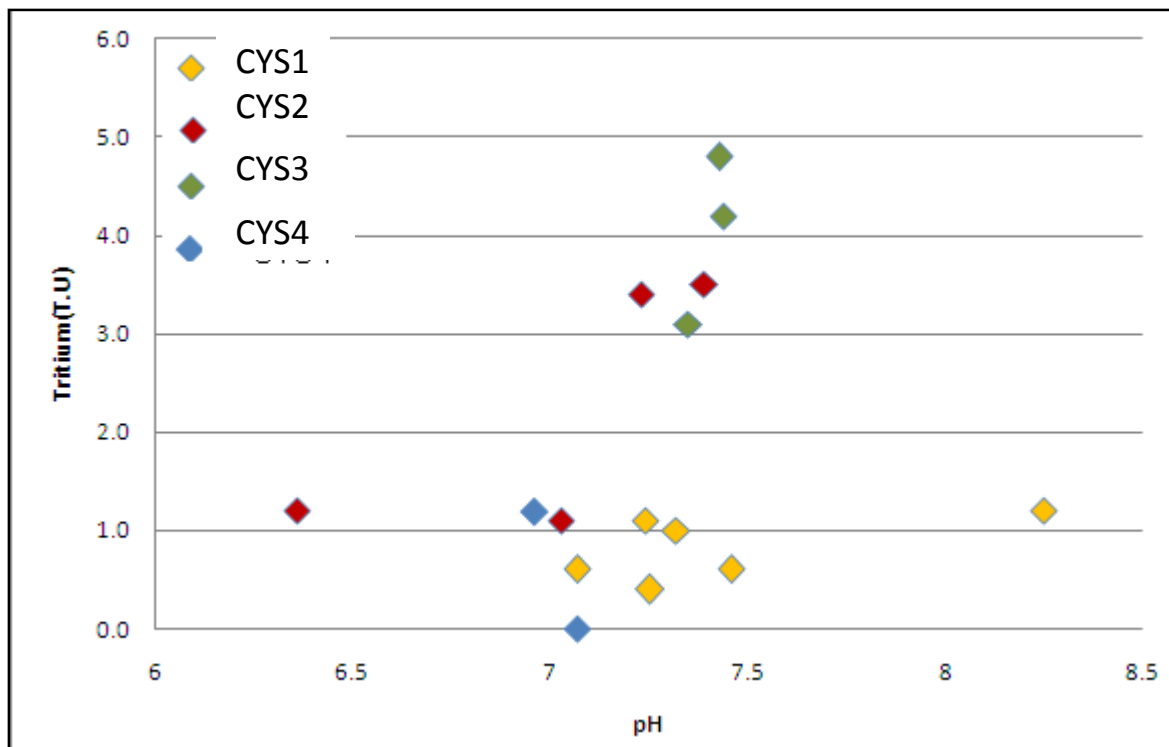


Figure 5-13: Plot of Tritium concentrations based on pH.

The study area is located on the farm and closed to constantly irrigated fields. Isotopes can demonstrate the irrigation return flow and pollution hazard. The plot of tritium against nitrate concentrations (Figure 5-14) highlights the fact that the sample show less nitrate content (WRC South African National Standards, 1998: 10- 20 mg/l as N). The groundwater samples with the lowest nitrate concentration are also the ones with the lowest tritium level indicating that, although the groundwater source lies on agricultural land, it has not been contaminated by nitrate fertilizers.

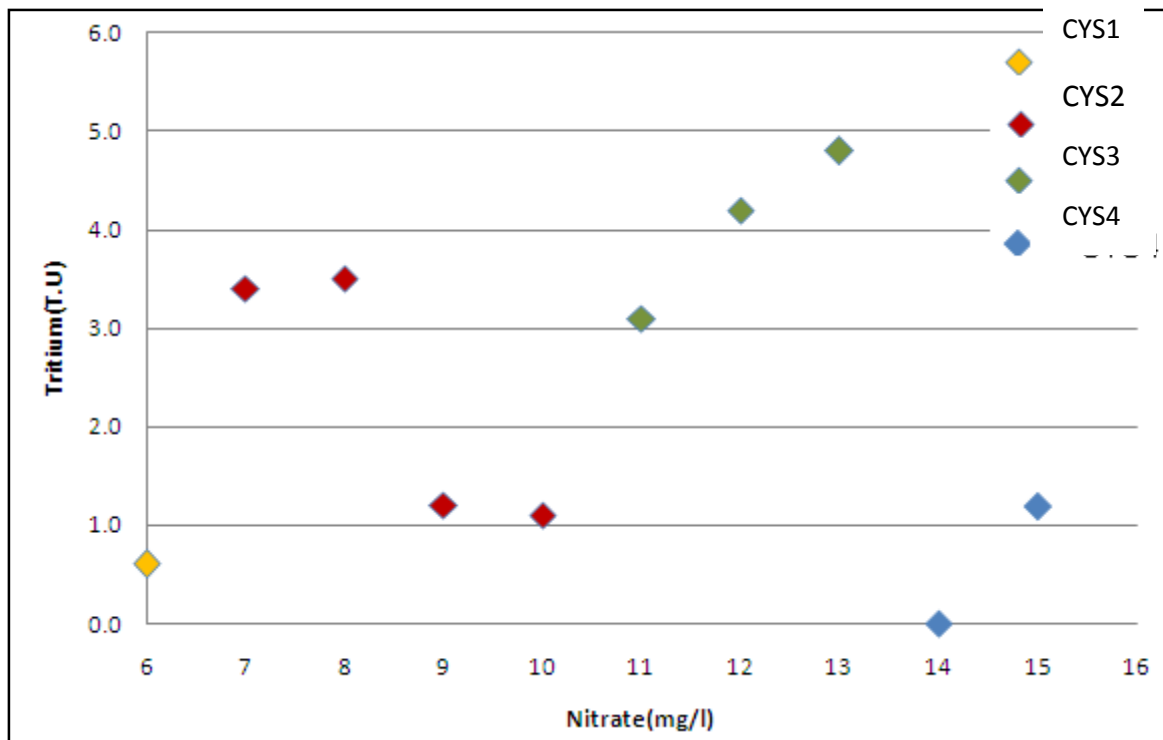


Figure 5-14: Plot of Tritium concentrations based on nitrate.

## 5.5 Conclusions

### 5.5.1 Hydrogeochemical characteristics

In general, all the samples together with the river water are bicarbonate type water and fall along a mixing line from sulfate-chloride type water to calcium-magnesium type water. The Piper diagram further indicated that analysed water is both unpolluted sodium enriched and chloride enriched. However, river water seems to fall between calcium/magnesium bicarbonate type water and sodium bicarbonate/chloride water. This attribute indicates almost the same source of water between river water and groundwater. It should be noted that water from CYS1BH2 seem to differ with the rest of the wells because it is characteristic as sodium potassium bicarbonate water. This characteristic is similar to that of river water indicating more mixing between the two. It should also be noted in this regard that CYS1BH2 never intercepted the gravel unit so that the most source of its water might be the inflow of the river water rather than the aquifer water.

Analytical results of the river water show that chloride and calcium were the predominant cations in solution from the six wells sampled (CYS1BH1, CYS1BH2, CYS1BH3, CYS1BH4, CYS1BH5 and CYS1BH6). The elevated concentrations of calcium and chloride in groundwater might strongly be attributed to forestation of the site where evapotranspiration rates are widespread. Natural groundwater chemistry is largely influenced by vegetation (evapotranspiration) in that salts not used up by plants tend to accumulate in the soil horizon thereby being leached by infiltrating and percolating water down to the water table. This process is therefore attributed to the elevated salt species in groundwater in the area. The other possible source might be the dissolution of calcium-rich calcrete identifiable in the study area.

Wells CYS1BH1, CYS1BH3 and CYS1BH4 are Ca–Cl waters that have undergone evolution through ion exchange from recharge to discharge areas in the groundwater flow system. These results are not questionable as the three wells display similar geological makeup. These waters are differentiated slightly by their EC values in which CYS1BH3 falls towards the end of the 50% percentile with CYS1BH1 falling mid 50% percentile while CYS1BH4 falls in the 95% percentile. Wells CYS1BH2 is Na+K-HCO<sub>3</sub> waters while CYS1BH6 is Ca-Cl- HCO<sub>3</sub> waters. River water on the other hand shows more of Na+K-Mg- HCO<sub>3</sub> type water characteristic.

### 5.5.2 Isotopic characteristics

Water from most of the wells (CYS1BH1, CYS1BH2, CYS1BH3, CYS1BH4, CYS1BH5, CYS1BH6, CYS2BH1, CYS2BH8 and CYS3BH2) plot close and parallel to GMWL indicating that recharge is primarily derived from the direct infiltration of precipitation or from the infiltration of seepage from the river (Figure 5-9). This conclusion is accentuated by the plot of river samples along the same position and trend as the groundwater samples (Figure 5-9). Water from CYS2BH2, CYS3BH1 and CYS3BH3 tend to scatter and their plot deviates from the GMWL indicating different groundwater ages and perhaps mixing of infiltrated surface water and precipitation with other contributing sources.

The  $\delta^{18}\text{O}$  and  $\delta\text{D}$  composition of water from the sampled wells indicates that water from all wells (CYS1BH1, CYS1BH2, CYS1BH3) drilled in the Riparian or Bank

storage aquifer (Figure 5-15) is isotopically lighter than water from wells located on the “Terrestrial” aquifer.



Figure 5-15: A Google image showing wells drilled in the bank storage aquifer (enclose).

The recorded environmental  $^3\text{H}$  content in 15 groundwater samples used for analysis at the study area varied from 0 T.U. to 4.8 T.U. with an average of 1.8 T.U. On comparing these results with standard  $^3\text{H}$ , it is evident that almost all the samples exhibited radioactive decay (0.1 to 5 T.U.) having a mixture of pre-modern (old water) water mixed with modern (new water) recharge. Usually, natural tritium in precipitation varies approximately from 1 TU in high-precipitation regions to as high as 10 TU in arid areas. Most samples (70%) from the study area lay beyond 1T.U. when only 30% falls below 1T.U (Figure 5-12) indicative of modern water and suggesting that the possible influx source might have been precipitation or precipitation derived water. In other words, the groundwater gets recharged with modern rainfalls and has short circulation time in the ground indicative of short travel time. The aforementioned interpretation hold true because sampling was carried it out during torrents of rains.

Most wells (except CYS3 wellfield) and river water are new (modern waters) having average tritium concentrations of 0.9T.U. Contrarily, CYS3 wells have average tritium content of 4T.U indicative of a mixture of old and new water (radioactive decay). Water from CYS2BH1 and CYS1BH2 has an average of 3.5T.U. indicative of mixture of old and new water

The plot of pH-Tritium indicated that majority of the samples fall within the pH range of 6 to 8.5 attributed to recharges with modern and highly neutralised rainfalls with minerals present in the aquifer lithology and have short circulation time in the ground (Figure 4-13). Since rain water has no minerals, when rain (modern recharge) falls down to the earth, it collects the environmental impurities along with minerals, dominated by alkaline components, particularly bicarbonates, carbonates.

The plot of tritium against nitrate concentrations highlights the fact that the samples show less nitrate content (Figure 5-14). The groundwater samples with the lowest nitrate concentration are also the ones with the lowest tritium level indicating that, although the groundwater source lies on agricultural land, it has not been contaminated by nitrate fertilizers.

## **6 GENERAL GROUNDWATER FLOW AND GRADIENTS**

### **6.1 Introduction**

One of the common calculations in hydrogeological studies is the determination of a single and representative hydraulic gradient and its sloping direction. These properties become useful in inferring the subsequent groundwater velocities and many other related parameters. More importantly, calculations of hydraulic gradient and directions become very much handy in the studies of surface water groundwater interactions by giving an indication of the nature of interaction, for example, 1) whether or not the aquifer is depleting or discharging into a given water body, 2) groundwater baseflow is usually controlled by the difference in hydraulic heads (water levels), between the river stage and the piezometric surface of groundwater (Department of Water Affairs, 2006).

Like fractured aquifer systems where identification and differentiation of fracture to matrix water is vital, identification of main water conduit in the alluvial aquifers is equally of utmost importance. This is because overlying fine sand does not transmit water in the same manner with an underlying gravel deposit. As a result therefore, this chapter's objectives are to, calculate magnitude and direction of groundwater flow gradient and deduce flow section.

### **6.2 Magnitude and direction of gradient**

Determination of the horizontal component of hydraulic gradient may be used to ascertain and give an indication of groundwater flow direction. This information was obtained from analysis of the water table elevations in the monitoring wells at the site. Hydraulic gradient is defined as the slope of the water table or piezometric surface defined by the change in the hydraulic head over a given distance (Groundwater dictionary, IGS).

### 6.2.1 Groundwater levels

As part of a groundwater monitoring programme, water levels from the six boreholes (CYS1BH1, CYS1BH2, CYS1BH3, CYS1BH4, CYS1BH5, and CYS1BH6) were measured. Measurements of water levels in wells provide the most fundamental indicator of the status of groundwater and are critical to meaningful evaluations of its quantity and so is its interaction with surface water. Water-level measurements from observation wells are the principal source of information about the hydrologic stress acting on aquifers and how these stress affect ground-water recharge, storage, and discharge (Taylor and Alley, 2001).

Ground-water levels are controlled by the balance among recharge to, storage in, and discharge from an aquifer. Regional groundwater levels are indicative of the direction of groundwater movement. A change in the natural water-table gradient indicates that external forces are acting upon the aquifer. Such forces may be groundwater discharge or recharge through nearby water bodies. In unconfined aquifers, hydraulic heads fluctuate freely in response to changes in recharge and discharge (Kok, 2002). Table 6-1 summarises the average groundwater level data for respective boreholes.

TABLE 6-1: SUMMARY OF MEASURED WATER LEVELS 2011/02/09

BH ID	Y-coord	X-coord	Elevation (mamsl)	Groundwater rest depth (mbgl)	Groundwater rest elevation (mamsl)
CYS1BH1	-3196646.31	90733.00	1226.00	3.31	1222.69
CYS1BH2	-3196640.77	90733.04	1225.98	3.27	1222.71
CYS1BH3	-3196650.46	90696.87	1233.78	10.79	1222.99
CYS1BH4	-3196840.59	90629.04	1235.73	12.45	1223.28
CYS1BH5	-3196624.69	90661.95	1235.66	12.73	1222.93
CYS1BH6	-3196668.19	90554.29	1238.84	15.54	1223.30

Figure 6-1 shows the water level depth fluctuations with time together with precipitation amounts during the field survey at the site. Some boreholes indicate similar trends in groundwater level fluctuation in response to rainfall. CYS1BH1 and



CYS1BH2 were completed in the upper unit consisting of a mixture of silty clay and sand approximately 12mbgl thick, while well CYS1BH4, CYS1BH3 and CYS1BH5 were completed in a deeper aquifer zone consisting of a mixture of sand and gravel. Because the silty clay does not easily transmit water, the shallow wells (CYS1BH1 and CYS1BH2) exhibit relatively muted response to increase in recharge (Figure 6-1). In contrast, the more permeable sand and gravel in the deeper aquifer zone transmits water very easily, and the deeper aquifer zone exhibits a much greater response to increase in recharge. On the same note, groundwater levels seem to respond to rise with precipitation although the response is not almost immediate as recharging water takes time to reach the water table (Figure 6-1).

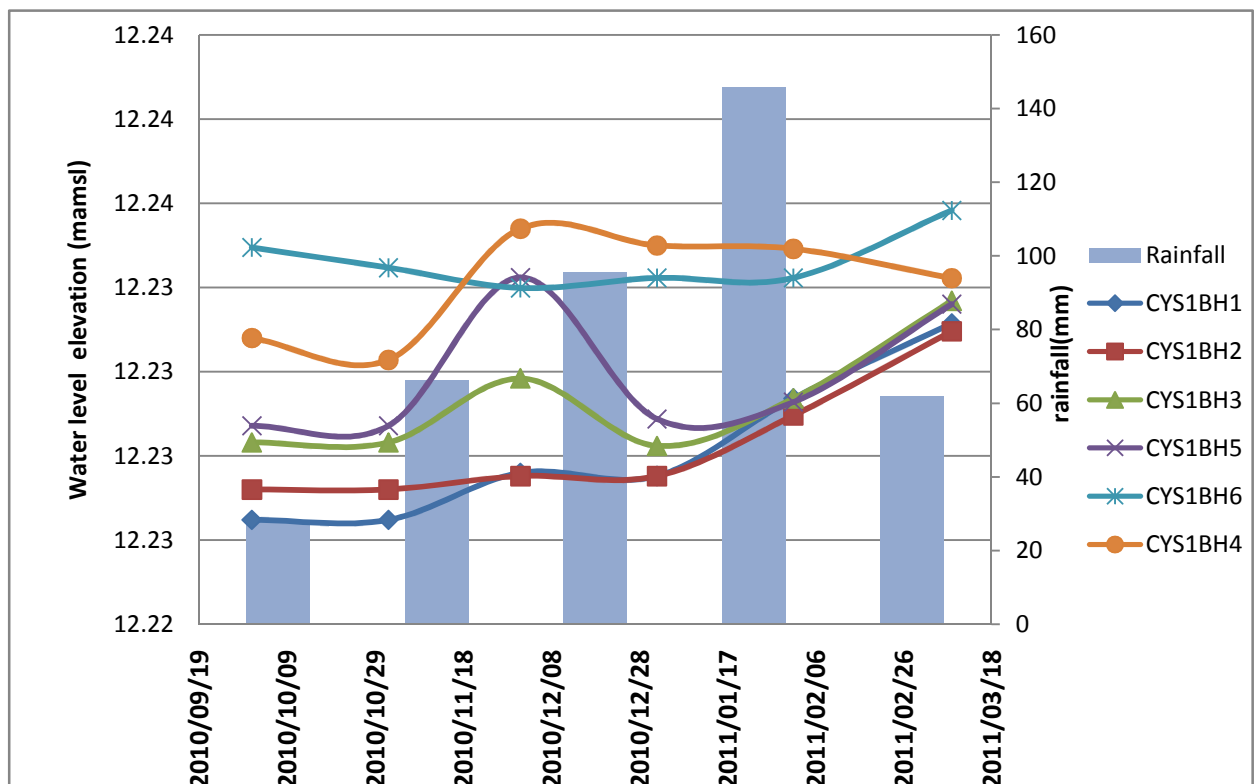


Figure 6-1: A hydrograph of monthly groundwater levels and bar graph of monthly precipitation.

On the hydrograph, the water elevation for CYS1BH3, CYS1BH4 and CYS1BH5, decrease sharply from November then increase sharply (comparatively) from January 2011 to February 2011. The possible bulkflow parameters that might be

attributed to this behaviour are high transmissivities and/or specific yields and hydraulic conductivity of the unsaturated alluvium gravel resulting in rapid flow of infiltrated water. CYS1BH2 shows almost the same behaviour as the rest of the wells because it overlies the gravel unit and hence might be feeding water from beneath. The water level elevations were falling in the period between September and October 2010 in response to low rainfall events (Figure 6-1). CYS1BH6 exhibits a complete different behaviour where water levels only fluctuate slightly from September to February. This borehole was dry when it was drilled and the water measured must have hypothetically been due to recharge from local precipitation events. When there has not been any shear stresses induced by tectonic movement or nonhydrostatic stresses on the mudstone formation, the dilatant structures do not increase and hence low permeability and transport properties of the strata (Ishii *et al.*, 2011) Indeed a major characteristic of the Karoo Supergroup, which consists mainly of sandstone, mudstone, shale and siltstone, is their low permeability such that the majority of boreholes drilled in the Karoo formations have very low immediate yields (<1 l/s) (Woodford and Chevallier, 2002).

The plot of groundwater level data against elevations for each well from which the water levels were measured indicate 81% correlation (Figure 6-2). It is subsequently inferred that groundwater elevation follows topography along the site drainage pattern. The water levels deepen with distance towards the southern at the study area while progressively diminishing with distance towards the river where boreholes close to the river show deeper static water levels. This observation presumably indicates the dominance of downward groundwater flow at the site.

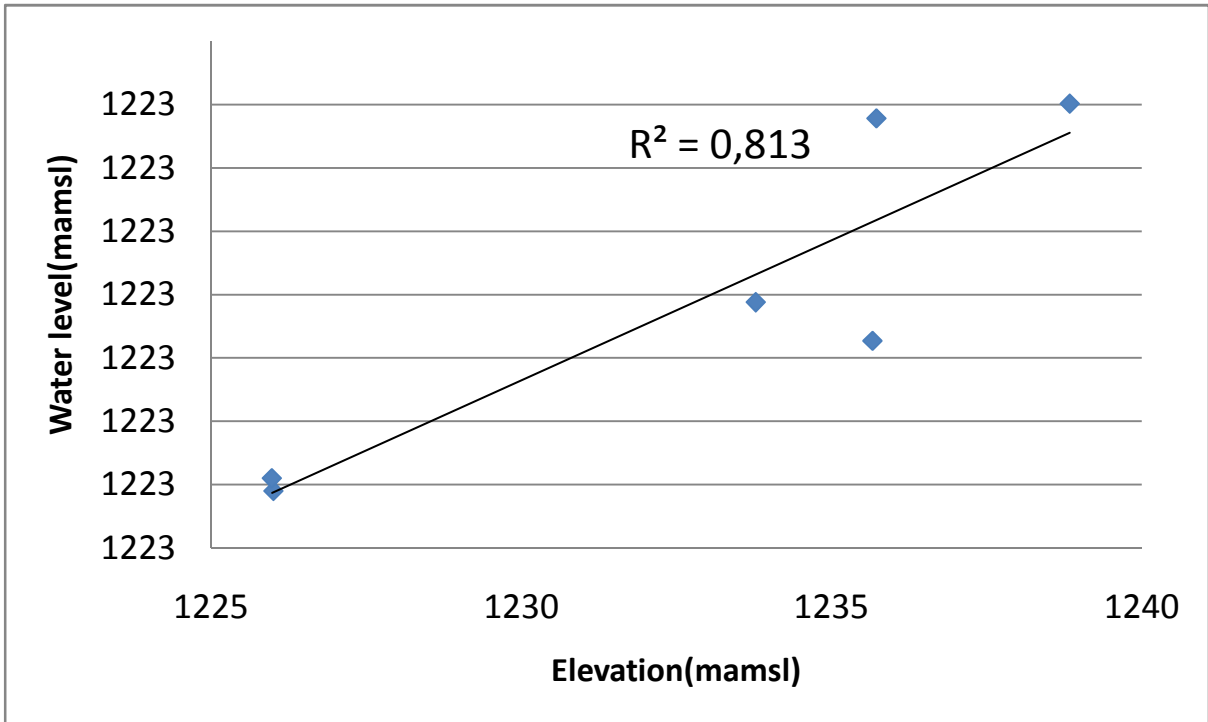


Figure 6-2: Water level as a function of elevation.

**6.2.2 Groundwater direction and slope**

A minimum of three hydraulic heads measurement from wells in a triangular arrangement are required to determine hydraulic gradient and the direction of flow (Schwartz, 2003). As a result therefore, the groundwater flow direction and slope for the study domain defined were determined by examining both small scale magnitudes of gradients using two sets of three-well elements to generate gradient field (triangle one: CYS1BH1, CYS1BH2 and CYS1BH3, triangle two: CYS1BH5, CYS1BH1, and CYS1BH2). It was also useful to determine a single large-scale gradient for the site in which all the wells in the study domain were used to determining the direction and magnitude of the hydraulic gradient. This criterion can only be used when the gradient obtained from at least two three-well elements show the gradient to be almost uniform. All the six wells were used in this criterion.

### 6.2.2.1 Small-scale gradients and mathematical preliminary

The groundwater small-scale magnitudes of gradients and direction of flow were determined using two sets of three-well element to generate gradient field (Figure 6-3 and Figure 6-4). The triangular interpolation technique using the cross product (a binary operation on two vectors in three- dimensional plane) methodology:

If the Cartesian component vectors of BH1= (x<sub>1</sub> y<sub>1</sub> z<sub>1</sub>), BH2= (x<sub>2</sub> y<sub>2</sub> z<sub>2</sub>), and of BH3= (x<sub>3</sub> y<sub>3</sub> z<sub>3</sub>) then:

A= BH<sub>2</sub> - BH<sub>1</sub>= (a<sub>1</sub>, a<sub>2</sub>, a<sub>3</sub>), and

B= BH<sub>3</sub> - BH<sub>1</sub>= (b<sub>1</sub>, b<sub>2</sub>, b<sub>3</sub>).

The vector product of the two vectors (A and B) in matrix form is given by:

$$A \times B = \begin{vmatrix} i & j & k \\ a_1 & a_2 & a_3 \\ b_1 & b_2 & b_3 \end{vmatrix}$$

Equation 6-1

Where (i, j, k) are unit Cartesian vectors.

Using Sarrus' rule, the expanded form of the above matrix is:

$$\begin{aligned} A \times B = & [(y_1 - y_2)(z_3 - z_1) - (z_2 - z_1)(y_3 - y_1)]i \\ & + [(z_2 - y_1)(x_3 - z_1) - (x_2 - z_1)(z_3 - z_1)]j \\ & + [(x_2 - x_1)(y_3 - y_1) - (y_2 - y_1)(x_3 - x_1)]k \end{aligned}$$

Equation 6-2 (Botha, 1994)

$$\therefore \alpha \cong \cos^{-1} \left[ \frac{A \cdot B}{\sqrt{A \times B}} \right]$$

Equation 6-3

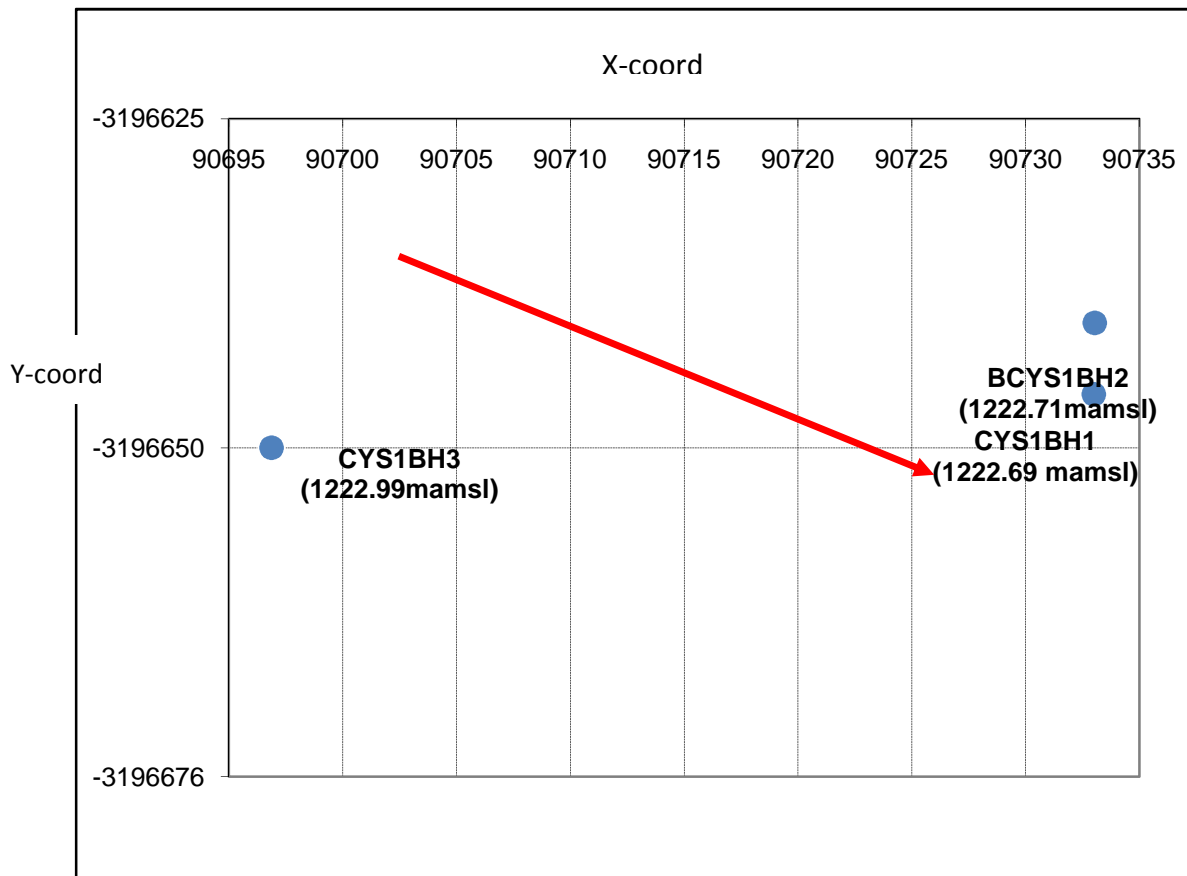


Figure 6-3: Cross product output depicting estimated groundwater flow direction inferred from CYS1BH3, CYS1BH1 and CYS1BH2.

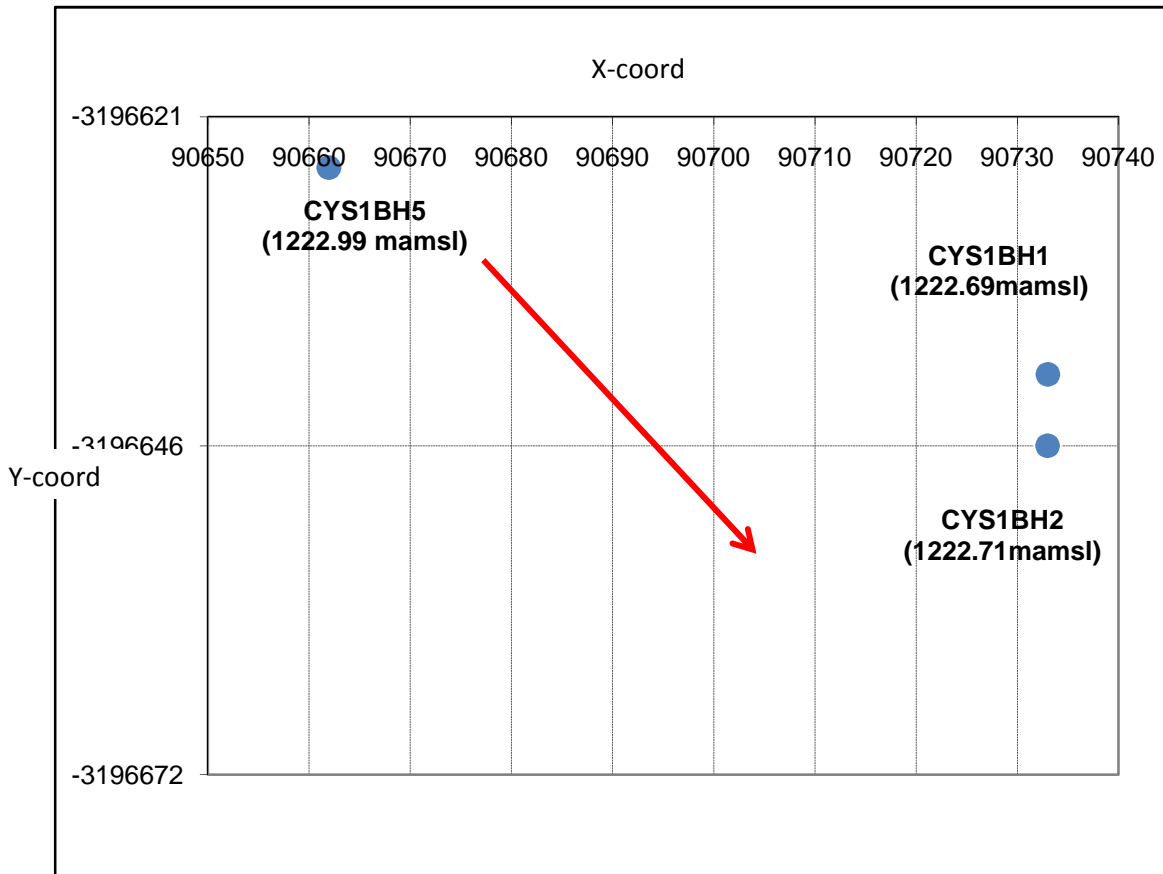


Figure 6-4: Cross product output depicting estimated groundwater flow direction inferred from CYS1BH5, CYS1BH1 and CYS1BH2.

### 6.2.2.2 Single large-scale gradient

Groundwater gradient and direction were estimated using the triangular Interpolation technique that defines the plane through three Cartesian component vectors [ $P_1=(x_1, y_1, z_1)$ ,  $P_2=(x_2, y_2, z_2)$  and  $P_3=(x_3, y_3, z_3)$ ] by the following equation of the plane:

$$Ax + By + Cz - D = 0$$

Equation 6-4

Where; A, B and C are the vectors defining the plane. D is the vector representing the position of an arbitrary but fixed point on the plane. Therefore, A, B, and C can be visualised as vectors starting at D and pointing in different directions along the plane.

In explaining the Cartesian co-ordinate system, Botha (1994) says one firstly choses a position of an arbitrary but fixed point called origin. From this point, three principal and mutually perpendicular straight lines (known as axes of the coordinate system) parallel to the three directions in space are established. The set of integers equidistance along each of the axes starting from the prescribed origin are assigned. Subsequently, the spatial position of any point can be specified from the origin. The distance are commonly denoted by  $(x,y,z)$  set of spatial coordinates (Botha, 1994).

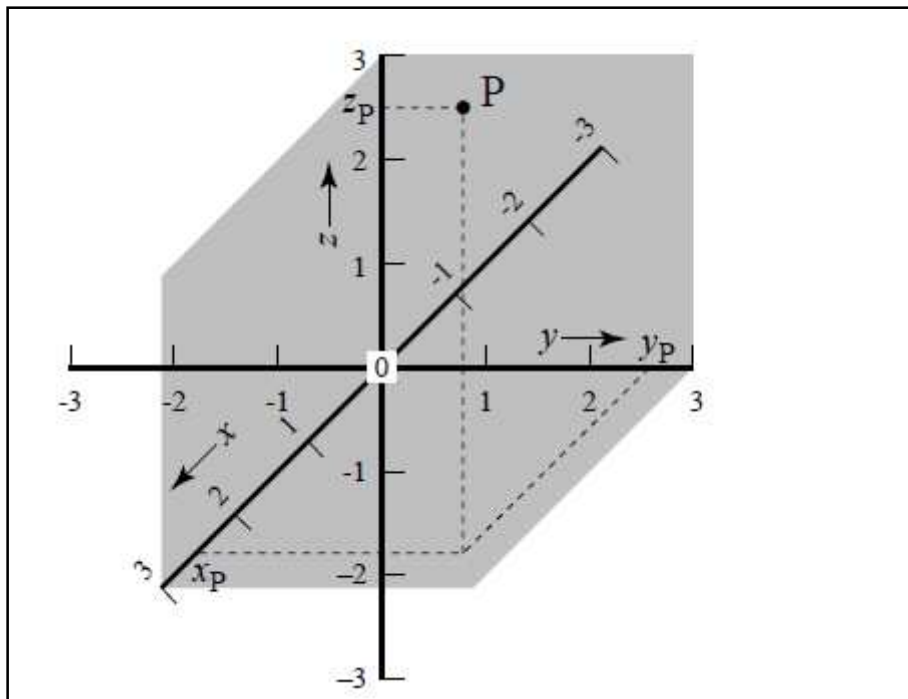


Figure 6-5: Schematic illustration of a right handed Cartesian co-ordinate system (Botha, 1994).

In this instance, the plane is thought to be representing the water table or piezometric surface so that  $x$  and  $y$  become the horizontal coordinates of the given well and  $z$  is the static water table elevation. The gradient and direction of flow between  $P_1$ ,  $P_2$  and  $P_3$  can then successfully be estimated by calculating  $A$ ,  $B$ ,  $C$  and  $D$  (Devlin, 2002).

The groundwater flow direction and gradient were calculated by the methodology adopted from “A spreadsheet method of estimating best-fit hydraulic gradients using

*head data from multiple wells*” by Devlin (2002) for each of the monthly water table data collected over a period of five consecutive months. In his paper, Devlin (2002) represents the water table surface by the plane in which the intercepts in each of the principal axes (Figure 6-6) are easily calculated from Equation 6-4. The matrix solving functions of the Microsoft excel spreadsheet (GRADIENT.XLS) by Devlin were used to determine the equation of the water table plane. The coefficients of the equation of the plane solved and used to determine the magnitude of the hydraulic gradient and direction of flow using Equation 6-5 and Equation 6-6 whose complete derivations can be found in the priori mentioned paper by Devlin.

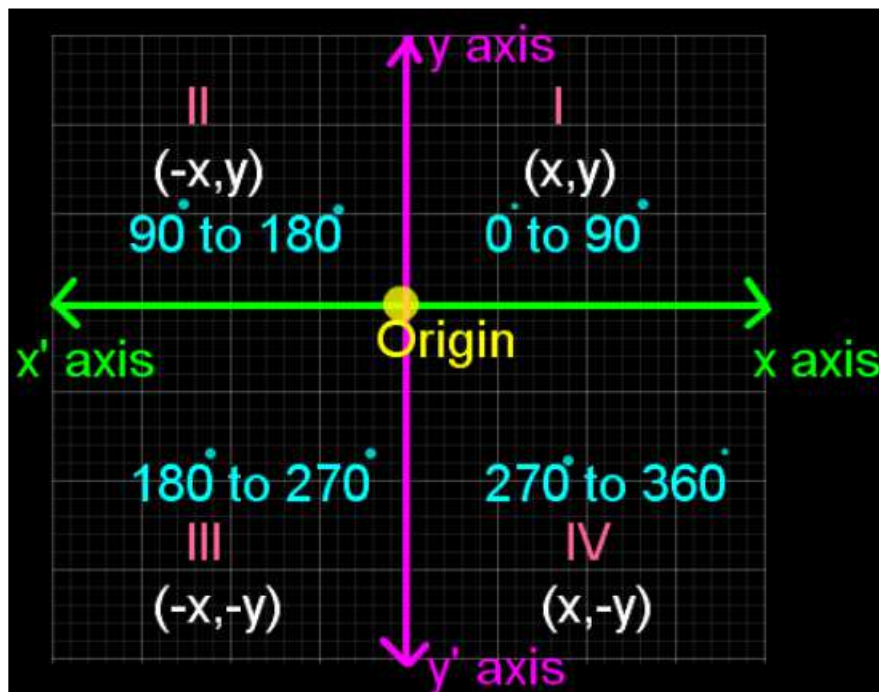


Figure 6-6: Schematic of Cartesian graph plane illustration on which the groundwater direction is read on the plane.

$$gradient = \sqrt{\frac{A^2 + B^2}{C^2}}$$

Equation 6-5



$$\alpha = \arctan \frac{B}{A}$$

Equation 6-6

### 6.2.2.3 Results and discussions

The movement of groundwater within a given flow domain is governed by head differences between the water levels as measured from each of the boreholes in a domain. Darcy's law accentuates that the direction of the exchange processes varies with hydraulic head so that flow occurs if and only if there is a difference in hydraulic heads creating a gradient in a given direction. In this particular instance, head differences yield the hydraulic gradients towards the river. On average the hydraulic gradient is 0.0083. Both small scale and large scale methods yield flow direction estimates in the same order. Flow direction varied by  $45^{\circ}$  (this angle is read from the Cartesian graph plane) over the entire study domain, but generally trended SE, sub-perpendicular to the regional surface water flow direction inferred.

The inferred groundwater flow direction complies with the principle of water level-elevation correlation in which flow is along the site drainage pattern (i.e. south-east towards the river). The wire frame visualisation (surfer interpolation) of the site in three dimensions with flow direction is also shown in Figure 6-7. The direction of flow is read relative to the Cartesian graph plane. For detailed explanation on the system, the reader is referred to "*Models and Theory of Groundwater Motion. Unpublished report*" by Botha (1994).

TABLE 6-2: GROUNDWATER GRADIENT AND DIRECTION OF FLOW.

Date	Gradient	Direction of flow (degrees)
22/10/2010	0.0071	45
14/11/2010	0.015	45
01/12/2010	0.0044	45
13/01/2011	0.014	45
09/02/2011	0.0024	45

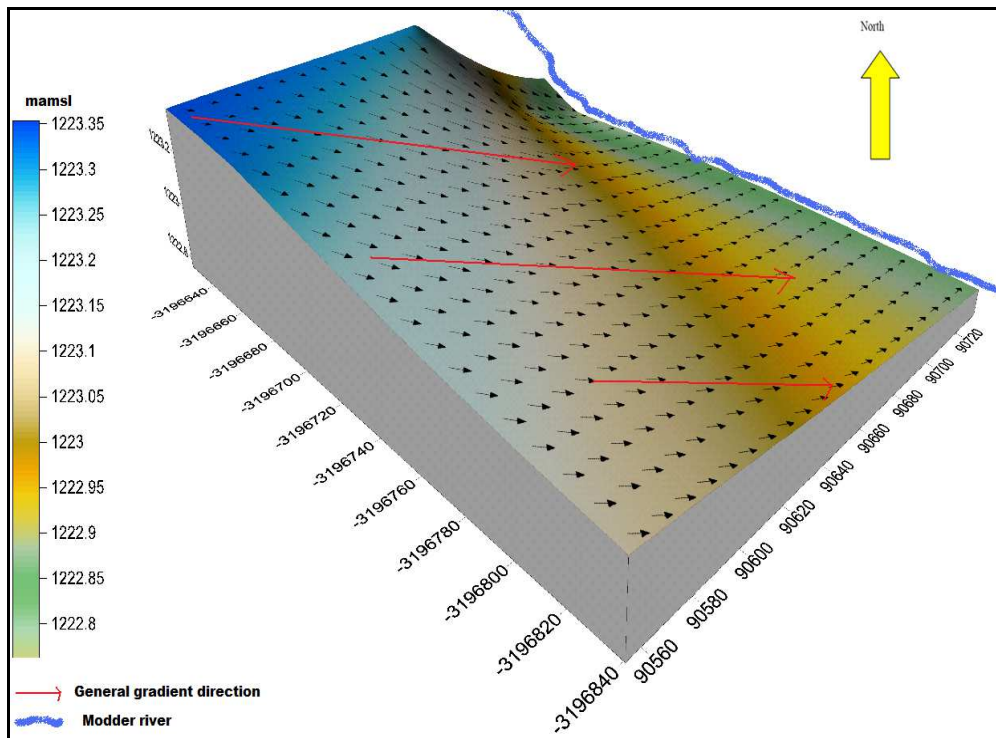


Figure 6-7: The contour map showing horizontal groundwater flow direction in three dimensions.

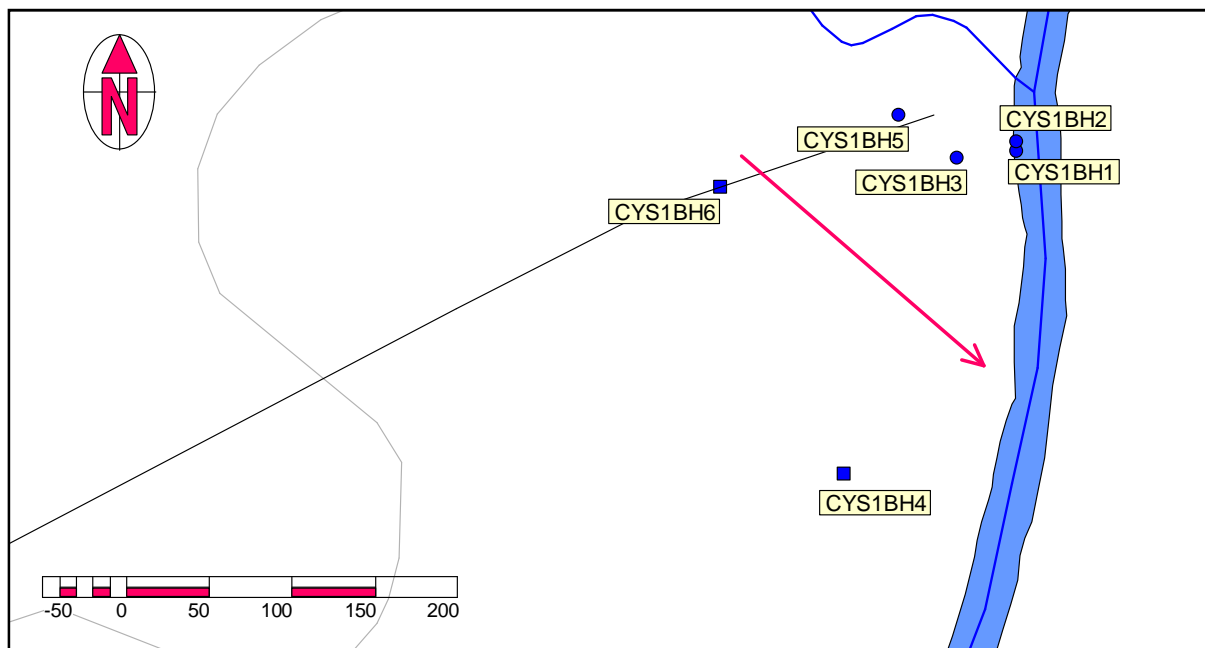


Figure 6-8: A map illustrating and depicting groundwater flow direction.

## 6.3 Deducing flow section

### 6.3.1 Borehole Electrical Conductivity (EC) Profiling

Borehole conductivity logs, measured with an EC-meter under natural conditions, give a good estimation of the depth of the flow zones hence aid in identifying section at which flow occurs in each well. By using salt as a tracer, the estimated position of the geological section acting as the flow conduit can be verified. In CYS1BH3, CYS1BH4 and CYS1BH5, the EC-profiles show flow zones at 11m, 16m and 19m respectively as seen from the jump in the EC-concentrations (Figure 6-9, Figure 6-10 and Figure 6-11). The increase in the EC-concentration from 12.9 and 24 metres for CYS1BH3 and CYS1BH4 respectively may be due to increased flow because of the sand gravel fraction at these depths. Usually, coarser sand particles with larger in diameter tend to settle first so that the hydraulically conductivity is increased at the deeper depths.

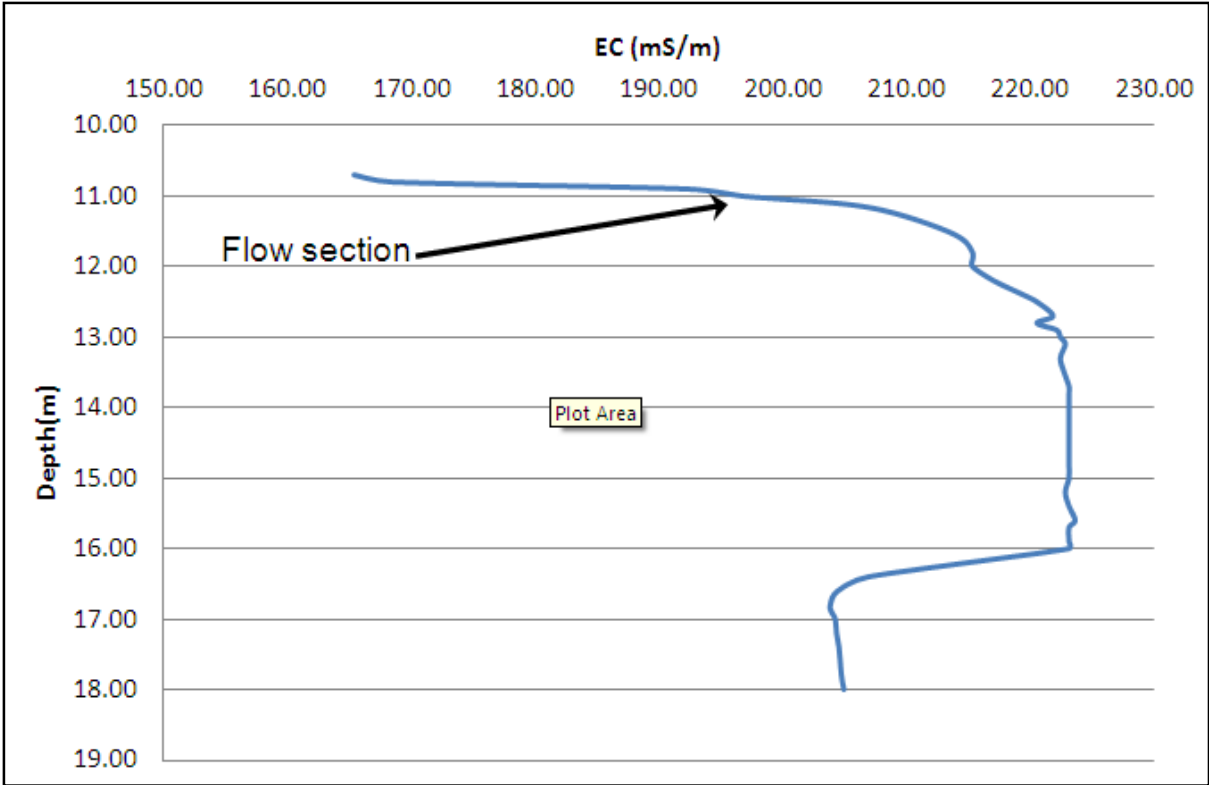


Figure 6-9: Borehole conductivity log for CYS1BH3

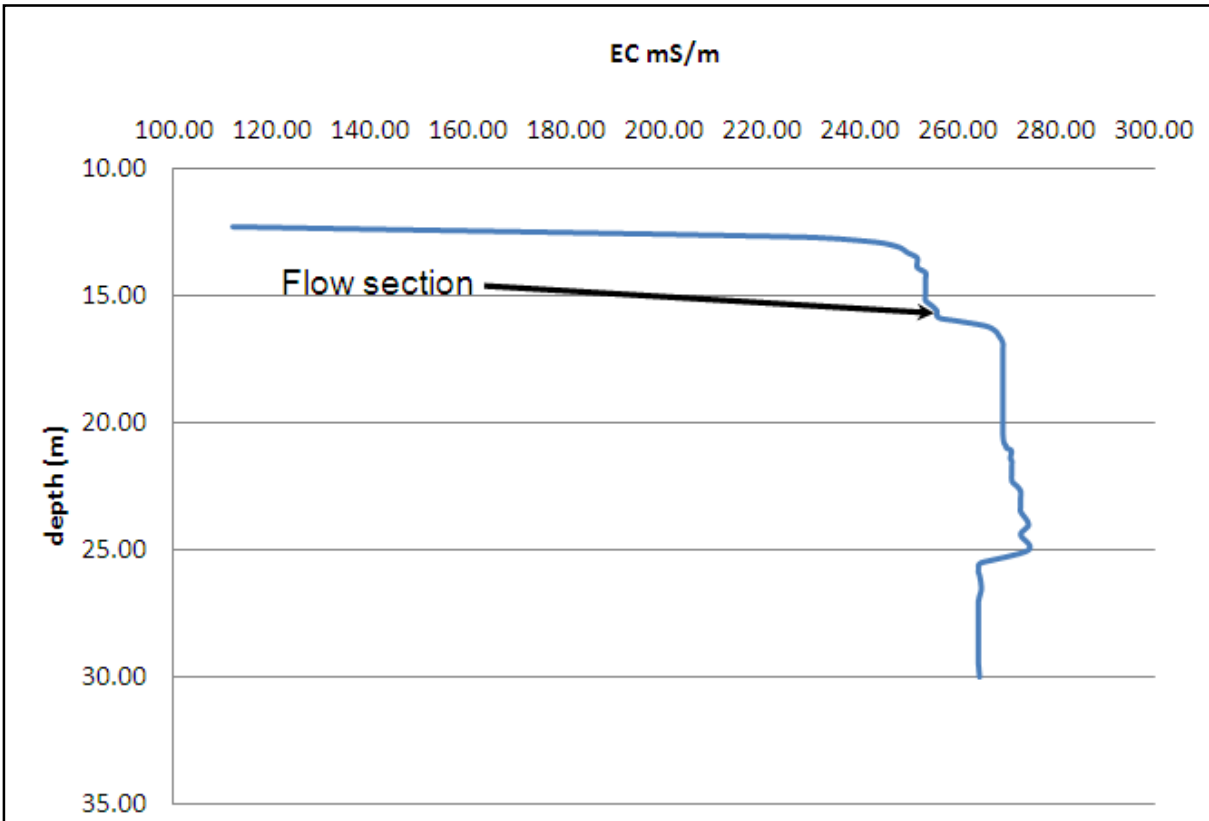


Figure 6-10: Borehole conductivity log for CYS1BH4.

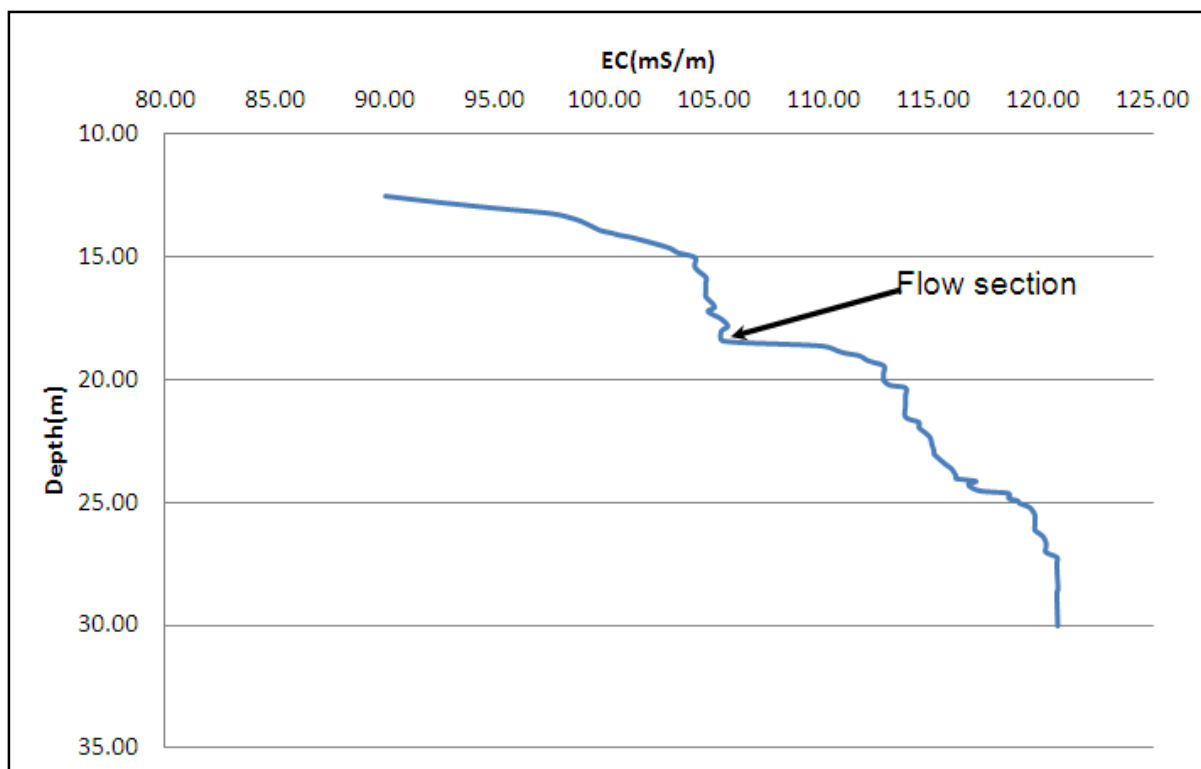


Figure 6-11: Borehole conductivity log for CYS1BH5.

### 6.3.2 Pumping test

Following the identification of the lithological unit that serves as the flow section, pumping test was used in this part to infer whether or not the gravel intercepted by the wells was the common source for all these wells. During this test, water was abstracted from borehole CYS1BH3 at a constant rate of 0.82 l/s and water levels were measured with levelloggers in boreholes CYS1BH5 (distance 34 m from the pumping well). Both wells intersected the same aquifer unit; more importantly the gravel unit which was confirmed from borehole EC logging to be the major flow conduit. Figure 6-12 shows the measured drawdown values of the test in CYS1BH3 together with the drawdown values measured in CYS1BH5 used as the observation. A very interesting feature is that the water level drawdowns in the boreholes that intersected the same flow source were very alike.

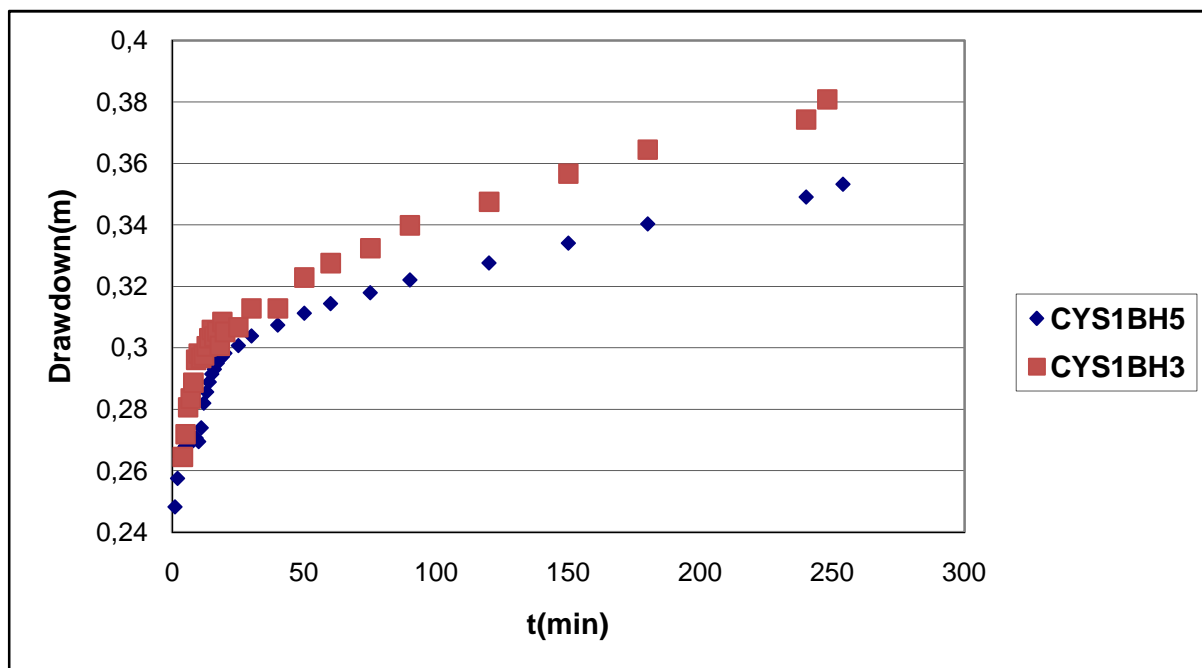


Figure 6-12: Pumping test showing the drawdown behaviour in boreholes CYS1BH3 and CYS1BH5.

### 6.4 Conclusions

On the hydrograph for CYS1BH3, CYS1BH4 and CYS1BH5, water levels decrease sharply from November then increase sharply from January of the following year to February. CYS1BH2 shows almost the same behaviour as the rest of the wells because it overlies the gravel unit and hence might be feeding water from beneath. CYS1BH6 exhibits a complete different behaviour where water levels only fluctuate slightly from September to February hypothetically in response to recharge from local precipitation events.

Head differences yield the hydraulic gradients from the terrestrial aquifer towards the riparian aquifer and into the channel aquifer. On average the hydraulic gradient is 0.0083. Both small scale and large scale methods yield flow direction estimates in the same order. Flow direction varied by 45° (read on the Cartesian coordinate system) over the entire study domain, but generally trended SE, sub-perpendicular to the regional surface water flow direction.

In CYS1BH3, CYS1BH4 and CYS1BH5, the EC-profiles show flow zone at 11 m, 16 m and 19m respectively as seen from the jump in the EC-concentrations. Significant or increased flow for CYS1BH3 is however noticed at 12.9m while that of CYS1BH5 is at 24m.

When water was abstracted from borehole CYS1BH3 while observing the water level in CYS1BH5 (distance 34 m from the pumping well) the water-level drawdowns in the boreholes that intersected the same flow source were very similar.

## 7 AQUIFER HYDRAULIC AND PHYSICAL PARAMETISATION

### 7.1 Introduction

Determination of aquifer hydraulic and transport properties is an important step in understanding groundwater flow systems. Pumping and tracer tests are widely used as *in-situ* techniques for measurements of hydraulic and transport properties of an aquifer. Appropriately planned and conducted, these tests help define the overall hydrogeologic regime of ground water flow systems.

This chapter is aimed at applying suitable techniques in order to measure and estimate aquifer hydraulic and transport properties as well as the baseflow contribution of the aquifer system at the study area.

### 7.2 Hydraulic parameters

Hydraulic characteristics of an aquifer are usually determined by hydraulic tests normally conducted to measure the drawdown or pressure response in one or more boreholes, and to relate this response to the hydraulic properties of the aquifer. The pumping test data is then analysed using graphical or computational methods which are based on the analytical solutions for groundwater flow. Analysis of aquifer tests are frequently carried out with the analytical model from which aquifer parameters are estimated and measured by fitting a straight line to drawdown on an arithmetic axis vs. time on a logarithmic axis in a semilog plot (Kruseman and De Ridder, 1994).

The most common hydraulic test is the constant discharge test or constant rate test, where water is abstracted from a borehole at a constant discharge rate. The change in pressure or drawdown in the borehole or observation boreholes is measured and can be related to the aquifer properties.



### 7.2.1 Fieldwork, results and discussion

Pumping tests were undertaken in three main phases. The first was an equilibration period (head equilibration) where transient effects in the test zone were allowed to dissipate. The second was diagnostic and main phase where the order of magnitude of pumping response was observed; allowing selection of an appropriate hydraulic test discharge rate. In this phase, hydraulic response was monitored over a period of four hours. The last was a recovery phase where the flow field was reversed and residual drawdown data was collected.

Constant discharge hydraulic tests were executed on all the wells over a period of four hours (except for CYS1BH2 and CYS1BH6) using a submersible pump. Pumping tests on both CYS1BH2 and CYS1BH6 were stopped once the wells dried out. The wells were pumped at a constant rate of 0.82l/s pumping rate while the wells that dried out (CYS1BH2 and CYS1BH6) were pumped at 0.28l/s and 0.2l/s respectively. Drawdown recovery period data were collected with the solinst levelloggers installed in both pumping and observation wells. After the pumping test ended, the levelloggers remained in the wells to record residual/recovery drawdown.

Both the resultant pumping and residual drawdowns were analysed as a function of time (Figure 7-1 and Figure 7-2). Transmissivity values were estimated by applying the Cooper-Jacob method to the late-time drawdown data. Specific yields were estimated by deploying the water table (Neuman) method (Figure 7-3) that treats the aquifer as a compressible system and the watertable as a moving material boundary while taking into account the existence of vertical flow components (Kruseman and De Ridder, 1994) The analytical solving functions of the excel spreadsheet (FC-method) was used to calculate the four aquifer parameters using pumping test drawdown and residual drawdown. Table 7-1 summarises the values of T, and  $S_y$  for the aquifer under study.

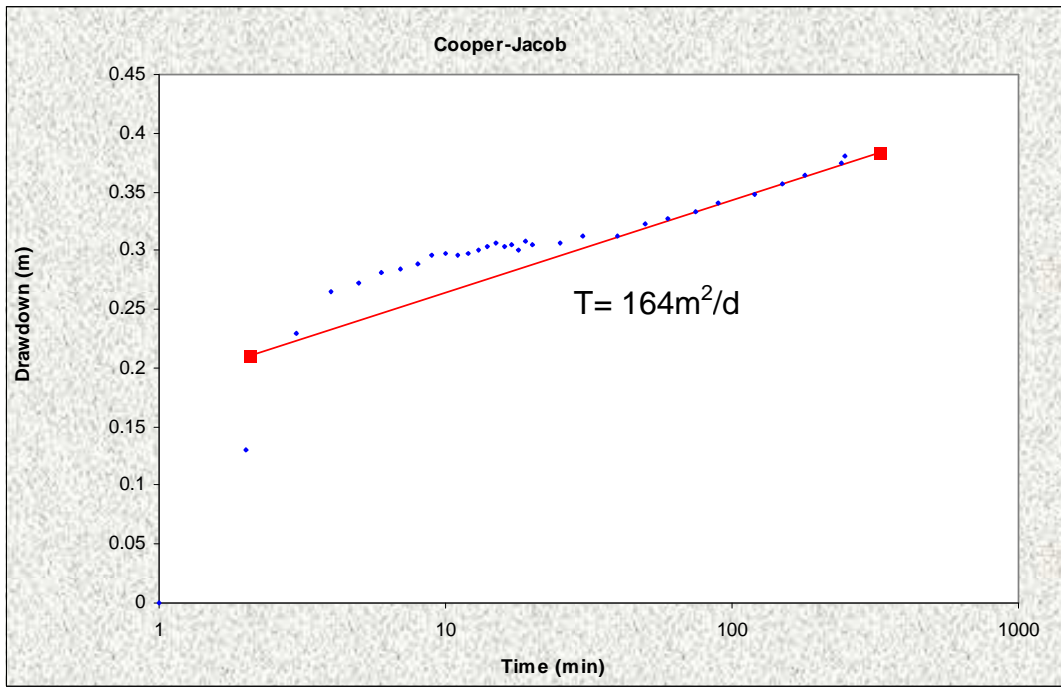


Figure 7-1: A Cooper Jacob fit for CYS1BH3.

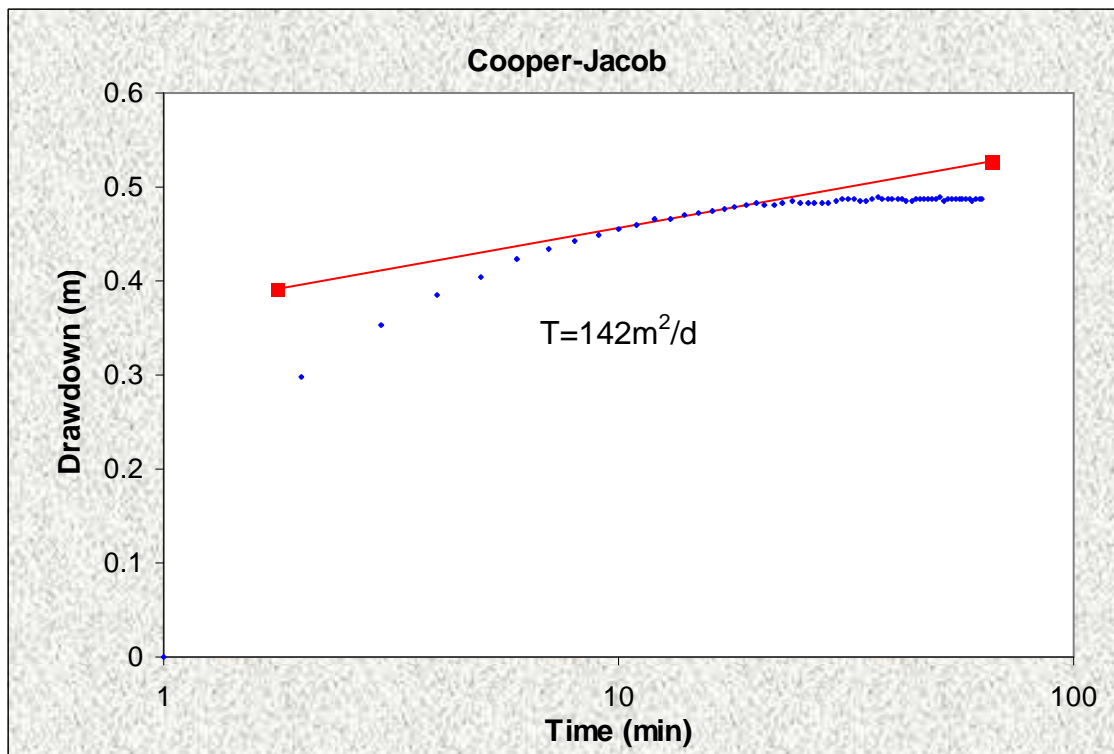


Figure 7-2: A Cooper Jacob fit for CYS1BH1.

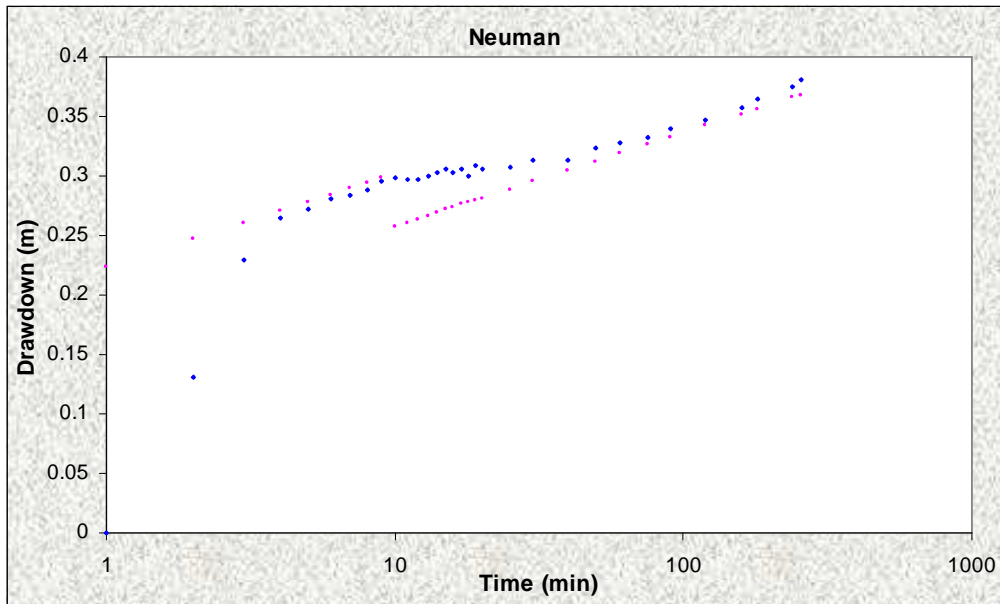


Figure 7-3: Neuman fit for CYS1BH3 pumping test data.

TABLE 7-1: AQUIFER PARAMETERS ESTIMATED FROM PUMPING TEST

Borehole ID	CYS1BH1	CYS1BH2	CYS1BH3	CYS1BH4	CYS1BH5	CYS1BH6
T (m <sup>2</sup> /d)	142.00	0.30	164.00	130.00	138.00	0.70
S <sub>y</sub>	-	-	0.02	-	0.005	-

### 7.3 Baseflow component

This section’s aim was achieved by focusing on the groundwater-surface water interaction needs of the site characterisation and considering chiefly the groundwater situation in relation to the adjacent river. In this regard, baseflow contribution component to the river flow is of utmost importance to estimate. Following the hydrocensus or the author’s consensus, there are no additional users of groundwater in the vicinity of the study area. The biggest users of groundwater however are the riparian vegetation through evapotranspiration. As the result therefore, the following relationship was used to obtain a guestimate value of the baseflow contribution into the river flow:

Baseflow= Net flow-Abstraction

Flow in the area= Flow<sub>riparian</sub> + Flow<sub>terrestrial</sub>

Flow<sub>riparian</sub>

Q= TiL

$$=142\text{m}^2/\text{d} \cdot 0.0086 \cdot 237\text{m} = 291.4\text{m}^3/\text{d}$$

Flow<sub>terrestrial</sub>

Q= TiL

$$= 0.7\text{m}^2/\text{d} \cdot 0.0086 \cdot 237\text{m} = 1.43\text{m}^3/\text{d}$$

Netflow= 291.4 + 1.43

$$=293\text{m}^3/\text{d}$$

Evapotranspiration value was taken from the reference evapotranspiration map (Figure 7-4) because no evapotranspiration studies had been undertaken at this stage of the project; subsequently, computations resulting from the use of this value are just guesstimate. The evapotranspiration used here is 0.0062m/d.

Abstraction= evapotranspiration \* total area

$$=0.0062\text{m}/\text{d} \cdot 47400\text{m}^2 = 294\text{m}^3/\text{d}$$

Therefore:

Baseflow = 293m<sup>3</sup>/d- 294m<sup>3</sup>/d

$$=-1\text{m}^3/\text{d}$$

The minus value signifies that there is no base flow contribution of groundwater into the river suggesting that most groundwater is used up by the riparian vegetation. It is important to note however that not all baseflow is derived from groundwater but baseflow also includes the contribution of interflow discharged into streams and rivers from the unsaturated zone (Parsons, 2004).

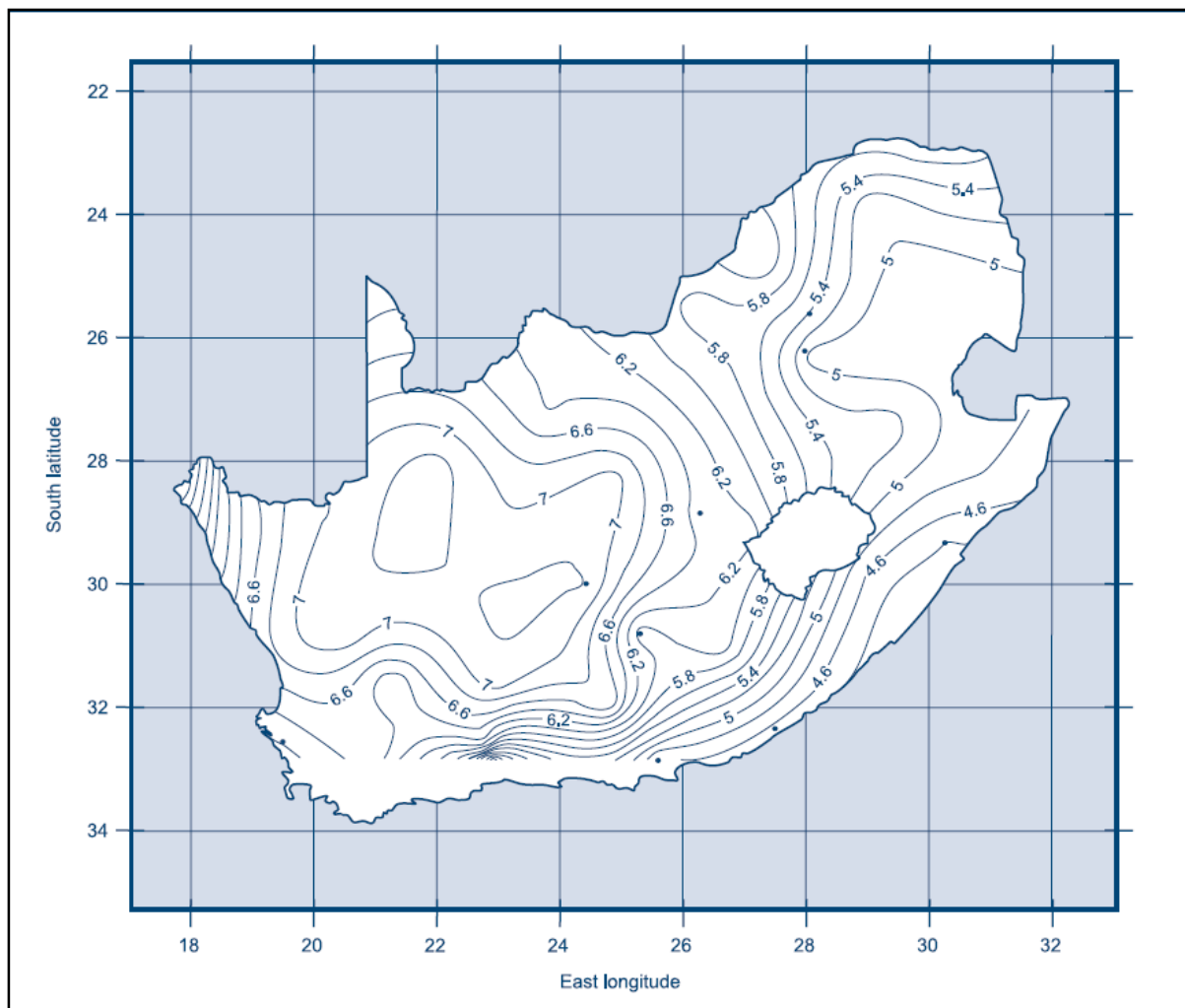


Figure 7-4: Reference evapotranspiration (mm/d) map of South Africa for the month of January (Sawva and Frenken, 2002).

## 7.4 Transport parameters

The transport parameters describe the behaviour of groundwater transport and commonly investigated using tracer tests. Tracer tests are field methods for obtaining data to describe flow and transport parameters of the aquifer using tracer substances. A tracer is a substance, which moves with the groundwater flow and can easily and accurately be detected (Guyen *et al.*, 1986). There are basically three main classes of tests: 1) single well tests, 2) two-well tests, and 3) natural gradient tests.

### 7.4.1 Groundwater tracer testing

Borehole dilution test have proved to be a powerful and simple hydrogeological tool for estimating some basic transport parameters. Therefore, a single well (point dilution) dispersion field tracer test was carried out. A particle tracer of the known mass was used and the dilution of concentration of tracer in the well monitored. The whole purpose of this test was to estimate the seepage velocity ( $v$ ), and bulk velocity ( $q$ ) of the aquifer system.

#### 7.4.1.1 Background to Single well point dilution test

A point dilution test is a single-well tracer test commonly used to estimate the flow rate within aquifers in which a tracer is introduced into a borehole and its decreasing concentration is measured over time. In other words, the single-well point dilution test relates the rate at which the tracer is diluted in a borehole to the average groundwater velocity in the aquifer (Freeze and Cherry, 1979). The principle is that the groundwater through-flow gradually removes a tracer introduced to the well from the well bore to produce a time-concentration relationship. The equation describing the dilution rate of the tracer and, under steady-state conditions, leading to a dilution curve that follows an exponential trend is as follows (Drost and Neumaier, 1974):

$$q = \frac{W}{\alpha A t} \ln \left( \frac{C_0}{C} \right)$$

Equation 7-1

Where:  $W$ = volume of fluid contained in the test section

$C_0$ = Tracer concentration at  $t = 0$ ,

$C$ = Tracer concentration at  $t = t$ .

$\alpha$ = Borehole distortion factor

$t$ = Time

$A$ = cross sectional area normal to the direction of flow ( $A = \pi r_w L$ ).

Where:  $r_w$  = Well radius;  $L$  = the length of the tested section in the borehole).

#### 7.4.1.2 *Fieldwork, results and discussion*

Well borehole dilution tests were conducted under natural gradient conditions. The tracer was injected discretely into CYS1BH3, CYS1BH4 and CYS1BH5 from a tracer injection tank. A decrease in concentration was measured over time by taking measurements of the electrical conductivity (EC) of the water using Temperature Level conductance meter (TLC). The results were analysed by generalised fractional-flow dimension equations for analysing tracer tests to estimate transport parameters. The fractional-flow dimension requires that flow dimension ( $n$ ) and flow thickness ( $b$ ) be known a priori. Flow dimension and flow thickness for respective wells were then obtained from Barker model using the pumping test data performed prior to tracer test (Table 7-2). Figure 7-5 shows a fitted Barker model of a constant discharge pumping test of CYS1BH4. It is worth noting in this regard however that, since transport parameters depend more on the geometry of the flow system than the hydraulic properties of the aquifer, the estimated flow dimension could differ from the flow dimension during the tracer test due to the scale effect (van Tonder, *et al.*, 2002).

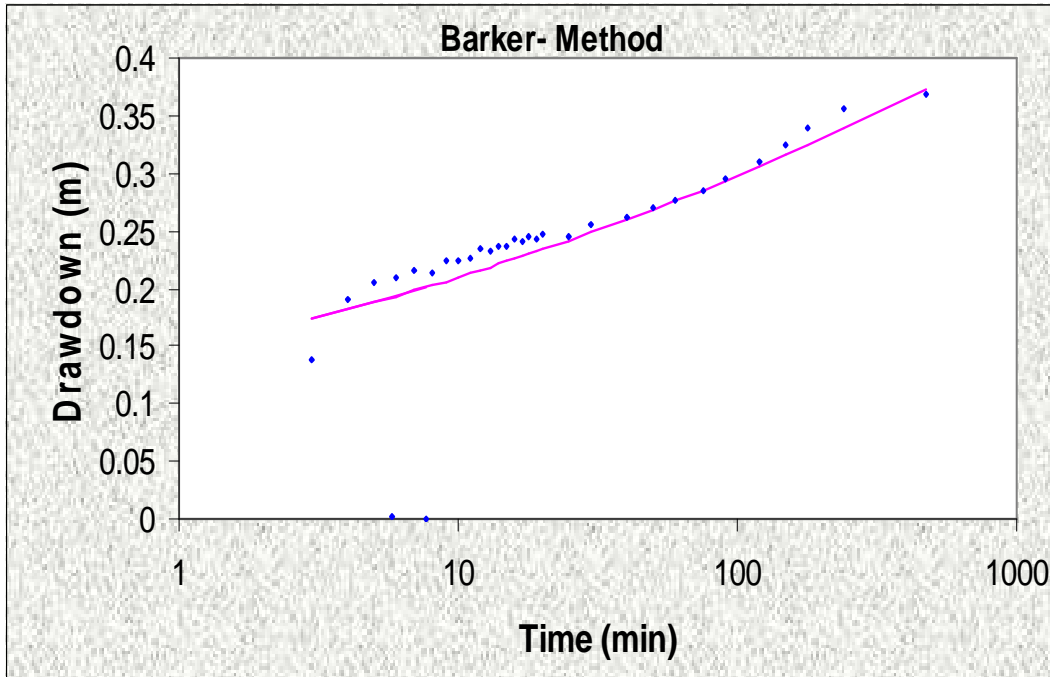


Figure 7-5: Barker model applied to CYS1BH4 used for as abstraction borehole during pumping test.

TABLE 7-2: FLOW DIMENSION (n) AND FLOW THICKNESS (b) FOR RESPECTIVE WELLS OBTAINED FROM BARKER MODEL.

Borehole ID	b(m)	n
CYS1BH3	3.37	1.75
CYS1BH4	4.48	1.75
CYS1BH5	0.2	1.75

#### 7.4.1.3 Methodology

##### ➤ CYS1BH4

A point dilution test was performed on CYS1BH4 by introducing 0.5 kg NaCl into the tested section. The setup to execute the test in this well was such that the pump was placed at 20 metres while the tracer injection inlet was placed at 15.5 metres just above the tested section (16-30 metres). The tracer concentration was then kept



constant in the tested section by constantly circulating the section's water through the tracer injection tank by pumping constantly with the 0.75l/s yield. There was no standard way in which the yield was selected, but the overall aim was to keep the water level in the tracer injection tank constant. This circulation was carried out for 24 minutes after which circulation was stopped. The circulation time was estimated as follows:

$$t_c = \frac{V_c}{Q_c}$$

Where;  $V_c$  = Volume of water in tested section

$Q_c$  = Flow rate of circulating pump

Tracer dilution was then monitored and measured for a period of 240 minutes. The EC measurements were then plotted against the time of measurements. Figure 7-8 shows the results of the dilution test. Using a flow dimension of 1.75, the Darcy velocity was estimated at 4.16 m/d. Since unconfined aquifer's specific yield equals the effective porosity because it represents the drainable pore volume (Roscoe Moss Company, 1990), estimated specific yield was used for effective porosity so that the natural flow velocity was ultimately estimated at 1.81 m/d.

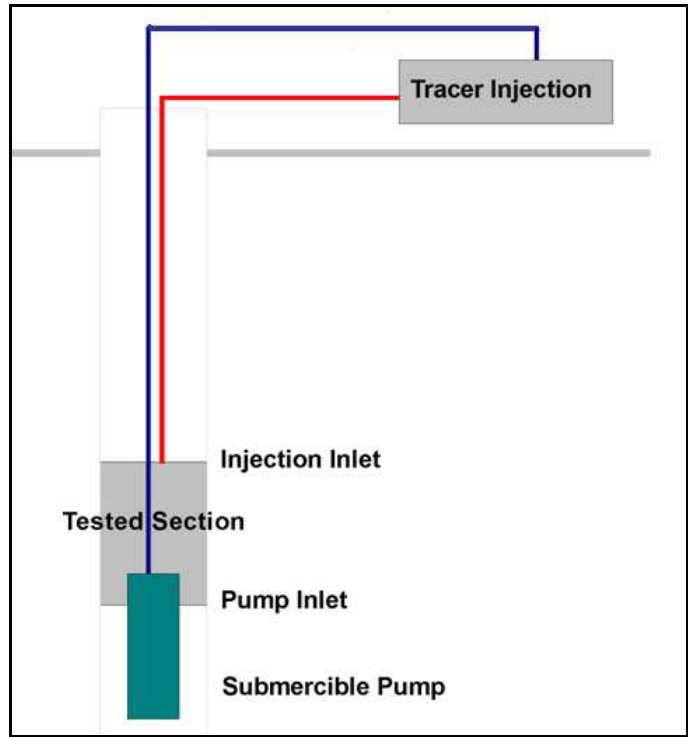


Figure 7-6: Set-up schematisation for point dilution test used during tracer testing (modified from GHR 611, 2010).

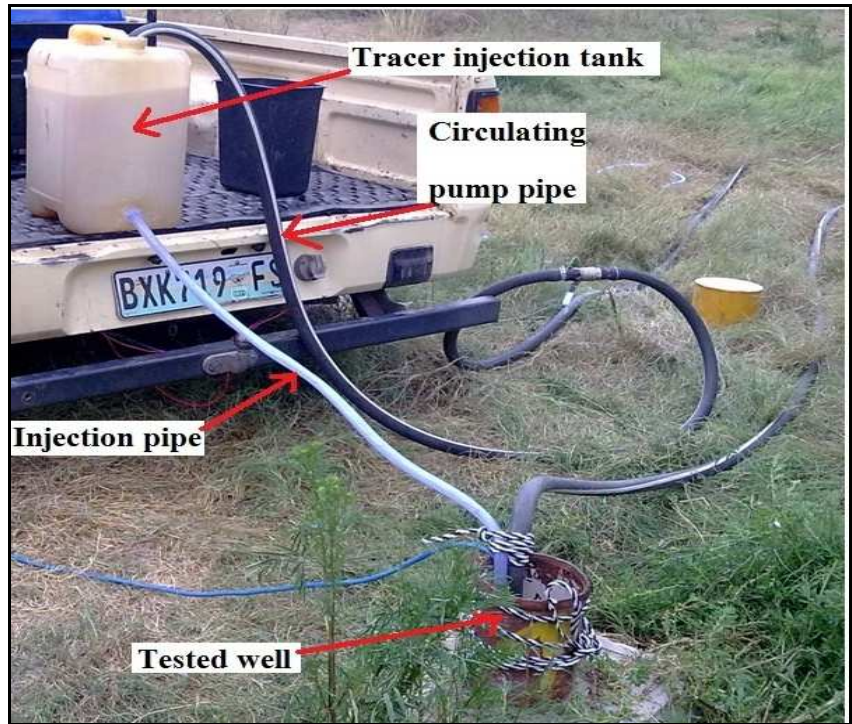


Figure 7-7: Field setup for executed point dilution test.

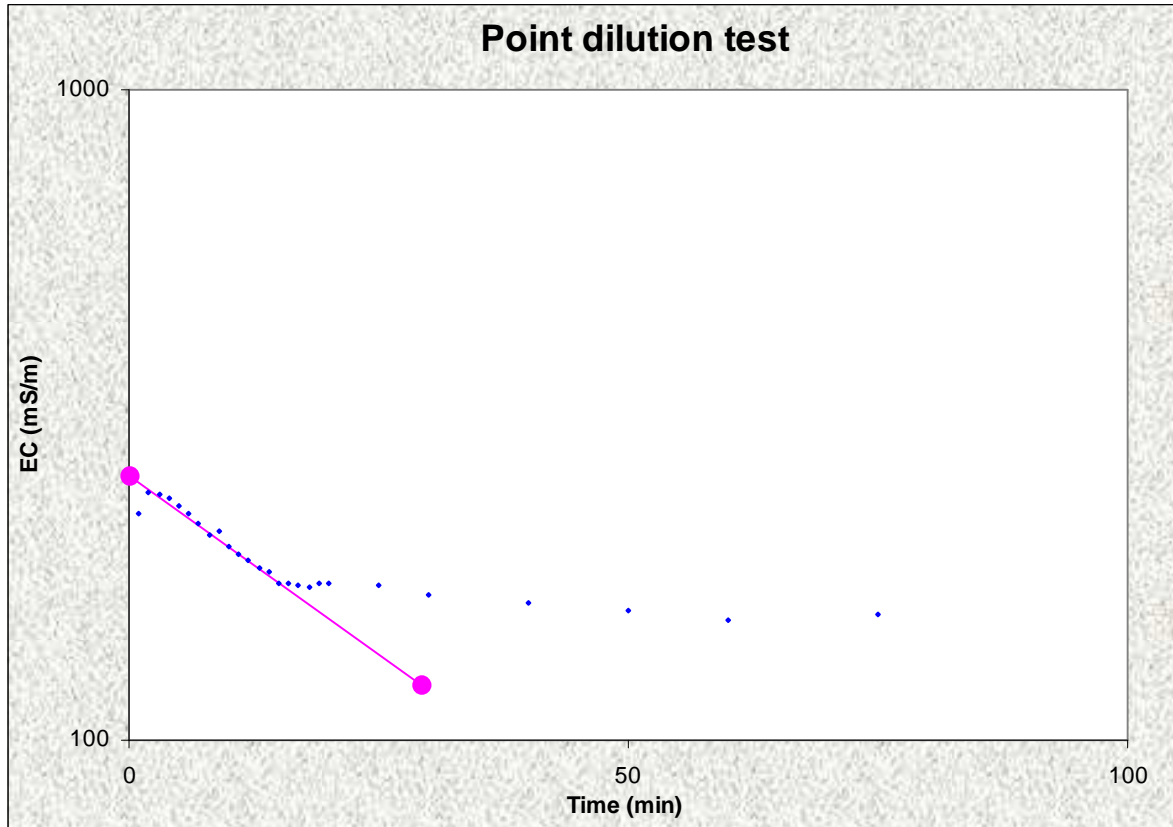


Figure 7-8: Point-dilution curve obtained during the CYS1BH4 tracer test.

➤ *CYS1BH3*

A point dilution test was performed on CYS1BH3 by introducing 0.5 kg NaCl in a section from 11 to 18 metres in the borehole. The concentration was continuously mixed by circulating the water for 10 minutes with a submersible pump at a rate of 0.75l/s in order to maintain the concentration level.

Tracer dilution was then monitored and measured for a period of 240 minutes. Likewise, the resultant EC measurements were then plotted against the time of measurements. Assuming a radial-flow field, a flow dimension of  $n=1.75$  was used to estimate the through-flow area and this area was used to estimate the Darcy velocity and hence the flow velocity. Figure 7-9 shows the results of the dilution test from which the Darcy velocity was estimated at 9.01m/d and natural flow velocity ultimately estimated at 3.92m/d.

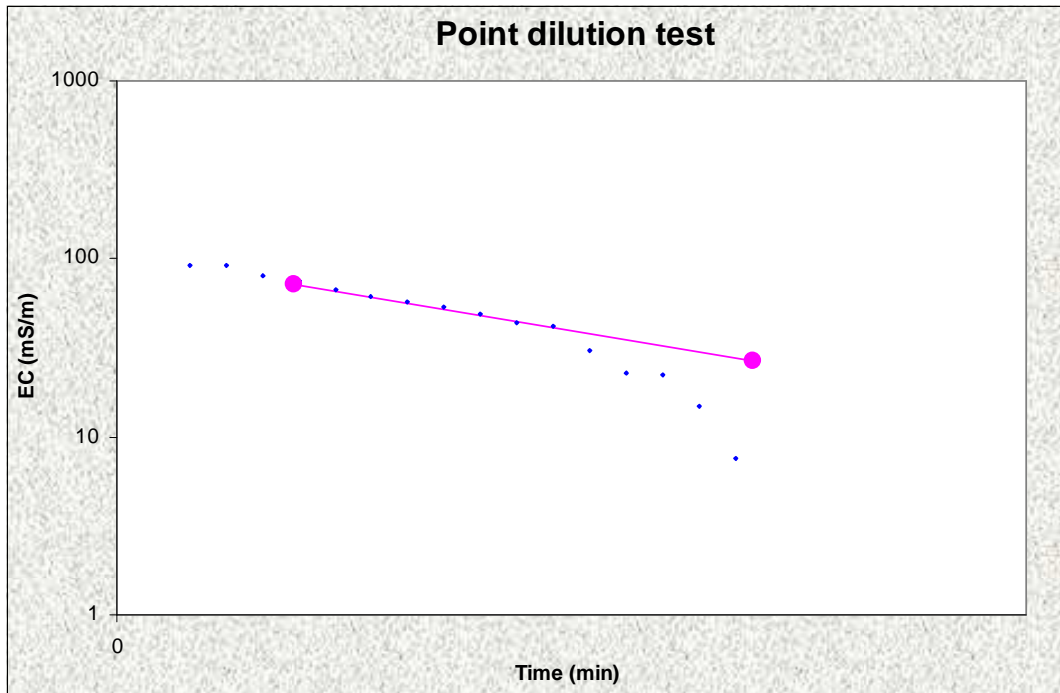


Figure 7-9: Point-dilution curve obtained during the CYS1BH3 tracer test.

➤ *CYS1BH5*

The setup to execute the test in this well was such that the pump was placed at 21 metres while the tracer injection inlet was placed just above the tested section (18.5 metres). The tested section’s water was circulated through the tracer injection tank by pumping constantly with the 0.75l/s yield in order to maintain the concentration level. The circulation was carried out for about 17 minutes following which circulation was halted. Tracer dilution was then monitored and measure for a period of 240 minutes. Figure 7-10 shows the results of the dilution test. Using a flow dimension of 1.75, the Darcy velocity was estimated at 11.24m/d and natural flow velocity ultimately estimated at 22.4m/d

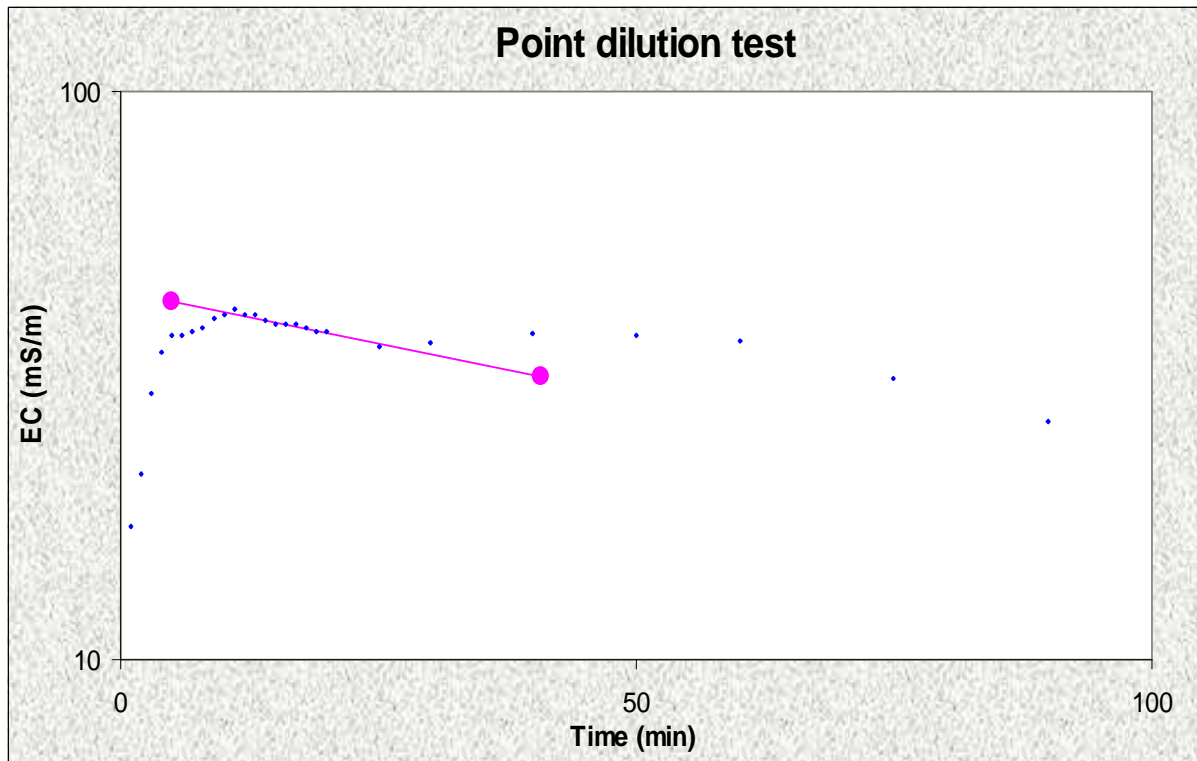


Figure 7-10: Point-dilution curve obtained during the CYS1BH5 tracer test.

TABLE 7-3: PARAMETER VALUES OBTAINED FROM THE TRACER TEST

Borehole ID	CYS1BH3	CYS1BH4	CYS1BH5
<i>Darcy Velocity (m/d)</i>	9.01	4.16	11.24
<i>Seepage Velocity</i>	3.92	1.81	22.47

## 7.5 Conclusions

The results of the constant discharge test indicate that the transmissivity of the site's aquifer ranges between  $0.3\text{m}^2/\text{d}$  and  $164\text{m}^2/\text{d}$ . Highest transmissivity estimated at a maximum level are observed in CYS1BH3, CYS1BH4 and CYS1BH5 ( $164\text{m}^2/\text{d}$ ,  $130\text{m}^2/\text{d}$  and  $138\text{m}^2/\text{d}$  respectively). An overall conclusion drawn from this is that wells located in the riparian aquifer generally have high transmissivity values while low transmissivity values ( $0.7\text{m}^2/\text{d}$ ) are associated with terrestrial aquifers. However well as wells in the riparian aquifer whose depth is limited in the upper fine sand unit have low transmissivity values ( $0.3\text{m}^2/\text{d}$ ).

The local transmissivity values from the wells drilled in the gravel of the aquifer is around  $143\text{m}^2/\text{d}$  (harmonic mean). The unconfined aquifer specific yield is in the order of 0.005(CYS1BH5) to 0.023(CYS1BH3) respectively. These values are expected to represent the gravel porosity because the pumping tests were carried out for a relatively short period during which only the gravel unit was dewatered.

Specific yields for CYS1BH2 and CYS1BH6 were not estimated as neither of the wells in the wellfield responded upon pumping of either of the wells in the study site. The guesstimate of the baseflow contribution to river flow yields a negative value that signifies that there is no base flow contribution of groundwater into the river suggesting that most groundwater is used up by the riparian vegetation.

Using a flow dimension of 1.75 for all the wells tested, the Darcy velocity was estimated at  $4.16\text{m}/\text{d}$  for CYS1BH4. Estimated specific yield was used for effective porosity so that the natural flow velocity for this well was ultimately estimated at  $1.81\text{m}/\text{d}$ . On the other hand, Darcy velocity for CYS1BH3 was estimated at  $9.01\text{m}/\text{d}$  with natural flow velocity ultimately estimated at  $3.92\text{m}/\text{d}$ . Lastly was CYS1BH5 whose Darcy velocity was estimated at  $11.24\text{m}/\text{d}$  and natural flow velocity ultimately estimated at  $22.4\text{m}/\text{d}$ . The estimated velocities are relatively high and this observation holds true for transmissivities so high.

## 8 CONCLUSIONS, PERSPECTIVES AND FLOW SYSTEM CONCEPTION

### 8.1 Introduction

The overall aim of this study was to undertake a hydrogeological characterisation in order to develop a groundwater flow system conception. This was achieved by focusing on the groundwater-surface water interaction needs of the site characterisation and considering chiefly the groundwater situation in relation to the adjacent river. After the assimilation and interpretation of the site characterisation data (Figure 8-1), a revised conceptual model that best suits the observed data or conclusions from each of the thesis' chapters for the aquifer in question is developed in this chapter. In other words, lithological characteristics, aquifer hydrogeology, and groundwater hydrogeochemistry from the previous chapters are synthesised to produce a detailed conceptual model for the site.

### 8.2 Characterisation Methodology

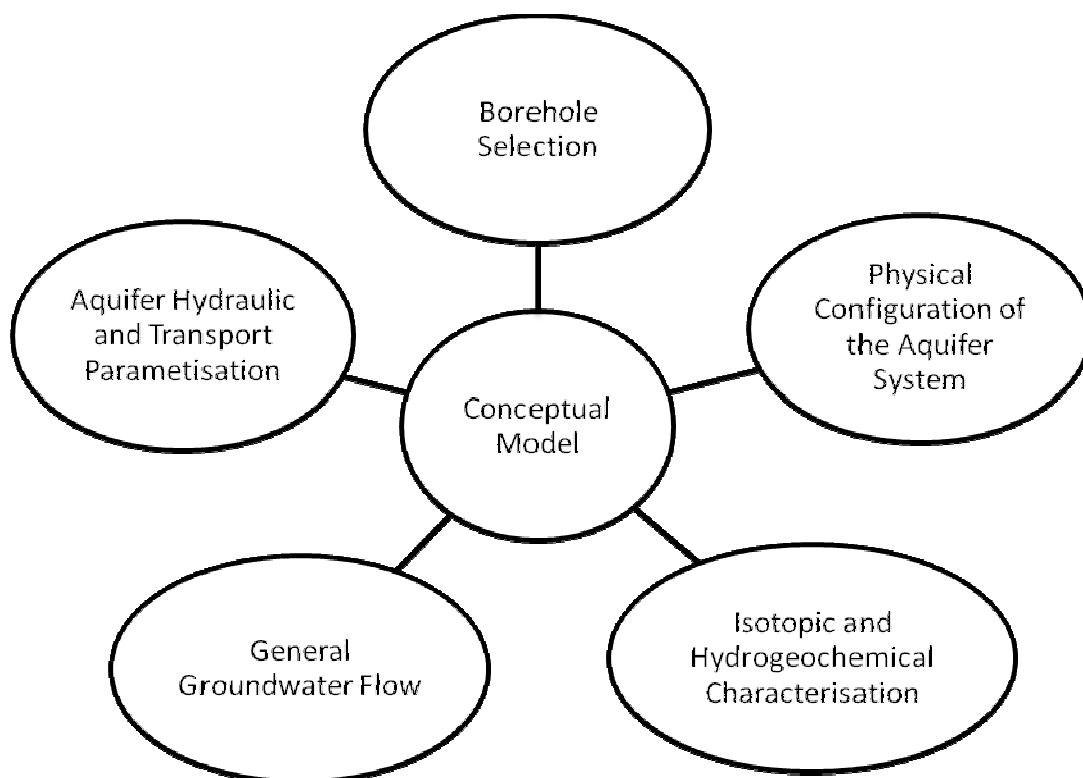


Figure 8-1: A Proposed methodology to constructing the conceptual model.

### **8.2.1 Borehole selection**

The study was conducted on the 6-spot pattern well array of CYS1 (BH1, BH2, BH3, BH4, BH5 and BH6) cluster of CYS wellfield at the Modder river project site. The study site, comprising approximating two triangulated arrays, measures ~200m by 190m over which the six boreholes of varying depths below ground surface were selected.

Boreholes were constructed in a partial gravel envelope type fashion to meet stipulated project objectives with each borehole constructed differently depending on the encountered subsurface strata. All the wells were developed until the discharge water was essentially sediment free.

### **8.2.2 Physical configuration of the aquifer system**

Overburden was concluded to be of average permeability; K calculated from infiltration test is approximately equal to 2.4m/d respectively. The regional geological setting of the study area consists mainly of rocks of the Karoo Sequence and Karoo Super Group comprising the Ecca and Beaufort Groups. The aquifer is a three unit unconfined alluvial stream aquifer situated in the alluvial deposits along the course of the river. The main units of the system are the upper unit, middle unit and lower unit aquitard made up of the overbank-fine sand deposits, gravel and mudstone respectively.

### **8.2.3 Isotopic and hydrochemical characteristics**

Analytical results show that all the samples are bicarbonate type water and fall along a mixing line from sulfate-chloride type water to calcium-magnesium type water. Analysed water is both unpolluted sodium enriched and chloride enriched. However, river water seems to fall between calcium/magnesium bicarbonate type water and sodium bicarbonate/chloride water. This attribute indicates the mixing phenomena between river water and groundwater. Water from CYS1BH2 seems to differ with the rest of the wells because it is characteristic of sodium potassium bicarbonate water.



This characteristic is similar to that of river water indicating more mixing between the two. CYS1BH2 never intercepted the gravel unit so that the most source of its water might be the inflow of the river water rather than the aquifer water.

Analytical results of the river water show that chloride and calcium were the predominant cations in solution from the six wells sampled. The elevated concentrations of calcium and chloride in groundwater might strongly be attributed to forestation of the site where evapotranspiration rates are widespread. Natural groundwater chemistry is largely influenced by vegetation (evapotranspiration) in that salts not used up by plants tend to accumulate in the soil horizon thereby being leached by infiltrating and percolating water down to the water table. This process is therefore attributed to the elevated salt species in groundwater in the area. The other possible source might be the dissolution of calcium-rich calcrete identifiable in the study area.

Wells CYS1BH1, CYS1BH3 and CYS1BH4 are Ca–Cl waters that have undergone evolution through ion exchange from recharge to discharge areas in the groundwater flow system. These results are not questionable as the three wells display similar geological makeup. These waters are differentiated slightly by their EC values in which CYS1BH3 falls towards the end of the 50% percentile with CYS1BH1 falling in the mid 50% percentile while CYS1BH4 falls in the 95% percentile. Wells CYS1BH2 is Na+K-HCO<sub>3</sub> waters while CYS1BH6 is Ca-Cl- HCO<sub>3</sub> waters. River water on the other hand shows more of Na+K-Mg- HCO<sub>3</sub> type water characteristic.

#### **8.2.4 General groundwater flow**

On the hydrograph for CYS1BH3, CYS1BH4 and CYS1BH5, water levels decrease sharply from November then increase sharply from January of the following year to February. CYS1BH2 shows almost the same behaviour as the rest of the wells because it overlies the gravel unit and hence might be feeding water from beneath. CYS1BH6 exhibits a complete different behaviour where water levels only fluctuate slightly from September to February hypothetically in response to recharge from local precipitation events. CYS1BH1 and CYS1BH2 are, during torrents of rains, flooded by overbank floods.

Head differences yield the hydraulic gradients towards the river indicating groundwater directions towards the river although most might be used up by riparian vegetation during evapotranspiration. On average the hydraulic gradient is 0.0083 (Figure 8-2). Both small scale and large scale methods yield flow direction estimates in the same mould where flow direction varied by 45° over the entire study domain, but generally trended SE, sub-perpendicular to the regional groundwater flow direction.

In CYS1BH3, CYS1BH4 and CYS1BH5, the EC-profiles show flow zone at 11m, 16m and 19m respectively as seen from the jump in the EC-concentrations. Significant or increased flow for CYS1BH3 is however noticed at 12.9m while that of CYS1BH5 is at 24m.

When water was abstracted from borehole CYS1BH3 while observing the water level in CYS1BH5 (distance 34m from the pumping well) the water-level drawdowns in the boreholes that intersected the same flow source were very similar.

### **8.2.5 Physical hydraulic characterisation**

The results of the constant discharge test indicated that the transmissivity of the site's aquifer ranges between 0.3m<sup>2</sup>/d to 164m<sup>2</sup>/d with specific yields ranging between 0.005 and 0.023 (Figure 8-2). These values are expected to represent the gravel layer porosity since this has been inferred in the thesis to be the chief water source. The guesstimate of the baseflow contribution to river flow yields a negative value that signifies a no base-flow-contribution of groundwater into the river suggesting that most groundwater is used up by the riparian vegetation.

## **8.3 Proposed Conceptual model (Schematisation)**

An important tool to characterise the aquifer are hydrogeological profiles. From the geological modelling (3D, cross-sections and borehole logs), the aquifer system is classified as an unconfined aquifer with two laterally zoned and three vertically zoned characteristics of alluvial structures. The lateral zones herein referred to are

the proximal and distal measured relative to the river. The proximal comprises an accumulation of fine sands, coarse gravel with poorly sorted pebbles, cobbles and boulders and mudstone. The distal zone is completely dominated by mudstone and fine sands

The groundwater system can schematically be subdivided into three hydrogeological layers that coincide with the wellfield inventory by the defined geologic logs. The upper layer whose thickness varies from 11 metres to 19 metres is mostly the unsaturated alluvial fine and single grained sand whose harmonic hydraulic conductivity is 2.42m/d calculated from *in situ* infiltration test. The second layer consists of coarse to sandy gravel decreasing in size to sand and mudstone upstream and completely dissipating further to the eastern side as depicted by geological log of CYS1BH6. The lower boundary is a highly impervious mudstone as revealed by CYS1BH5. This formation entirely blankets the distal zone (Figure 8-3). The aquifer here is believed to source its water from the rainfall infiltration. The aquifer system is bounded to the southern side by and abuts the river (Modder River).

The aquifer and the river in the study area form mixed systems characterised by transmission losses of a temporary nature. The river alternately recharges the bank storage in alluvial systems during high flows, which are subsequently released from the same material to the channel during low flows loses (Figure 8-3).

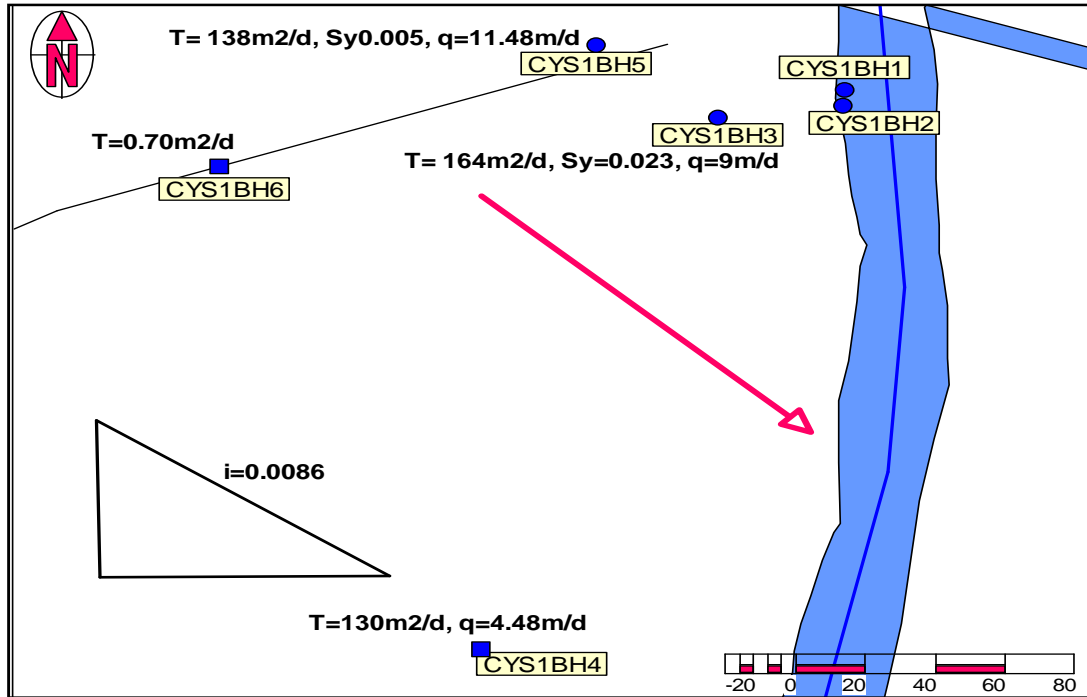


Figure 8-2: Map showing the estimated hydraulic properties of the site water bearing material.

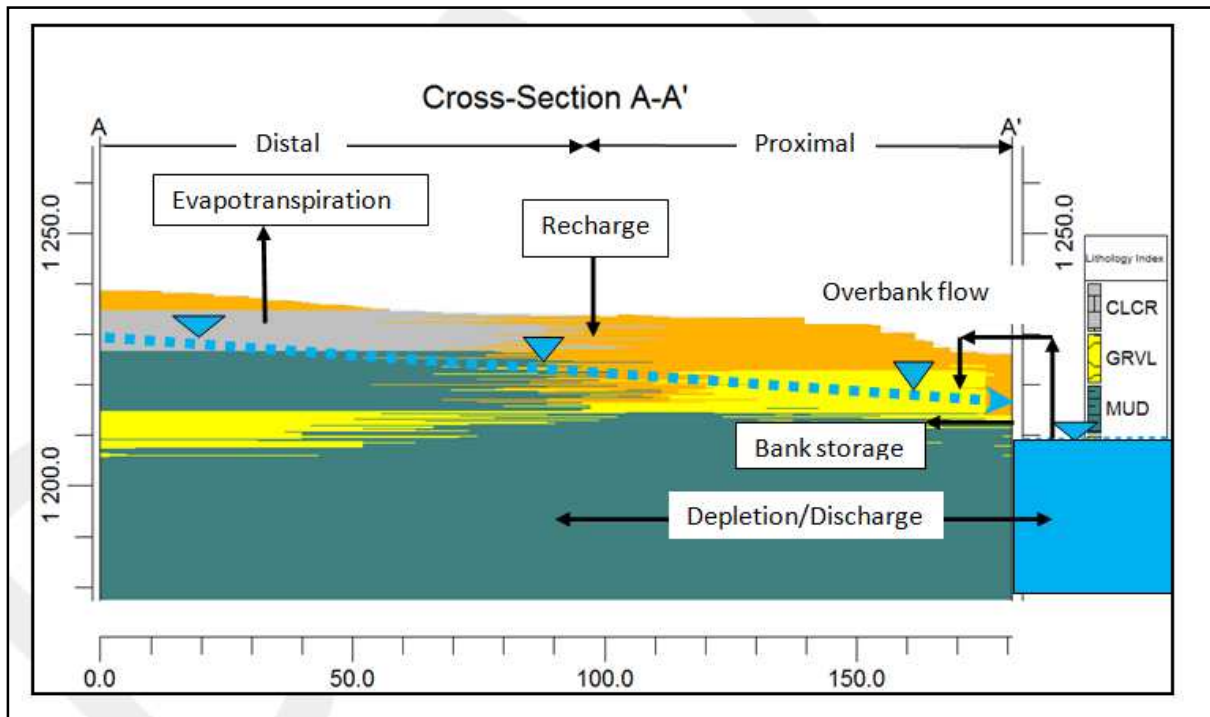


Figure 8-3: Schematic section for the hydrogeologic conceptual model.

## 9 REFERENCES

- Bagarello, V., and Provenzano, G. (1996). Factors affecting field and laboratory measurement of saturated hydraulic conductivity. *Transactions of the ASAE* 39, no. 1: 153–159.
- Bear, J. (1979). *Hydraulics of Groundwater: McGraw-Hill Series in water Resources and Environmental engineering*. McGraw-Hill Inc, Israel.
- Bell, F.G. (1993). *Engineering geology*. London: Blackwell Scientific Publications.
- BKS. (2002). Catchment Management Strategy for the Modder and Riet Rivers- Water Quality Assessment Report. Unpublished (progress) report prepared by DWAF Free State Region, June 2002.
- Botha, J. F. (1994). Models and Theory of Groundwater Motion. Unpublished report. Institute for Groundwater Studies, University of the Free- state, P.O. Box 339, Bloemfontein, p. 124-127.
- Botha, J.F. (1998). Karoo Aquifers, their Geology, Geometry and Physical Properties. WRC report no; 487/1/98. Pretoria: Water Research Commission.
- Bouwer, H. and Jackson, R. D. (1974). (Cited 2010, April 20) Determining soil properties. In: J. van Schilfgaarde (ed.), *Drainage for Agriculture*. Agronomy 17. American Society of Agronomy, Madison, pp. 611-672. Available from: [www.waterlog.info](http://www.waterlog.info)
- Carl, F. E., Craig, G. C. and Robert, G. S. (Cited 2010, October 11). Clean Water for Washington: Role of Soil in Groundwater: Washington State university Extension, USA, Available from: <http://www.cru.cahe.wsu.edu/CEPublications/eb1633/eb1633.html>
- Clark, I. and Fritz, P. (1997) *Environmental Isotopes in Hydrogeology*. Lewis Publ., Boca Raton. 323.

- Conrad, L. P. and Beljin, M. S. (1996). Evolution of an Induced Infiltration Model as Applied to Glacial Aquifer System. *Water Resources Bulletin* 32, no.6; 1209-1220.
- Cook, M.G. (1990) (Cited, 2010, October 11). Good Soil Management Helps protect Groundwater. North Carolina Cooperative Extension Services, USA. Available from: <http://www.soil.cnsu.edu/publications/soifacts/AG-439-09/>.
- Coplen, T.B., (1988). Normalization of oxygen and hydrogen isotope data. *Chemical Geology* 72 (4), 293–297.
- Craig, H. (1961). Isotopic variations in meteoric water. *Science* 133: 1702–1703.
- Darcy Groundwater Consultants. (2004). Establishment of a Groundwater Management Plan for the Kalkveld WUA, Progress Report 1, Geohydrology, Free State Regional Office, the Department of Water Affairs & Forestry, Bloemfontein.
- DEAT (Department of Environment and Tourism). (2001). Environmental Potential Atlas of South Africa. Pretoria: DEAT.
- DEAT (Department of Environment and Tourism). (1999). Environmental Potential Atlas of South Africa. Pretoria: DEAT.
- Department of Water Affairs, South Africa. (2004). *Internal Strategic Perspective: Upper Orange Water Management Area*. Prepared by PDNA, WRP Consulting Engineers (Pty) Ltd, WMB and Kwezi-V3 on behalf of the Directorate: National Water Resource Planning. DWAF Report No P WMA.
- Department of Water Affairs, South Africa. (2006). Final Report: Groundwater-surface water interactions, Project 2003-150, Rep. 3Bc, DWAF.
- Devlin, J. F. (2002). A Spreadsheet method of estimating best-fit hydraulic gradients Using Head Data from multiple wells. Geology Department, University of Kansas, 1475 Jayhawk Blvd.

- Drost W. and Neumaier, F. (1974). Application of single borehole methods in groundwater research. Proceedings, Symposium on Isotope Techniques in Groundwater Hydrology 1974, Vienna, pp 241-254.
- Du Press, M. (2007). Experimental Determination of Rock Hydrological Properties Using Elastic Parameters: Masters of Science thesis. IGS: University of the Free State, South Africa.
- Eagle. C.F., Cogger, C. G. and Stevens, R. G. (1991). Role of Water in Groundwater Protection. Washington State university Cooperative Extension and the U.S Department of Agriculture, USA.
- Farrar, C. D., Metzger, L. F., Nishikawa, T., Koczot, K. M., Eric G. and Reichard, E. G. (2006). Geohydrologic Characterization, Water- Chemistry, and Ground-Water Flow Simulation Model of the Sonoma Valley Area, Sonoma County, California. Scientific Investigations Report 2006-5092: U.S. U.S. Geological Survey, Reston, Virginia.
- Freeze, R. A., and , J. A, Cherry (1979). Groundwater. Prentice Hall Inc., Englewood Cliffs, New Jersey.
- Fritz, P. and Fontes, J. C. (1980). Introduction. In P. Fritz and J. C. Fontes (ed), Handbook of Environmental Isotope Geochemistry, v. 1. Elsevier, Amsterdam, p. 1-19.
- Gasca, D. and Ross, D. (2009). (Cited, 2010, October 11). The use of wetland water balances to link hydrogeological processes to ecological effects. Atkins Ltd, Woodcote Grove, Ashley Road, Epsom, Surrey KT18 5BW, UK. Available from: <http://www.springerlink.com/content/r4q0p30885550143/fulltext.pdf>
- Gat, J.R. and Gonfiantini, R. (1981). Stable Isotope Hydrology: Deuterium and Oxygen-18 in the Water Cycle. International Atomic Energy Agency: Vienna, Austria; 210.
- Gemici, U.F.S. (2001). Hydrochemistry of the geothermal area in western Turdey. *Journal of Volcanology and Geothermal Research* 110: 171–187.

- GHR611. (2010). Conducting Hydraulic and Tracer Tests: Class Notes. University of the Free State, Institute for Groundwater Studies, Box 339, Bloemfontein 9300, South Africa.
- Gugulethu, N.C., Zuma-Netshiukhwi and Walker, S. (2009). Crop-climate matching for south-western Free State, University of the Free State P. O. Box 339, Bloemfontein.
- Guyen, O., Falta, R. W., Molz, F.J. and Melville, J.G. (1986). A Simplified Analysis of Two-well Tracer tests in stratified Aquifers. Vol. 24. No.1-Groundwater. Department of Civil Engineering, Auburn University, Alabama.
- Han, D., Liang, X., Currell, M.J. Song, X., Chen, Z., Jin, M., Liu, C. and Han, Y. (2010). Environmental isotopic and hydrochemical characteristics of groundwater systems in Daying and Qicun geothermal fields, Xinzhou Basin, Shanxi, China. *Hydrol. Process.* 24, 3157–3176 (2010) Published online 11 June 2010 in Wiley Online Library (wileyonlinelibrary.com) DOI: 10.1002/hyp.7742.
- Heath, R. C. (1987). Basic Ground-Water Hydrology. U.S. Geological Survey, Federal Centre, Box 25425, Denver, CO 80225.
- Hem, J. D. (1970). Study and Interpretation of the Chemical Characteristics of Natural Water, 2<sup>nd</sup> ed., U. S. Geological Survey Water Survey Paper No. 1473, 363 pp., Washington, D.C.
- Hermance, J. F. (2003). (cited 2010, October 2008). Department of Geosciences course notes: Environmental Geophysics/Hydrology (internet). Province, USA: Brown University. Available from:  
[http://www.brown.edu/courses/Geo158/ge158web/classsupplements/2010/St\\_OrangePropertiesOfAquifers.ppt](http://www.brown.edu/courses/Geo158/ge158web/classsupplements/2010/St_OrangePropertiesOfAquifers.ppt)
- Hillel, D. (1980). Fundamentals of Soil Physics. Academic Press, New York.
- Hogan, C. (2008). Groundwater Management Plan for the Kalkveld Area: Groundwater Resource Directed Measures, Establishment of a Management



and Monitoring plan for the Kalkveld Area in order to ensure sustainable use of the groundwater resource. 10/17/2008.

Institute for Groundwater Studies. (2007). Groundwater Dictionary. University of the Free- state, P.O. Box 339, Bloemfontein.

Ishii, E., H. Sanada, H. Funaki, Y. Sugita, and H. Kurikami (2011). (cited 2010, October 08). The relationships among brittleness, deformation behaviour, and transport properties in mudstones: An example from the Horonobe Underground Research Laboratory, Japan, *J. Geophys. Res.*, 116, B09206, doi:10.1029/2011JB008279. Available from:

<http://www.agu.org/pubs/crossref/2011/2011JB008279.shtml>

Johanson, M. R., Van Vuuren, C. J., Hegenberger, W. F., Key, R., and Shoko, U., (1996). Stratigraphy of the Karoo Supergroup in Southern Africa: An overview. *Journal of African Earth Sciences*, Vol.23, No. 1, pp3-15. Elsevier Science Ltd: Great Britain.

Jousma, G. and Roelofsen, F.J. (2004). World-wide Inventory on Groundwater monitoring: *International Groundwater Resources Assessment Centre Utrecht*.

Kok, A. (2002). Groundwater Monitoring: Past & Future: 17th Salt Water Intrusion Meeting, Delft, The Netherlands, 6-10 May 2002. Nuon Water, P.O. Box 400, 8901 Leeuwarden, the Netherlands.

Kruseman, G. P. and de Ridder, N.A. (1994). Analysis and Evaluation of Pumping Test Data Second Edition. International Institute for Land Reclamation and Improvement, P.O. Box 45, 6700 AA Wageningen, the Netherlands.

Kuchment, L.S. (2004), The Hydrological Cycle and Human Impact on it, in *Water Resources Management*, [Eds. Arjen Y. Hoekstra, and Hubert H.G. Savenije], in *Encyclopedia of Life Support Systems (EOLSS)*, Developed under the Auspices of the UNESCO, Eolss Publishers, Oxford, UK, [<http://www.eolss.net>]

- Larkin, R.G. and Sharp, J.M. (1992). On the Relationship between River-basin Geomorphology, Aquifer Hydraulics, and Groundwater Flow Direction in Alluvial Aquifers, Geological Society of America Bulletin 04, no. 12; 1608-1620.
- Lory, J. (2010). (Cited 2010, April 02). The Cooperative Soil Survey: Soil Bulk Density- Physical Properties. Available from: <http://www.soilsurvey.org/tutorial/page10.asp>
- Lloyd, J.W. (2006). The difficulties of regional groundwater resources assessments in arid areas. Based on a presentation at the 2nd International Conference on Water Resources and Arid Environment, Prince Sultan Research Centre for Environment, Water and Desert, King Saud University, Riyadh, Kingdom Of Saudi Arabia, November 2006.
- Meyer, P.S. (2003). An explanation of the 1:500 000 General Hydrogeological Map, Bloemfontein 2924. Directorate: Geohydrology, Department of Water Affairs & Forestry, Pretoria.
- Midgley, D.C., Pitman, W.V. and Middleton, B.J. (1994a). Surface Water Resources of South Africa. Vol. 2, Drainage C, Vaal. Appendices. WRC report no. 298/2.1/94. Pretoria: Water Research Commission.
- McKinney, D.C. (2009). (Cited 2010, October 01) CE374L Darcy's law: Groundwater Hydraulics notes. Available from: [www.ce.utexas.edu/prof/mckinney/ce374l/ce374l.html](http://www.ce.utexas.edu/prof/mckinney/ce374l/ce374l.html)
- Odong, J. (2007). Evaluation of Empirical Formulae for Determination of Hydraulic Conductivity based on Grain-Size Analysis School of Environmental Studies China University of Geosciences 388 Lumo Road Wuchang, Wuhan, Hubei 430074, China.
- Oosterbaan, R. J. and Nijland H.J. (1994). (Cited 2010, September 01) Determining the Saturated Hydraulic Conductivity. Chapter 12 in: H.P.Ritzema (Ed.), Drainage Principles and Applications. International Institute for Land Reclamation and Improvement (ILRI), Publication 16, second revised edition,

1994, Wageningen, The Netherlands. ISBN 90 70754 3 39. Available from:  
[www.waterlog.info](http://www.waterlog.info)

Parsons, R. (2004). Surface Water–Groundwater Interaction in a Southern African Context: Geohydrological Perspective. WRC report no. 116-F1. Pretoria: Water Research Commission.

Rădulescu, V., Rădulescu, F. and Stan, L. (2006). Geoelectrical Measurements Applied to the Assessment of Groundwater Quality. National Institute of Marine Geology and Geo-ecology (GeoEcoMar), 23-25 Dimitrie Onciul St 024053, Bucharest, Romania.

Ravikumar, P. and Somashekar, R.K. (2010). Environmental Tritium ( $^3\text{H}$ ) and hydrogeochemical investigations to evaluate groundwater in Varahi and Markandeya basin, Karnaka, India.

RockWorkks15. (2010). Rockworks15 manual, Third edition. 2221 East St., Suite 101 Golden, CO 80401 USA.

Roscoe Moss Company. (1990). Handbook of Ground water Development. John Wiley & Sons: Los Angeles, California.

Rosenshein, J.S. (1998). Hydrology of the North America, Region 18, Alluvial Valleys. In The Geology of North America, ed, W,Back, J.S. Rosenshein, and P.R. Seaber, 0-2, 165-176. Boulder, Colorado: Geological Society of North America.

Savva, A. P. and Frenken, K. (2002). Crop Water Requirements and Irrigation Scheduling. Water Resources Development and Management Officers FAO Sub-Regional Office for East and Southern Africa, Harare.

Shahin, M. (2002). Hydrology and water resources of Africa. Kluwer Academic Publishers, P.O. Box 17, 3300 AA Dordrecht, the Netherlands.

Smedema, L.K. and D.W. Rycroft (1983). Land drainage: planning and design of Agricultural Drainage Systems. Batsford, London, 376 p.

Spitz, K. and Moreno, J. (1996). A practical guide to groundwater and solute transport modelling. Canada: John Willey and Sons.

Schwartz, F. W. (2003). Fundamentals of groundwater. John & Wiley, Inc. USA.

Sophocleous, M. (2002). (Cited 2010, October) Interactions between groundwater and surface water: the state of the science. Kansas Geological Survey, University of Kansas, 1930 Constant Ave., Lawrence, Kansas 66047, USA. Available from:

[http://www.kgs.ku.edu/General/Personnel/rs/mas/2002/Sophocleous\\_GW-SW.pdf](http://www.kgs.ku.edu/General/Personnel/rs/mas/2002/Sophocleous_GW-SW.pdf).

Sturchio, N.C., Ohsawa, S., Sano, Y., Arehart, G., Kitaoka, K. and Yusa, Y. (1996). Geochemical characteristics of the Yufuin outflow plume, Beppu hydrothermal system, Japan. *Geothermics* 25 (2): 215–230.

Taylor, C. J. and Alley W.M. (2001). Ground-water-Level Monitoring and the Importance of Long term Water-Level Data: U.S. Geological Survey Circular. Denver, Colorado.

Troeh, F. R. and Thompson, M.L. (1993). Soils and Soil fertility. Oxford University press: New York.

Tsokeli, R. D. (2005). Masters Thesis: An evaluation of the spatial variability of Sediment Sources along the Banks of the Modder River. Free State Province, South Africa. Department of Geography Faculty of Natural and Agricultural Sciences University of the Free State, Bloemfontein.

Usher, B.H. (2008). Hydrochemistry and pollution: GHR612 lecture notes. Institute for Groundwater Studies, University of the Free State, Bloemfontein, South Africa.

van Tonder, G. and Rudolph, D. (2003). Rapid Determination of the Groundwater Component of the Reserve for Bainsvlei, Quaternary Catchments (C52G, C52H and C52J). The Department of Water Affairs, Pretoria.

van Tonder, G., Riemann, G. and Dzanga, P. (2002). Interpretation of single-well tracer tests using fractional-flow dimensions. Part 1: Theory and

mathematical models. University of the Free State, Institute for Groundwater Studies, Box 339, Bloemfontein 9300, South Africa.

van Tonder, G., Riemann, K. and Dennis, I. (2002). Interpretation of single-well tracer tests using fractional-flow dimensions. Part 2: Theory and mathematical models. University of the Free State, Institute for Groundwater Studies, Box 339, Bloemfontein 9300, South Africa.

van Tonder, G. (2011). Non-Perennial Rivers: Unpublished Workshop Presentation. University of the Free State, Institute for Groundwater Studies, Box 339, Bloemfontein 9300, South Africa.

Vermaak, J.J.G. and van Schalkwyk, A. (2000). The Relationship Between the Geotechnical and Hydrogeological Properties of Soils and Rocks in the Vadose Zone. WRC report no. 701/1/00. Pretoria: Water Research Commission.

Walton, C. W. (1970). Groundwater Resource Evaluation. New York, McGraw-Hill Book Company.

Winter, T. C., Harvey, J. W., Franke, O. L. and Alley, W. M. (1998). Ground Water and Surface Water A Single Resource: U.S. Geological Survey Circular 1139. U.S. Geological Survey, Branch of Information Services, P.O. Box 25286, Denver, CO 80225-0286.

Woodford, A. C. and Chevallier, L. (2002). Hydrogeology of the Main Karoo Basin: Current Knowledge and Future Research Needs. WRC report no. TT 179/02. Pretoria: Water Research Commission.

WRC. (1998). Quality of Domestic Water Supplies. Volume 1: Assessment Guide. WRC report no. TT 101/98. Standard South Africa, 1 dr Lategan Road Groenkloof, Pretoria.

Yangxiao, Z. (1994). Objectives, criteria and methodologies for the design of primary groundwater monitoring networks. International Institute for Infrastructural,

Hydraulic and Environmental Engineering, PO Box 3015, 2601 DA Delft, The Netherlands.

Zouari, K., Hkir, N. and Ouda, B. (2003). Palaeoclimatic Variation in Maknassi Basin (Central Tunisia) During Holocene Period Using Pluridisciplinary Approaches. Technical Document. IAEA, Vienna. 2” 80-88.

## 10 ANNEXE A: SOIL ANALYSIS

### 10.1 Infiltration Test

TABLE 10-1: INFILTRATION TEST RESULTS CYS1\_ABH2

t(min)	WL(m)	Ht	ht+r/2
0	0.30	0.700	0.753
1	0.350	0.6500	0.703
2	0.370	0.630	0.683
3	0.412	0.588	0.641
4	0.398	0.602	0.655
5	0.414	0.586	0.639
6	0.431	0.569	0.622
7	0.461	0.539	0.592
8	0.475	0.525	0.578
9	0.490	0.510	0.563
10	0.502	0.498	0.551
11	0.520	0.480	0.533
12	0.529	0.471	0.524
13	0.540	0.460	0.513
14	0.556	0.444	0.497
15	0.560	0.440	0.493
16	0.566	0.434	0.487
17	0.570	0.430	0.483
18	0.578	0.422	0.475
19	0.584	0.416	0.469
20	0.600	0.40	0.453

TABLE 10-2: INFILTRATION TEST RESULTS CYS1\_ABH3

t(min)	WL(m)	ht	ht+r/2
0	0.300	0.700	0.753
1	0.348	0.652	0.705
2	0.356	0.644	0.697
3	0.412	0.588	0.641
4	0.424	0.576	0.629
5	0.454	0.546	0.599
6	0.458	0.542	0.595
7	0.464	0.536	0.589
8	0.488	0.512	0.565
9	0.520	0.480	0.533

10	0.536	0.464	0.517
11	0.546	0.454	0.507
12	0.549	0.451	0.504
13	0.569	0.431	0.484
14	0.574	0.426	0.479
15	0.592	0.408	0.461
16	0.61	0.39	0.443
17	0.624	0.376	0.429
18	0.626	0.374	0.427

TABLE 10-3: INFILTRATION TEST RESULTS FOR CYS1\_ABH4

t(min)	WL(m)	ht	ht+r/2
0	0.300	0.700	0.750
1	0.370	0.630	0.680
2	0.390	0.610	0.660
3	0.432	0.568	0.620
4	0.458	0.542	0.590
5	0.485	0.515	0.570
6	0.494	0.506	0.560
7	0.530	0.470	0.520
8	0.550	0.450	0.500
9	0.564	0.436	0.490
10	0.580	0.420	0.470
11	0.599	0.401	0.450
12	0.612	0.388	0.440
13	0.629	0.371	0.420

TABLE 10-4: INFILTRATION TEST RESULTS FOR CYS1\_ABH5

t(min)	WL(m)	ht	ht+r/2
0	0.300	0.700	0.750
1	0.330	0.670	0.720
2	0.360	0.640	0.690
3	0.390	0.610	0.660
4	0.410	0.590	0.640
5	0.430	0.570	0.620
6	0.450	0.550	0.600
7	0.480	0.520	0.570
8	0.490	0.510	0.560



9	0.540	0.460	0.510
10	0.550	0.450	0.500
11	0.550	0.440	0.500
12	0.550	0.450	0.500
13	0.560	0.440	0.500
14	0.560	0.440	0.490
15	0.570	0.430	
16	0.580	0.420	
17	0.590	0.410	
18	0.590	0.410	
19	0.60	0.40	
20	0.61	0.39	

## 10.2 Soil Index Properties

### 10.2.1 Bouyoucos procedure for soil classification

- **Separation of sand fraction:** The dispersed sample was washed on the 0.053mm size and passing the silt and clay through the funnel into 1m<sup>3</sup> cylinder. The washing was performed until the percolate was clear after which the size was removed from the cylinder and the sand quantitatively transferred to a tarred evaporating beaker and oven dried at 105°C to a constant mass. The resultant mass of sand was determined. The percentage sand was then computed using the following formula (department of Agriculture, 2010):

$$\text{percentage sand} = \frac{A \times 100}{M}$$

Equation 10-1

Where; M = mass (g) of soil used

A = mass (g) of sand fraction (>0.53)

- **Determination of clay:** the cylinder was filled with the silt and clay suspension to the 1m<sup>3</sup> mark, stirred for 30 seconds. A blank was prepared by adding 10cm<sup>3</sup> Calgon to 1cm<sup>3</sup> of water in a cylinder. After six hours, the hydrometer reading, **C**, and temperature, **T**, of the blank of the suspension was taken and

so is the hydrometer reading **B** of the blank. Hydrometer reading of the blank was subtracted from that of the suspension (**C-B**) and the percentage clay determined under appropriate temperature column in table X (department of Agriculture, 2010):

- Determination of silt:

$$\%silt = 100 - (\%sand + \%clay)$$

Equation 10-2

## 11 ANNEXE B: LITHOLOGIC DESCRIPTIONS

Well:CYS1BH1

Land Surface Elevation = 1226.004m.a.m.s.l

Depth (m)			Lithologic Description	Top Elev.
0	to	3	Sand	1226.004
3	to	6	Sand	1223.004
6	to	9	Sand	1220.004
9	to	11	Sand	1217.004
11	to	12	Sand and gravel with trace clay (dense)	1215.004

Well:CYS1BH2

Land Surface Elevation = 1225.98 m.a.m.s.l

Depth (m)			Lithologic Description	Top Elev.
0	to	3	Sand	1225.98
3	to	6	Sand	1222.98
6	to	9	Sand	1219.98
9	to	11	Sand	1216.98
11	to	12	Sand	1214.98

Well:SCYS1BH3

Land Surface Elevation = 1233.78 m.a.m.s.l

Depth (m)			Lithologic Description	Top Elev.
0	to	3	Sand	1233.78
3	to	6	Sand	1230.78
6	to	9	Sand	1227.78
9	to	11	Sand	1224.78
11	to	12	Sand	1222.78
12	to	18	Sand and gravel	1221.78

Well:CYS1BH4

Land Surface Elevation = 1235.725 m.a.m.s.l

Depth (m)			Lithologic Description	Top Elev.
0	to	11	Sand	1235.725
11	to	14	Sand and gravel	1224.73
14	to	16	Sand	1221.73
16	to	30	Sand and gravel	1219.73

Well: CYS1BH5

Land Surface Elevation = 1235.661 m.a.m.s.l

Depth (m)	Lithologic Description	Top Elev.
0.00 to 10.00	sand	1235.661
10.00 to 12.00	Silty sand	1225.661
12.00 to 13.00	Sand	1223.661
13.00 to 19.00	Silty sand	1222.661
19.00 to 20.00	Sand and gravel and silt (dense)	1216.661
20.00 to 21.00	Sand and gravel (dense)	1215.661
21.00 to 30.00	Bedrock (mudstone)	1214.661

Well: CYS1BH6

Land Surface Elevation = 1238.839m.a.m.s.l33

Depth (m)	Lithologic Description	Top Elev.
0 to 4	silty sand	1238.839
4 to 9	calcrete	1234.839
9 to 12	Sand	1229.839
12 to 24	Sand and gravel	1226.839

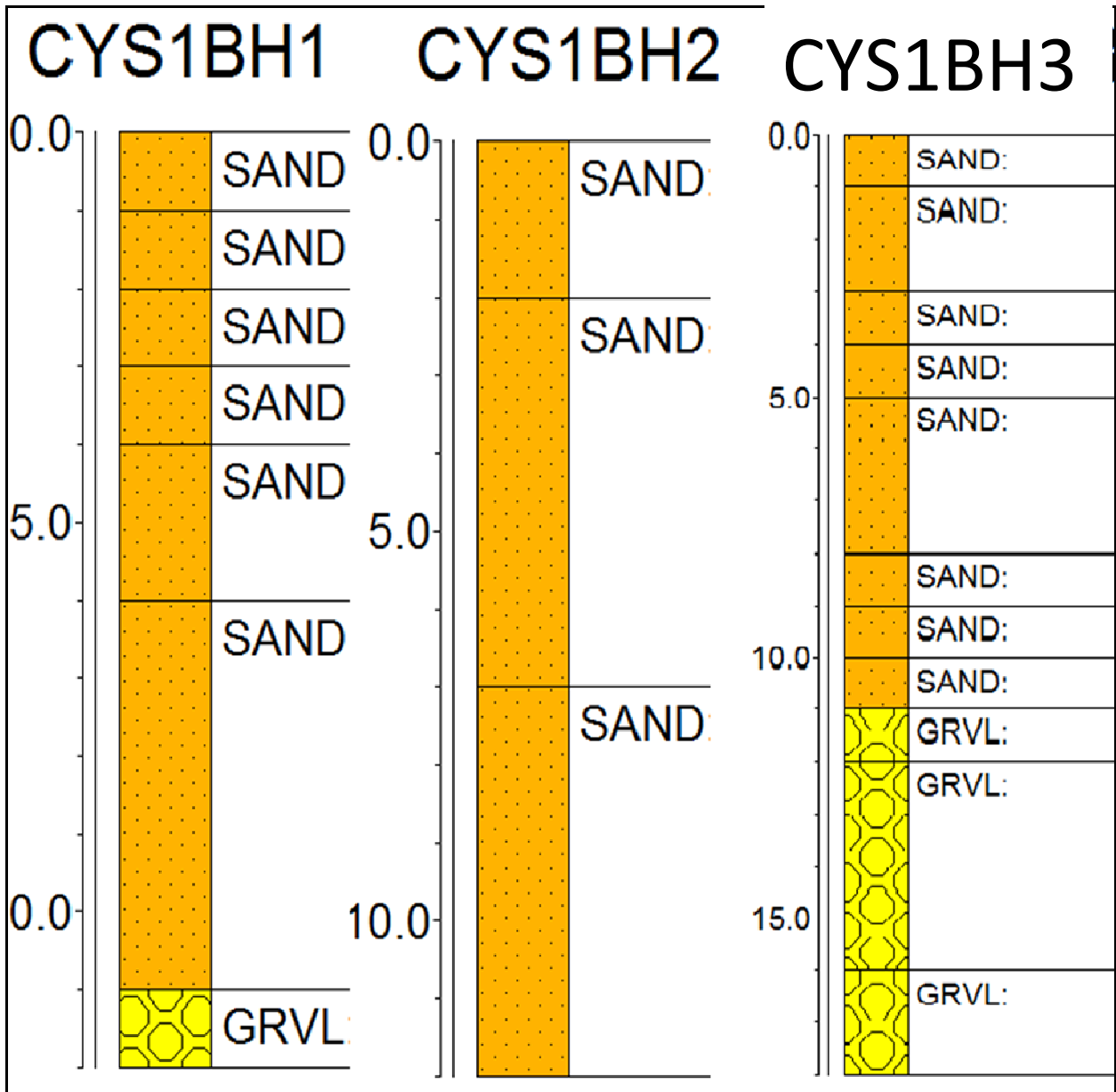


Figure 11-1: 2D lithological logs.

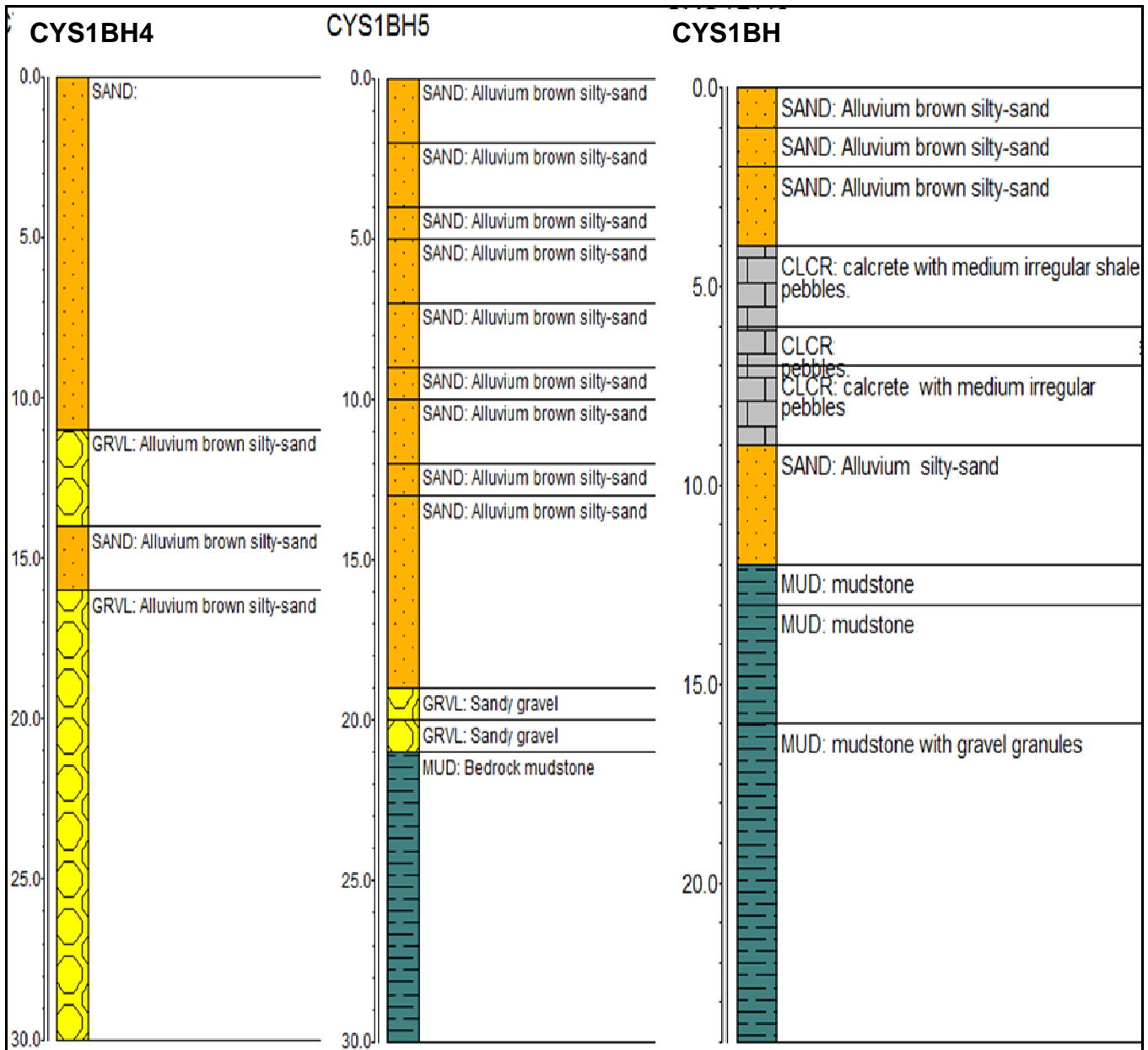


Figure 11-2: 2D lithological logs.

## 12 ANNEXE C: ENVIRONMENTAL ISOTOPIC AND HYDROCHEMICAL CHARACTERISTICS

TABLE 12-1: SUMMARISED WATER QUALITY DATA FROM DIFFERENT WELLS

SiteName	Ca(mg/l)	Mg(mg/l)	Na(mg/l)	K(mg/l)	MAIk	Cl(mg/l)	SO4(mg/l)	EC (mS/m)
CYS1 BH1	133.62	67.16	84.84	1.93	312	270.43	98.29	164
CYS1 BH2	85.07	39.47	130.78	4.36	384	195.50	4.45	126
CYS1 BH3	176.04	102.50	105.30	2.34	326	432.70	176.8	185
CYS1 BH4	185.9	91.5	131.4	3.8	286	420.16	282.30	216
CYS1 BH5	133.81	55.19	58.69	1.61	463	149.00	68.00	105
CYS1 BH6	77.5	41.0	62.9	2.2	239	184.00	31.79	103
River water_1	16.2	7.3	27.0	6.5	99	24.53	16.15	-
River water_2	22.0	8.9	23.5	6.6	99.7	22.16	15.08	-

### 13 ANNEXE C: GROUNDWATER FLOW AND HYDRAULIC PARAMETER CHARACTERISATION

TABLE 13-1: TIMELY GROUNDWATER LEVEL DATA (MEASUREMENTS ARE GIVEN IN MAMSL)

Date	CYS1BH1	CYS1BH2	CYS1BH3	CYS1BH5
2010/07/01	1222.56	1222.65	1222.79	1222.84
2010/09/01	1222.56	1222.65	1222.79	1222.84
2010/11/01	1222.7	1222.69	1222.98	1223.28
2010/12/01	1222.69	1222.69	1222.78	1222.86
2011/01/01	1222.92	1222.87	1222.92	1222.91



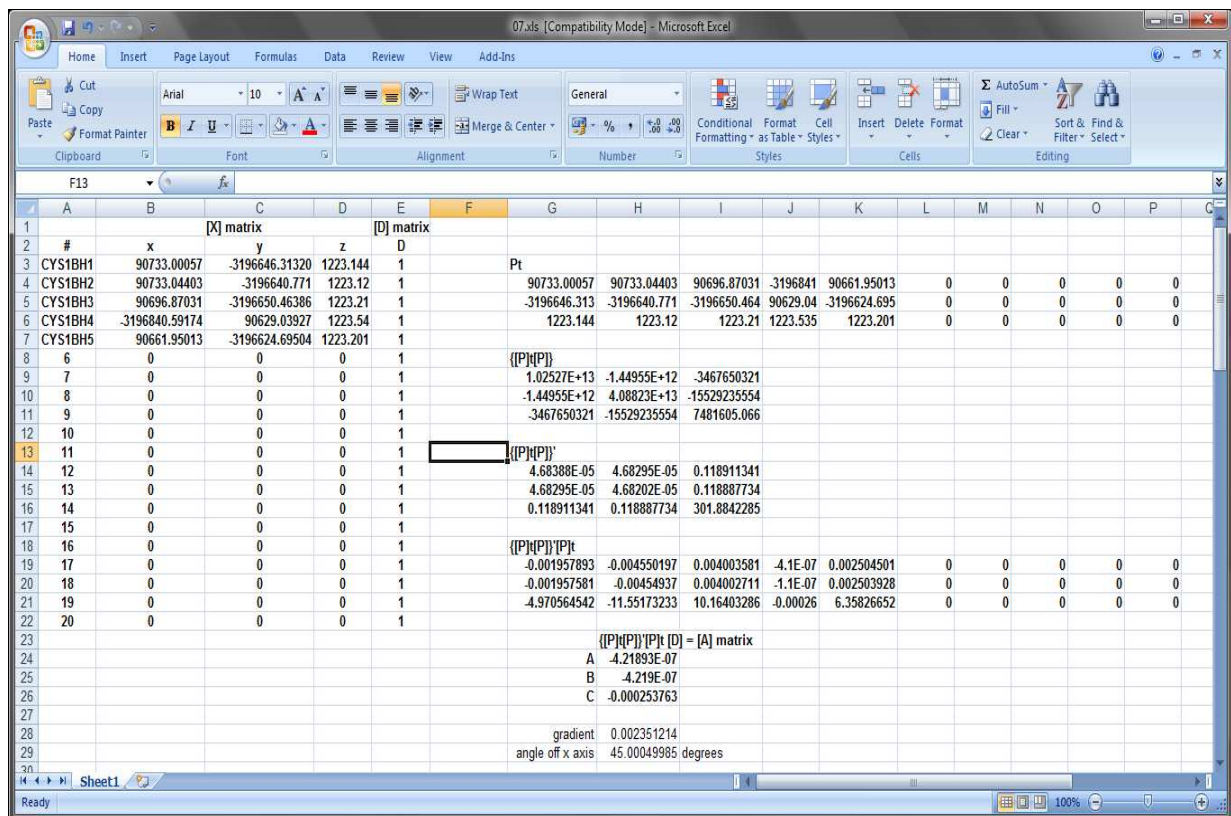


Figure 13-1: GRADIENT XLS Microsoft excel used to estimate the groundwater gradient and direction of flow (Devlin, 2002).

**NOTE:** To use the program, the coordinates for the well locations are entered in the columns labeled x and y (part of the [X] matrix), and the water levels in the z column. Water gradient is given by H34 whilst the direction is given by H35 (Devlin, 2002).

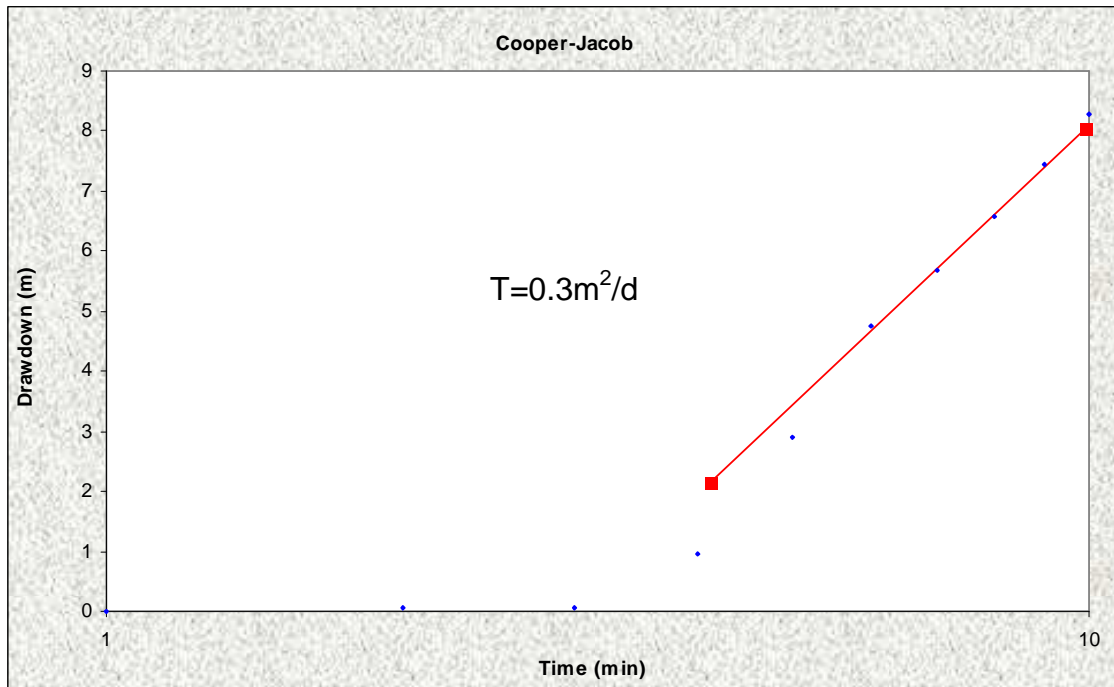


Figure 13-2: A cooper Jacob fit for CYS1BH2 (a drying well).

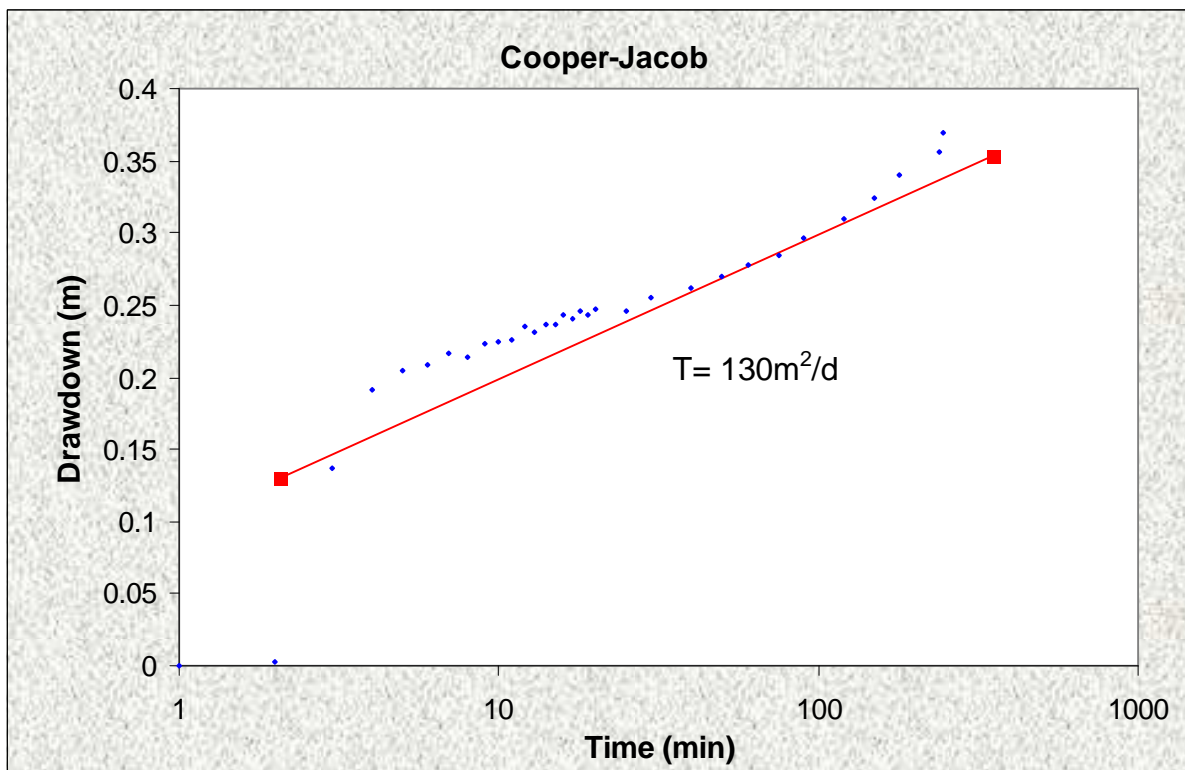


Figure 13-3: A Cooper Jacob fit for CYS1BH4.

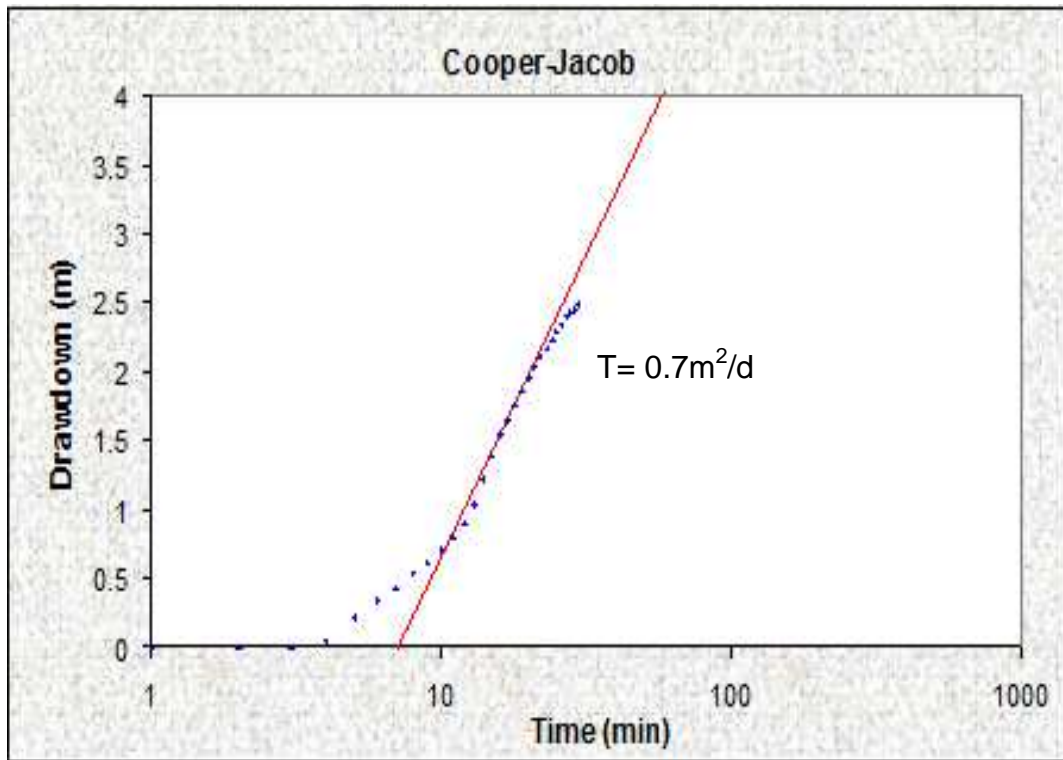


Figure 13-4: A Cooper Jacob fit for CYS1BH6 (a drying well).

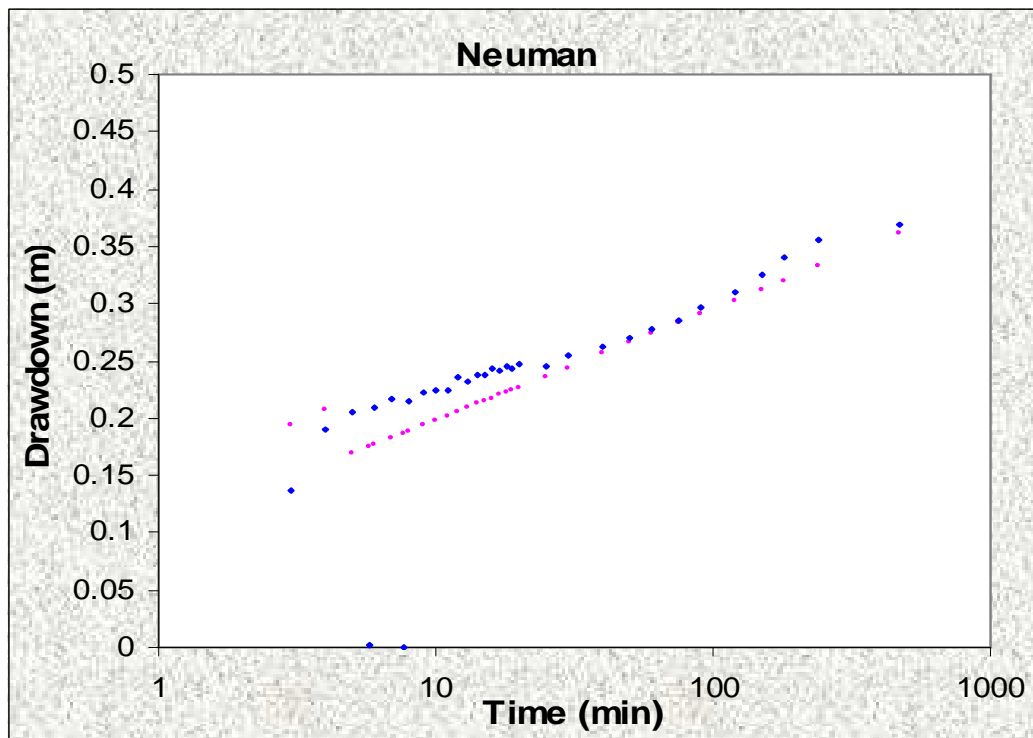


Figure 13-5: Neuman fit for CYS1BH3 pumping test data.

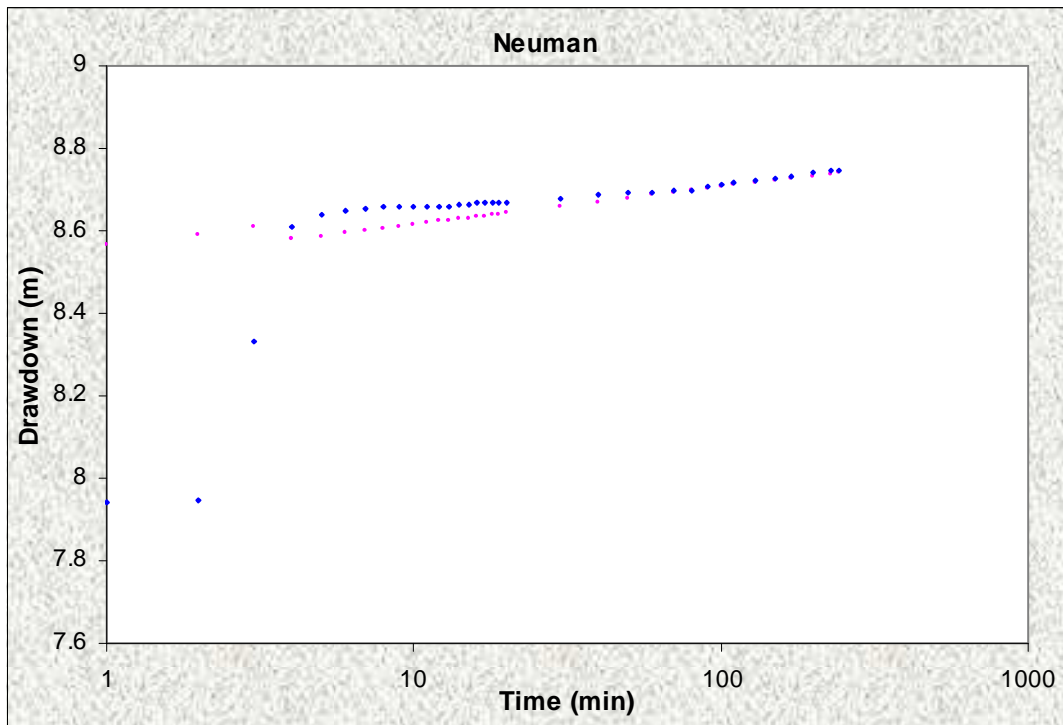


Figure 13-6: Neuman fit for CYS1BH5 data.